LOW FREQUENCY RADIO EMISSIONS

From

COSMIC RAY AIR SHOWERS

A thesis presented for the degree of

Doctor of Philosophy

by

PHILIP CHARLES CROUCH

PHYSICS DEPARTMENT

UNIVERSITY OF ADELAIDE

June 1979

...these matters I have very diligently analysed and pondered for a long time, and now having summarised them in a little book, I am sending them to Your Magnificence.

Niccolo Machiavelli

C O N T E N T S

SUMMARY

Between 1965 and 1975, there was considerable interest in radio pulses produced by extensive air showers. The main interest was centred on the expectation that studies of these pulses might reveal the nature of the high energy primary cosmic rays. A theory, based on the deflection of shower particles by the earth's magnetic field was developed, and proved successful in explaining features of the radiation at frequencies above 20 MHz. However, below this frequency there was gross disagreement between the theoretical prediction that the pulse amplitude would fall to zero at low frequencies, and a number of experimental measurements of very high pulse amplitudes. This project was conceived with the aim of determining the origin of these pulses.

A series of experiments was performed at a frequency of 2 MHz, but neither these experiments, nor the analysis of a previously unpublished 3.6 MHz experiment showed the presence of any signal. Upper limits, of the order of one-tenth of the previously reported field strengths were established.

However, experiments performed at 100 KHz confirmed the presence of variable, and on occasion very large, signals. Although the observing period was severely limited by these variations, the relationships of pulse amplitude to shower size and core distance were established. No indication of the nature of the production mechanism was found. However, it is suggested that the variations observed at 100 KHz extend to higher frequencies and are thus responsible for the confused situation at frequencies near 2 MHz, and also some apparently anomalous results at higher frequencies.

This thesis also includes a description of work carried out in connection with the air shower detector used in the above experiments. A system was designed and built to record data from this array on magnetic tape, and this was subsequently improved and extended to cater for more detectors. Some calculations were made to explore the capabilities of the array, how these capabilities can best be used, and the optimum siting of additional detectors.

This thesis contains neither material which has been accepted for the award of any other degree or diploma, nor, to the best of the author's knowledge and belief, any material previously published or written by any other person, except where due reference is made.

Signed

P. C. CROUCH

Acknowledgements

I would like to express my sincere thanks to my supervisor, Dr. A.G. Gregory, for his continued help throughout this project; his gentle guidance, patience and sence of humour were always appreciated.

I am also indebted to Dr. R.W. Clay for his infectious enthusiasm, and his valuable help in very many ways.

Dr. J.H. Hough kindly supplied some of the data used in this thesis.

I am grateful for the assistance I have received from many members of the Physics Department: particularly Judy Taylor, Ern Hindley, John Smith, Alex Didenko, Linsey Hettner, and the late Bill Jamieson. Without their help this project would have taken even longer.

Thanks are also due to Mr. Peter Paulos and his staff, and the C.R.G.G.C. for help at many crucial moments.

But without the support and encouragement of my wife Susan, this thesis would never have been completed.

CHAPTER ONE

INTRODUCTION

> When I was young, Cebes, I had an extraordinary passion for that branch of learning which is called natural science; I thought it would be marvellous to know the causes for which each thing comes and goes and continues to be.....
>
> Until at last I came to the conclusion that I was uniquely unfitted for this form of inquiry.
>
> Socrates

1.1 The Rise and Fall of Radio Pulses from Extensive Air Showers

In a short paper published in 1965 [1], Jelley et al. announced that following the theoretical prediction of Askaryan [2], radio pulses emitted by extensive air showers had been observed.

The summarised results of the early experiments [3] show many of the features that were to recur in later experiments. Only a few of the showers detected had clear, unambiguous radio pulses associated with them; for the vast majority of the showers detected, the presence of radio pulses could only be inferred by 'integrating' a large number of events. Some parts of the experiments (e.g. an attempt to measure polarisation) were inconclusive, and it was clear that many questions could not be answered unless information about the shower particles was known. The topic seemed to be rather a backwater in cosmic ray research.

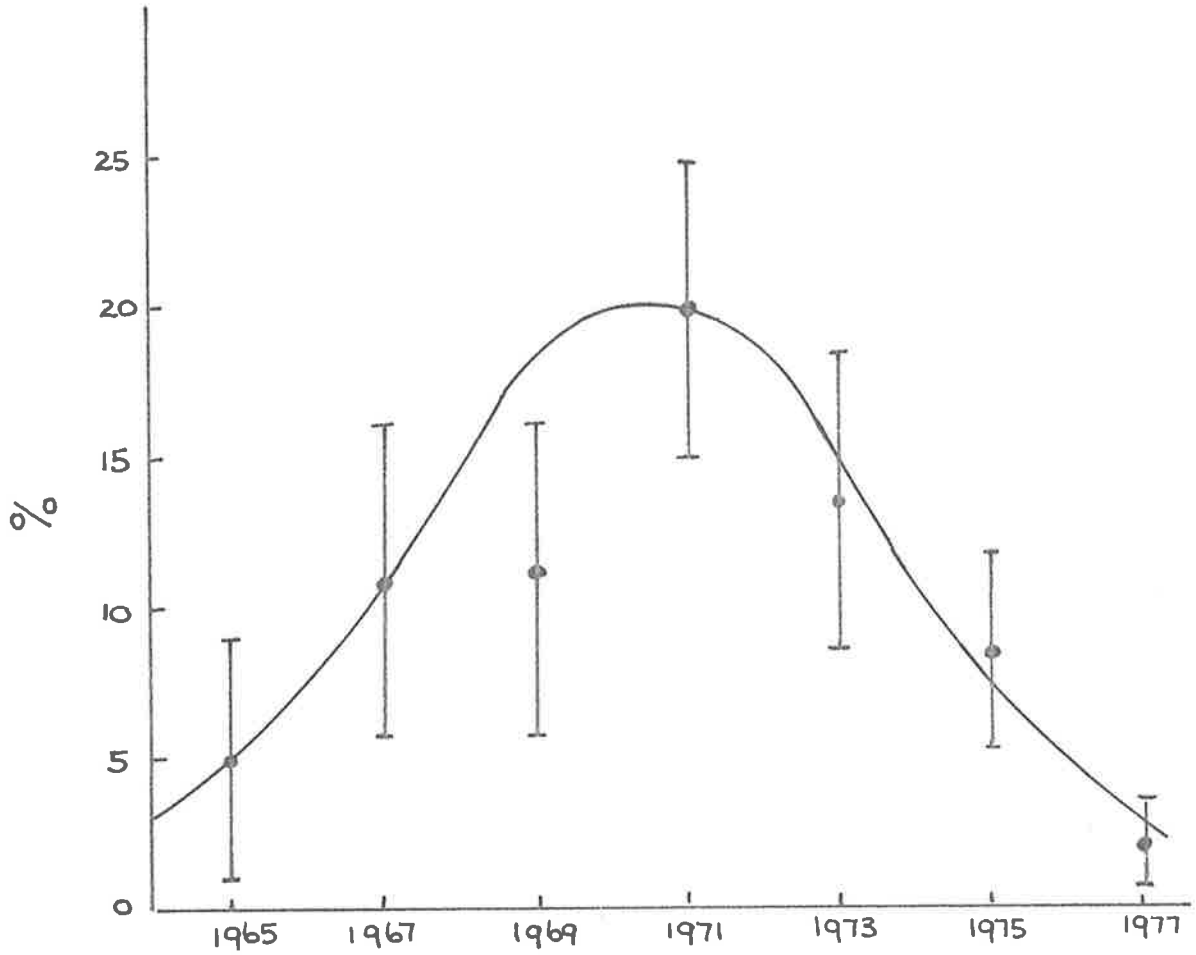

FIG 1·1

The Rise and Fall of Radio Emission from EAS.

[Ratio of "Radio emission" papers to "EAS" papers presented at International Conferences on Cosmic Rays.]

However, the result created a good deal of interest; 20% of all papers presented at 'Air Shower' sessions of the 1971 International Conference on Cosmic Rays were concerned with radio pulses. To understand the reasons, we should look at the state of high energy cosmic ray research at the time.

One of the main areas of interest was the behaviour of the high energy end of the cosmic ray spectrum, for it had been predicted that the spectrum might cut off sharply at energies above 5×10^{19} eV as a result of interactions with the microwave background radiation [4]. However, although the statistics were poor, the only measurement in this range appeared to show a flattening, not a steepening of the spectrum [5], and so the first results of the large air shower detectors at Haverah Park and Sydney were eagerly awaited. The wait would be a long one, however, for even the giant Sydney array, with 32 pairs of detectors over an area of 40 sq.km, would take a number of years to collect sufficient events to allow the spectrum above 10^{19} eV to be determined accurately. There was thus a good deal of interest in techniques which would enable air showers to be detected cheaply over large areas, and it was hoped that the radio emission phenomena would provide such a technique.

Several attempts were made to detect showers solely by means of their radio emission [6,7], but only limited success was reported, for the pulses were difficult to detect above the background noise. As the fairly limited lateral spread of the radio signal become clear (a few hundred metres at a few tens of MHz [8]) it became apparent that the spacing of receivers required for air shower detection would be much less than that used by conventional particle detecting arrays,

and all hopes of detecting air showers purely by radio means were abandoned.

Despite this disappointment, interest in radio work was maintained. The reason for this is to be found in the other major question of high energy cosmic ray research: what is the composition of the primary particles?

Below about 10^{15} eV the cosmic ray primaries are abundant enough to be observed directly in detectors flown above the atmosphere, and these experiments show that near 10^{12} eV the majority of primaries are protons, with some (15%) helium and a small amount (about 2%) of heavier nuclei; at higher energies this heavy component appears to increase [9]. However, above 10^{15} eV the cosmic ray primaries are far too rare to be detected in this way, and so the nature of the primary must be inferred from measurements on the cascade of secondary particles (called an extensive air shower, EAS) produced as it traverses the atmosphere. One line of approach is based on the expectation that changes of composition will, inter alia, result in changes in the height at which the number of secondary particles reaches a maximum. As the maximum radio emission will come from this region, the resulting radio pulse, and particularly its lateral distribution is expected to show corresponding changes. It was this aim, that is, of identifying the nature of the primary cosmic rays by means of a study of the lateral distributions of the radio pulses produced by the resulting extensive air showers, that sustained the impetus in this research.

Two groups, at Haverah Park and Moscow, were at the forefront of this research; other groups made important contributions, particularly

to the understanding of the production mechanisms, but were in general handicapped by their limited shower detection facilities. The experiments were difficult, for the background noise masks many of the pulses, but in 1973 (eight years after the discovery), the work appeared to be reaching fruition, for both the Moscow and Haverah Park groups reported that variations in lateral distribution were apparently being observed [10, 11]. In 1975, the position was reversed: both groups announced their retirement from the field, (for reasons discussed in chapter 2), without being able to draw firm conclusions about the primary mass . After ten years of activity, the study of radio pulses from extensive air showers was abandoned [12].

1.2 Low Frequency Radio Emission from Extensive Air Showers

This project is not, however, concerned directly with either of these major questions, viz. the spectrum or composition, but with an apparent discrepancy between theory and experiment. The theory developed to explain the radio emission has successfully withstood many experimental tests at frequencies above 20 MHz [13]. However, below 6 MHz there have been several reports of high field strengths, very much greater than those observed above 20 MHz. These are in complete disagreement with the theory, which predicts that the field strength should approach zero at these low frequencies [14]. This project was conceived with the aim of resolving this paradox.

1.3 The Astrophysical Problem

As a tool for the investigation of the cosmic ray composition, noise

problems were expected to limit the usefulness of the technique to energies above about 10^{17} eV. This energy region is very interesting astrophysically. At low energies, direct measurement of such features of the cosmic ray flux as isotope ratios, and abundances of elements (particularly Li, Be and B) are possible, and have enabled estimates of the source composition, and the amount of interstellar material traversed by the cosmic rays to be made. With this data, and the fact that these cosmic rays can be constrained to the galaxy by magnetic fields, and given the number of plausible sources of the radiation (pulsars, supernovae, galactic nucleus, etc.) it is relatively easy, at least on general energetic grounds, to account for the observed cosmic ray flux [15]. (This does not, of course, make it easy to choose the right explanation.)

Theories of the origin of the cosmic ray component above about 10^{19} eV, however, have (in the past) all been faced with an apparent paradox, based on two experimental observations. They were firstly, that the energy spectrum apparently continued on above 10^{20} eV with no sign of a cut off [16], and secondly, that the flux was apparently isotropic [17].

The first observation was interpreted as evidence that the sources of these cosmic rays are relatively local (i.e. within about 4×10^{23}m) for they would otherwise have lost most of their energy through photo-meson production interactions with the microwave background (for proton primaries) or through photodisintegration (for heavy primaries) during the journey from their source [4].

On the other hand, the second observation seemed to preclude their origin in this galaxy. A proton will have a curved trajectory in the

interstellar magnetic field of about 3×10^{-10}T, but for an energy of 10^{20} eV its radius of curvature will be about 10^{21}m, and as this is large with respect to the galactic dimensions (cf. disk thickness $\sim 10^{19}$m) any departure from rectilinear propagation will be small. Therefore, as the sun is by no means in a central location in the galaxy, the sources would be presumed to be non-uniformly distributed around us, resulting in an anisotropic cosmic ray flux.

There were two generally popular explanations of this apparent paradox. The first was to assume that the cosmic rays do originate in the galaxy, and are subsequently trapped in its neighbourhood, becoming so mixed that any original anisotropy is lost [15]. The trapping is accomplished by magnetic fields, either in the galactic disk, or more probably, in a large region surrounding the galaxy (the galactic halo). The most severe problem of this theory is that it is difficult to confine the highest energy cosmic rays to the galaxy, even with a halo. The problem is considerably reduced, however, if the cosmic ray particles are heavy nuclei, for then their radius of curvature in the galactic field is reduced, by a factor equal to the atomic number, from that of a proton of equal energy. Here, then, was a powerful motive for the determination of primary mass, for if it could be shown that the ultra high energy particles were protons, a galactic containment theory would become untenable. Even with heavy primaries, however, galactic origin theories still face problems, particularly in regard to the diffusion of particles between the disk and halo, for it appears that only a small fraction of the cosmic rays which enter the halo from the disk will ever return to the disk [18].

For these and other reasons there was some support for an extra-galactic origin theory, where the bulk of the highest energy

cosmic rays originate outside our galaxy and propagate through inter-galactic space to us [18]. This theory also removed some of the problems of constructing a model of the acceleration processes, for now such active objects as radio galaxies or Seyfert nuclei could be postulated as sources, instead of our rather ordinary spiral galaxy. Its major drawback was that the amount of energy required to fill all of inter-galactic space with the cosmic ray density observed near the sun would be equivalent to about 3×10^{-4} of the total mass observed in galaxies [15], and it is difficult to imagine any mechanism which would be this efficient at producing relativistic particles. This criticism can be circumvented to some extent if it is assumed that the cosmic rays originate, and are to some extent trapped, in the local 'supercluster' of galaxies (the Virgo supercluster), for here the density of galaxies appears to be some ten times greater than the average 'universal' density and it appears that the number of active galaxies is sufficient to supply the required energy [19]. The centre of the Virgo Supercluster is close enough to allow high energy cosmic rays to reach us without significant attenuation from the microwave background.

These, then, were the main rival theories of cosmic ray origin during the period in which the techniques of radio observation of air showers were being developed, and a knowledge of the nature of the primary particles was considered of central importance in discriminating between them.

More recent observations have, however, removed the basis of much of the above speculation. In the first place, the distribution of cosmic ray arrival directions has been shown to be anisotropic. Measurements of the anisotropy were at variance with that predicted from theories

of the galactic magnetic field, but were at first considered to support a galactic origin theory [20]. However, more recent reports, that many of the highest energy particles come from near the galactic pole have strengthened the claims of an extra-galactic origin [21, 22].

This theory has also gained support from the observation that the cosmic ray energy spectrum, instead of continuing on with constant slope, as had previously been believed, flattened out above 10^{19} eV [23]. A very natural explanation of this effect is that there are two components to the flux, a galactic component with a steep spectrum and an extra-galactic component with flatter spectrum, which becomes dominant at energies above the point where these spectra intersect, i.e. about 10^{19} eV (Figure 1-2) [23]. It is, however, possible that the extra-galactic component remains dominant below 10^{19} eV; the 'ankle' being due to some characteristic of either the source, or the propagation through the intergalactic medium. As little is known of either, the mystery of the origin of high energy cosmic rays remains.

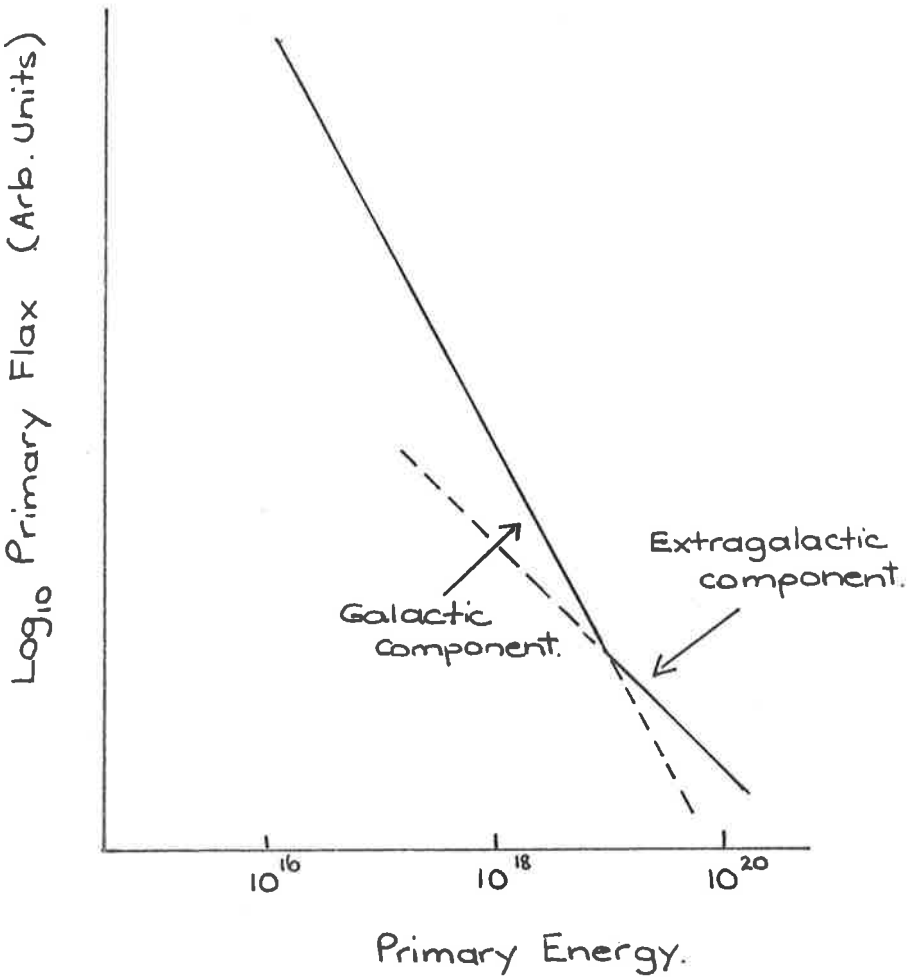

FIG 1·2

Possible explanation of the 'ankle' in the Cosmic Ray Spectrum, in terms of a 'two component' model.

CHAPTER TWO

RADIO EMISSION FROM AIR SHOWERS

2.1 Extensive air showers

The surface of the earth is shielded from the primary cosmic radiation by the atmosphere, the 'cosmic rays' observed at sea level being the result of (often very many) interactions in the atmosphere, initiated by the primary particle. Thus ground level studies must rely on a very complex, and at present incomplete, chain of reasoning in order to deduce the properties of the primaries from measurements of the 'secondary' particles. The missing steps in the argument lie mainly in the fields of high energy nuclear and particle physics, and although advances in the design and construction of particle accelerators are slowly allowing some of the gaps to be filled, it does not seem conceivable that machines could ever be constructed to enable the highest energy interactions to be studied directly. Instead, progress is made by the slow method of fitting theoretical predictions, and extrapolations of experimental data (often over many orders of magnitude), into self consistent models, which are then refined by experimental checks on their predictions.

Although the atmosphere masks the properties of the primary radiation, it also, paradoxically, provides the only practical method of observing the highest energy cosmic rays. Primary particles of

energy above 10^{17} eV are rare; even a detector with a sensitive area of 100 m^2 would only record one or two a year. However, the atmosphere is of sufficiently low density to enable the secondary particles to spread out significantly from the axis of the primary particle; at sea level, secondaries are found up to several kilometres from the axis of high energy primaries. These cascades of secondary particles or 'extensive air showers' (EAS) thus allow cosmic rays to be detected, over large areas, by means of coincidences between relatively few, widely spaced detectors.

As the goal of the study of radio pulses from EAS was the determination of the nature of the primary particles, the following sections, as well as providing a basis for the discussion of radio pulse production, will also outline some other approaches to this question.

2.1.1 The Nuclear Component

The first interaction of a cosmic ray particle with the atmosphere is a nuclear collision, between the primary particle (a proton or heavier nucleus) and a nucleus of oxygen or nitrogen in the air. The result is the emission of a number of high energy hadrons, which continue through the atmosphere, colliding with further atmospheric nuclei to produce more hadrons. This nuclear cascade is the core of the extensive air shower.

Practically none of the properties of the early, highest energy interactions are known precisely; even such basic parameters as the interaction cross sections, the energy lost in each interaction (the

inelasticity), the number of secondaries produced (the multiplicity), their nature, energy spectrum, and transverse momentum are all the subject of debate.

As the primary retains a sizeable fraction of its energy after each interaction (the inelasticity is about 0.5 [1]), its interactions govern the way in which energy flows to the shower secondaries, and hence the overall build up and decay of the shower. In the early stages, while the energy of the primary remains high, large amounts of energy are transferred to the secondaries at each interaction, and so the particle numbers increase (by means of the multiplication processes discussed later). Eventually the primary energy falls to a level at which the energy transferred to the secondaries is no longer sufficient to maintain their numbers in the face of losses by ionisation, etc., and the shower begins to decay. A higher energy primary will be able to sustain the build up of secondaries longer, and so the region of maximum shower development will be deeper in the atmosphere. (This increase in depth of maximum is about 50 to 90 gr cm^{-2} per decade of energy [2, 3].)

If we now compare the shower produced by a primary proton, with that produced by a heavy nucleus (say iron), of the same energy, we see that as the first interactions of the heavy nucleus essentially break it up into its constituents, the resulting shower consists of a large number of superimposed cascades [4], each carrying only a fraction of the primary energy. Thus the resulting shower will reach maximum development much higher in the atmosphere than the corresponding proton initiated shower [5].

As well as this difference in mean behaviour of the showers, the way

in which individual showers vary from the mean is also, to some extent, characteristic of the primary mass. The interaction length for a proton is about 80 gr. cm^{-2}, or approximately one-twelfth of the atmosphere. There is an appreciable probability that the first interaction will not occur until after 3 interaction lengths, and thus the development of the shower can be delayed by as much as one quarter of the atmosphere. The interaction length for a heavy primary is much less however, and the resulting fluctuations in shower maximum will not exceed 10% of the atmosphere [6]. This variation in depth of shower maximum is the basis of many attempts to determine the primary composition, in particular by means of studies of the Cerenkov light or radio pulses emitted by showers.

The multiplicity is also important in determining the flow of energy to the secondaries, and hence shower development, but there is probably more dispute over this parameter than any of the others. Some theoretical considerations [7] favour a logarithmic dependence of multiplicity on incident particle energy, and models of air showers have been produced with this basis [8], but other assumptions, including heavy primaries have been necessary to obtain agreement with experiment. Other models, with multiplicity rising as $E^{0.25}$ (CKP model), or as quickly as the square root of energy have been used [2,10]. These high multiplicity models [with predominantly proton primaries] are currently favoured [11], but by no means unanimously. Figure 2-1 illustrates some of the combinations of multiplicity and primary composition favoured at the last International Conference on Cosmic Rays (from Gaisser [12]).

Because of their relatively large masses and energies, the nuclear active particles do not move very far from the axis of the primary

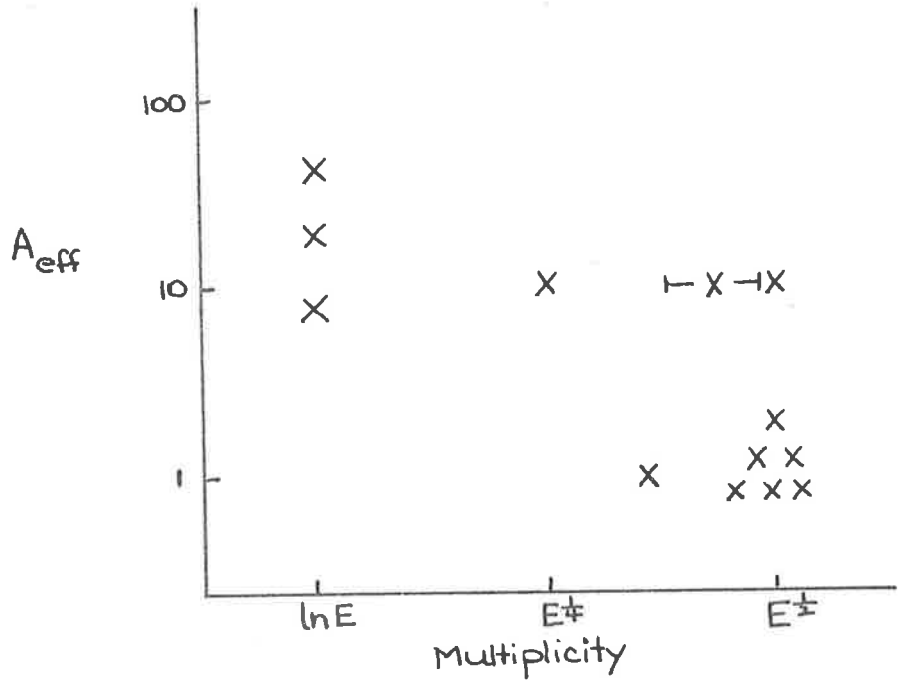

FIG 2·1 Combinations of particle physics and primary composition put forward at 15th ICCR

[After T·K Gaisser, Rapporteur paper 15th ICCR.]

particle, most of them being found within 3m of the axis. However, if the primary is a heavy nucleus, it is possible that the initial spallation reaction could result in two or more almost coaxial showers, resulting in several sub-cores being found in the nuclear cascade. Such sub-cores have been found, but there is dispute over their frequency, and interpretation [13, 14, 15].

One property of the nuclear cascade which is expected to be strongly dependent on the nature of the primaries is the energy spectrum of the hadrons [16]. Heavy initiated showers are expected to be deficient in high energy hadrons, compared to a proton initiated shower of the same energy, as a direct consequence of the heavy primaries' lower energy per nucleon. The experimental evidence at energies near 10^{16} eV would appear to favour proton primaries [11].

There are many species of nucleons, antinucleons, excited baryons, and mesons in the nuclear cascade, but the most important are the pions, for not only are they expected to be most numerous, but they also form the link with the other two components of the shower.

2.1.2 The Electromagnetic Component

Neutral pions decay very rapidly, their half-life being 10^{-16} seconds. Thus very few interact with the atmosphere, almost all of them decay, to two gamma rays. Each gamma ray initiates an electromagnetic cascade, in which the particle numbers increase by the repeated processes of pair production, producing an electron-positron pair from a gamma ray, and brehmsstrahlung, where an electron is scattered, and a gamma ray produced. The mean free path is about 40

g cm^{-2} for both of these processes, and is called the radiation length. The particle numbers continue increasing, and their energy decreasing, until the energy loss processes of ionisation and Compton scattering become important at energies below 100 MeV. The particle multiplication processes then become less important, and the cascade begins to die out. The multiplication processes are so efficient that, at shower maximum, the electromagnetic component comprises some 90% of the total particle number [17].

In contrast to the nuclear cascade, the processes involved in the electromagnetic cascade are well understood, and the properties of the cascade can be determined either through a (semi-analytic) solution of the 'diffusion equations' [18], or by means of a computer based Monte Carlo simultion of the shower [19]. However, the complexity of the calculation is such that, despite this firm basis, there is disagreement about such fundamental parameters as the cascade width [20].

The nuclear core of the shower is continually initiating these cascades, as it moves down through the atmosphere, so that the electromagnetic component of the shower consists of many overlapping cascades. The number of particles at the cascade maximum is proportional to the energy of the initiating gamma ray, and the cascade builds up rapidly to this maximum. The particle numbers in an air shower thus follow fairly closely the flow of energy from the nuclear core, building up to a maximum, then decaying. This shower maximum occurs well above sea level (for all but the highest energy showers) and the decay length is about 200 g cm^{-2} [17]. Thus, for a given primary energy, fluctuations in shower development of this order (as expected for proton initiated showers) will result in large

fluctuations in the sea level particle number [21]. (This may introduce undesirable selection effects into experiments searching for such fluctuations, for those showers exceeding a certain particle number at sea level will be preferentially late developing.)

The number of particles at a particular altitude is governed by the above factors; their distribution about the shower axis is determined by scattering from atmospheric atoms.

The mean scattering angle increases rapidly as the electron energy falls below 100 MeV, so the more energetic electrons stay closer to the core than those with less energy. The resulting distribution is generally represented by the 'NKG' formula [17]; this is a function of the shower 'age', that is, the position in the shower development curve, for in the early development, the mean particle energy is high, and thus the scattering is small, compared with later stages. It is also a function of altitude, for at high altitude the low air density allows the particles to move further from the axis before interacting.

Multiple scattering causes the particles to follow a more or less zig-zag path, thus as well as a lateral displacement, a scattered particle will have a longitudinal lag behind an unscattered particle. Again, this lag is more pronounced at low energies and high altitudes.

The nett result of this scattering is that the electromagnetic cascade takes up the form of a shallow dish as it moves down through the air; at sea level it is typically 100 m across and 5 m thick, with a radius of curvature of about a kilometre. The highest energy particles are concentrated at the front of the disk, and near the axis.

2.1.3 The Muon Component

At sea level, 10-20% of the particles in an air shower are muons, produced by the decay of charged pions and, to a lesser extent, kaons [17]. Muons have a very long interaction length, and so after production travel to the ground virtually unchanged. Thus they are capable of carrying information about the early stages of the nuclear cascade.

The interaction length of a pion is about 120 gr cm^{-2}, and this is about the amount of atmosphere that a $3x10^{10}$ eV pion, at an altitude of 5km, will traverse in its (time dilated) decay half life. Higher energy pions will be more likely to interact; lower energy pions will usually decay. High energy muons will generally be produced early in the shower, not only because of the higher hadron energies, but also because the lower air density reduces the pion interaction probability.

As the muon flux observed at sea level is essentially an integral of the muon production over the whole path of the shower through the atmosphere, the effect of fluctuations in shower development is much less than for the other components. In particular it has been shown that the muon density several hundred metres from the core is relatively insensitive to the primary mass, the details of the nuclear interactions, and to fluctuations, and so provides a reliable index of primary energy [22].

The muon component provides several approaches to the determination of shower development and primary composition. As the total number of

shower particles (mainly electrons) is decreasing rapidly at sea level (for all but the largest showers), while the muon number, as noted above is fairly constant, the ratio of muons to electrons is a measure of the height of shower maximum; a higher than usual proportion of muons indicates that the electron number has decayed further from maximum, and hence that the maximum was higher. This ratio has been extensively used by the Moscow University group, to assist in interpreting changes of radio lateral distribution in terms of height of shower maximum [23]. This effect will be somewhat enhanced for high energy muons, as they will be preferentially produced in showers developing early, where the air density is lower, as noted previously [16]. The very highest energy muons may have a significant fraction of the primary energy, and so would be expected to be relatively deficient in heavy primary showers, where the primary energy must be shared between a number of nucleons [24]. Unfortunately, however, this effect appears to be sensitive to the nuclear interaction parameters [11].

Another, conceptually very direct approach, which is made possible by the long interaction length and low scattering of the muons, is to trace their trajectories back to the shower axis, and so determine their height of origin [25]. Similar information is contained in the lateral distribution, for, if the mean production angle relative to the shower axis remains constant, muons produced high in the atmosphere will tend to be found far from the core. Unfortunately, the most useful information is carried by the high energy muons, and experimental data for these is sparse [11].

2.2 Radio Emission from Air Showers

The possibility of radio emission from air showers was considered by Jelley [26], who investigated the extension of Cerenkov emission from showers, previously detected in the optical region, into the radio bands. His conclusion was that no radio signal could be observed, since as the shower was electrically neutral (at least on scales greater than a wavelength at radio frequencies), the contributions from positive and negative charges would cancel out. For any significant radio signal to be produced, some mechanism had to break the charge balance of the shower. Several such mechanisms have been found and will be discussed in following sections.

There are two general approaches to the calculation of the radio field produced by some mechanism. The first, which might be termed a 'macroscopic' approach is to calculate, for the shower as a whole, the electrical characteristics which the mechanism produces, and then to solve Maxwell's equations for this distribution of charge and current. This was the approach used by Kahn and Lerche [27], in the first estimate of the field produced by the geomagnetic mechanism (see Section 2.2.3). The second approach, is a 'microscopic' one; the field produced by each shower particle is calculated separately, and then these fields are summed to find the resultant at the point of observation. This approach has been used extensively by Allan [28] and his colleagues [29,30].

The macroscopic approach suffers from the disadvantage that a large number of shower properties (for example the particle numbers and energies, and how these change with core distance, lag behind the leading particle, and altitude) must all be calculated and parametised

before they may be used. As these properties are generally calculated by using computer simulations to trace the histories of all shower particles (or a statistically significant fraction of them) through the atmosphere, it is relatively convenient to use the microscopic approach by including the contribution of each particle to the field in this calculation. This technique has been used to give the most complete treatment of the problem, and as it illustrates the direct links between shower particle motions and the resultant field, it will be discussed here.

2.2.1 Radio Emission from a Single Charged Particle

The most suitable formulation of electromagnetic theory for this purpose is that given by Feynman [31]; the field observed at a point, due to a charge q, a distance $\underset{\sim}{r} = r\hat{\underset{\sim}{r}}$ from the point is (in vacuo)

$$E = -\frac{q}{4\pi\epsilon_0}\left(\frac{\hat{\underset{\sim}{r}}}{r^2} + \frac{\hat{r}}{c}\frac{d}{dt}\left(\frac{\hat{\underset{\sim}{r}}}{r^2}\right) + \frac{1}{c^2}\frac{d^2}{dt^2}\hat{\underset{\sim}{r}}\right) \quad (1)$$

where the differentiation is with respect to the 'retarded time', i.e. the time at which the motion is observed by an observer at the field point. In the case of relativistic particles the first two terms are small, and so the field at a point reduces to

$$E = -\frac{q}{4\pi\epsilon_0}\left(\frac{1}{c^2}\frac{d^2}{dt^2}\hat{\underset{\sim}{r}}\right) \quad (2)$$

where the differentiation is again with respect to the retarded time. The term $\frac{d^2}{dt^2}\hat{\underset{\sim}{r}}$ is thus the apparent angular acceleration of the charge, as observed from the field point. The field calculated in this way includes both the 'near field' and 'far field' components of more conventional treatments [32]. Allan uses this equation as the basis of all his theoretical studies of radio pulse production and also shows that it produces 'correct' results for special cases such as Cerenkov radiation [28].

As an example of its use, consider the radiation from a short length of particle track, i.e. a particle initially at rest, which is suddenly accelerated, and moves a short distance (l) with velocity $v \approx c$, before being abruptly stopped. (An air shower model could be assembled from suitable selection of such tracks.) Suppose that during the motion, the angular displacement of the particle as observed at a point is $\delta\theta$, and that this point is sufficiently far from the particle that the angular velocity of the particle $\dot{\theta}$ appears constant during its motion [28].

The postulated infinite angular acceleration of the charge makes the direct application of equation (2) meaningless, but we can calculate the magnitude of the impulse in the electric field thus

$$\int \mathcal{E}\, dt = \frac{-q}{4\pi\epsilon_0 c^2} \int \ddot{\theta}\, dt$$

$$= \frac{-q}{4\pi\epsilon_0 c^2}\, \dot{\theta} \qquad (3)$$

No field will be observed while the particle is moving ($\dot{\theta}$ = constant) but the decelaration of the particle will produce an impulse, equal to that of equation (3), but of opposite sign. We can calculate the frequency spectrum ($\mathcal{E}_{(\nu)}$) of each of these impulses [33] using the Fourier transform

$$\mathcal{E}_{(\nu)} = \int_{-\infty}^{\infty} \mathcal{E}(t)\, e^{2\pi i \nu t}\, d\nu \qquad (4)$$

as $\mathcal{E}(t)$ is a delta function, and using positive frequencies only, we obtain

$$\mathcal{E}_{(\nu)} = 2\int_0^\infty \mathcal{E}(t)\,dt$$

thus from (3)

$$\mathcal{E}_{(\nu)} = \frac{q\nu}{2\pi\varepsilon_0 c^2}\,\dot{\theta} \qquad (5)$$

If the impulses are observed at the field point to be separated by a time τ, then provided $\tau \ll \frac{1}{2\pi\nu}$, we can add their contributions vectorially, and obtain

$$\mathcal{E}_{(\nu)} = \frac{q\nu}{2\pi\varepsilon_0 c^2}\,\dot{\theta}\,(2\pi\tau\nu)$$

that is,

$$\mathcal{E}_{(\nu)} = \frac{q\nu}{\varepsilon_0 c^2}\,\nu\delta\theta$$

, provided $\nu \ll \frac{1}{2\pi\tau}$ (6)

(The condition is satisfied for most particles in an air shower at frequencies below 100 M Hz.)

This result, a spectrum rising linearly with frequency, will be used in the following section.

2.2.2 Radiation from a Shower

This method can be extended to a complete shower. The technique used is to calculate the deflection of each particle in the shower, expressed as the angular displacement observed from the antenna. The nett angular displacement of charge is then calculated, as a function of the time at which the displacement is observed. This function is

then differentiated twice, to obtain the electric field as a function of (observed) time, and the frequency spectrum may be calculated by means of a Fourier transform [30, 34, 35].

We can generalise this approach somewhat, to obtain a qualitative estimate of the spectrum of the radiation, assuming that the signal is produced by the relativistic particles of the shower disk, but without knowing the details of the mechanism responsible for the deflections. Let us assume only that every particle makes the same contribution to the total charge deflection.

Suppose the geometry is as in Figure 2.2, where AB is the shower axis, and the antenna is at 0, say 100 m from the core. For showers of primary energy below about 10^{18} eV most of the particles in the shower are at heights above about 2 km, and all particles in this region will be observed almost simultaneously, as the path lengths $X_1 0$ AND $X_1 X_2 0$ are almost equal. However, as the shower nears the ground, the delays between successive points on the shower axis will increase ($Y_1 Y_2 0$ is significantly larger than $Y_1 0$). Particles in the last few hundred metres above the ground will be observed over a period of several hundred nanoseconds. The build-up of charge displacement, observed from 0 will then be of the form shown in Figure 2.3(a); most of the displacement will be observed in the first few tens of nanoseconds, although it will continue to increase slowly for several hundred nanoseconds. We now differentiate twice, to obtain the angular acceleration of the charge, and hence the electromagnetic pulse; it will be of the form shown in Figure 2.3(b), that is, a narrow pulse, followed by a long overswing. The areas of the two parts of the pulse will be equal.

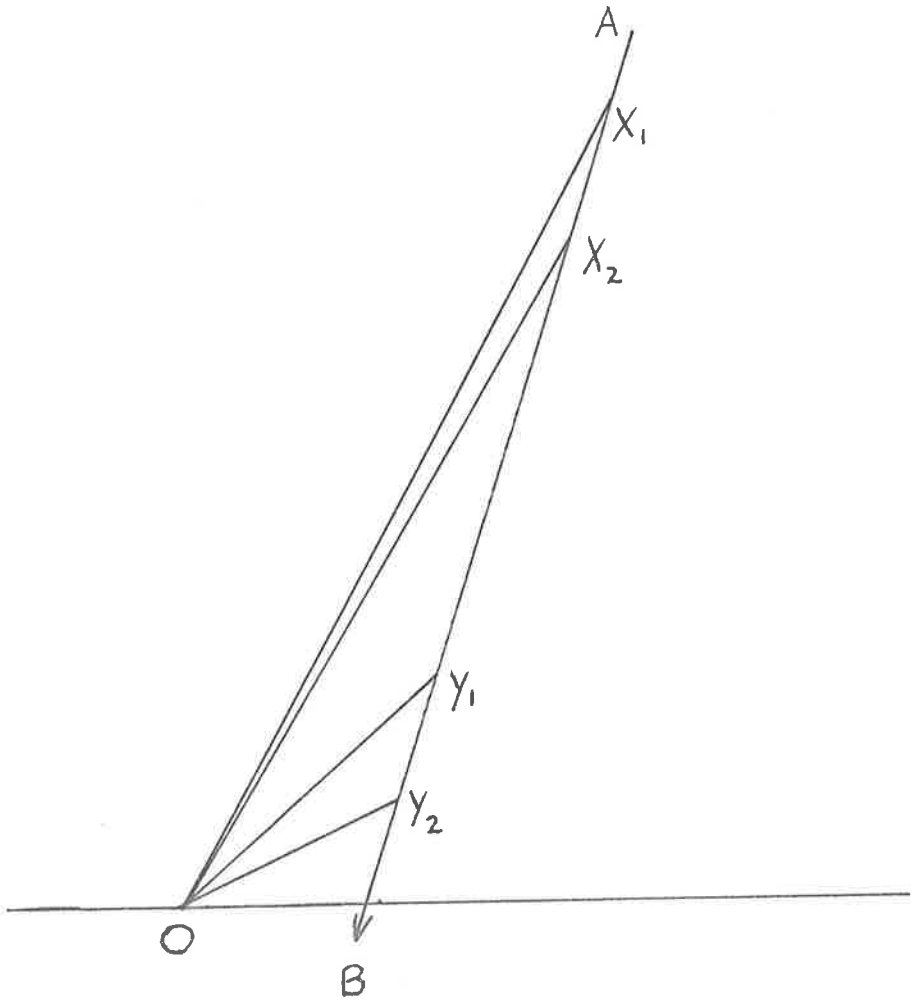

FIG 2·2 Geometry for calculation of the radio pulse from a shower.

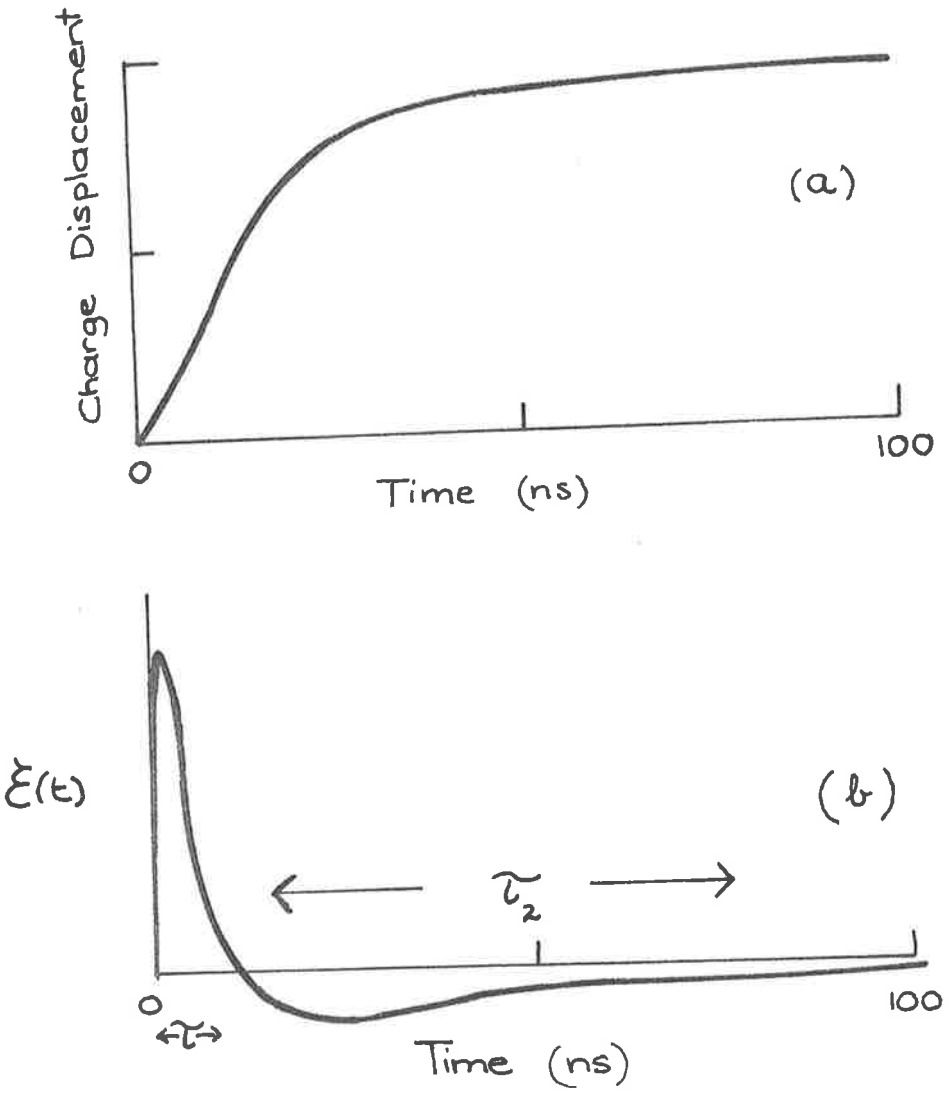

FIG 2·3

Build up of charge displacement, and resulting radio pulse waveform. (schematic.)

We can now estimate the frequency spectrum of this pulse. At very low frequencies, much less than $\nu_2 = \frac{1}{2\pi\tau_2}$, where τ_2 is the timescale of the overswing, both parts of the pulse will appear as narrow impulses; and so the overall pulse will be similar to that in the previous section. The spectrum will thus be similar, that is, rising linearly with frequency. At frequencies higher than ν_2, but less than $\nu_1 = \frac{1}{2\pi\tau_1}$ where τ_1 is the width of the first part of the pulse, the overswing is too slow to be observed, so only the first part of the pulse appears as an impulse. The spectrum in this region is thus approximately that of an impulse, that is, flat. At still higher frequencies, greater than ν_1 the initial pulse no longer appears as an impulse, and so the spectrum falls. The spectrum thus obtained is illustrated in Figure 2.4.

The detailed shape of the pulse, and thus the values of ν_1, ν_2 will depend on the details of the deflection mechanism (for example, in a mechanism where only the highest energy particles contribute, the initial pulse would be narrower, and the overswing shorter), but the values cannot be too far from those found here, from simple geometry, that is, $\nu_1 \approx 30$ MHz, $\nu_2 \approx 3$ MHz. (Allan finds [35], for the geomagnetic mechanism (see Section 3.2.2.2), $\nu_1 \approx 50$ MHz, $\nu_2 \approx 8$ MHz, and for charge excess (Section 3.2.2.1) $\nu_1 \approx 25$ MHz, $\nu_2 \approx 3$ MHz.)

We conclude that, if the radiation is produced by the shower particles, the spectrum must be of the form above, that is, flat between a few MHz and a few tens of MHz, and falling on either side. In particular, it must be monotonically rising from zero to at least 3 MHz.

2.2.3 Mechanisms of Charge Separation

As we have noted, the detailed neutrality of a shower would preclude the production of a radio pulse. In the terminology of the previous section, the nett charge displacement would be zero, as the movements of the positive charges would be exactly balanced by those of the equal number of negative charges. In this section, the main mechanisms responsible for breaking this nexus are examined, and in Section 2.3 The application of the resulting radio pulses will be discussed.

2.2.3.1 The Charge Excess Mechanism

Askaryan [36] was the first to suggest that, because of the annihilation of positrons in flight, an air shower would be expected to have an overall negative charge. Although this mechanism does contribute to an excess of negative charge, much larger contributions have been found to come from electrons produced in Compton collisions between shower photons and atmospheric atoms, and 'knock-on' electrons produced after an electron collides with an atom. Calculations by Fujii and Nishimura [37] show that this negative excess ranges from 1% for 100 MeV electrons to 20% at 2 MeV. Overall it is about 10%. Only 10% of this figure is due to positron annihilation.

Radiation from this mechanism can only be observed away from the shower axis, for on the axis, symmetry ensures that the nett charge displacement observed will be zero.

2.2.3.2 The Geomagnetic Deflection Mechanism

Askaryan [36] also pointed out an additional way in which the charge symmetry of a shower could be broken; as the shower moves through the atmosphere the earth's magnetic field will deflect the positive particles to one side of the shower, and negative particles to the other. As a result, the shower will acquire a dipole moment, which will radiate as it extends downwards at relativistic speed. Kahn and Lerche [27] investigated this mechanism and showed that it would produce significant radiation, but the main contribution was from the geomagnetically induced currents which produce the dipole rather than the dipole itself. Further calculations, by Castagnoli [38], and Fujii and Nishimura [39] confirmed the importance of the geomagnetic mechanism in the frequency range 10-100 MHz.

As the deflection is produced by the Lorenz force $\underline{V} \times \underline{B}$ where $\underline{V}$ is the particle velocity and $\underline{B}$ the magnetic field, the resulting radio pulse is proportional to the sine of the angle between these vectors. This relationship, and the predicted polarisation of the pulses (i.e. parallel to the deflection) have been used to confirm the importance of the mechanism [40, 41, 42].

There is, however, disagreement on the relative contribution of the charge excess, and geomagnetic mechanisms. Early estimates of a 90% geomagnetic component [39] appeared confirmed at 22 MHz [41], but more recent calcultions by Allan [35] estimate the charge excess component to be 30% in this frequency region, while Shutie [30] estimates that below 30 MHz charge excess exceeds geomagnetic.

This confusion would appear to be associated with the fact that the charge displacement due to the charge excess mechanism is mainly associated with low energy particles. These low energy particles produce difficulties in the calcultions, for the approximations used become poorer as the energy falls [30].

2.2.3.3 Geo-electric Mechanisms

A vertical electric field, which can vary from about 100 V/m in fine weather, to 10^4 V/m below thunderclouds is generally maintained in the atmosphere [43]. This field has the capacity to separate positive and negative charges in a shower, and so has been suggested as a possible mechanism of radio pulse production [44, 45].

For vertical showers, the positrons will be accelerated, and electrons retarded. The effect is slight (the separation is about 1 mm [45]) and as the deflections are in the approximate direction of the antenna, the angular deflection, and consequent radiation, is minimal. However, for showers with large zenith angles, the deflection is transverse, and the effect is analogous to the geomagnetic case although the deflections are in general much less. For fields greater than about 6×10^3 V/m, however, the deflection will be comparable to the geomagnetic [45] and so for fields above this, for example in thunderstorms, the geoelectric effect will be dominant.

Besides its effect on the relativistic electrons of the shower, the geoelectric field may produce important effects on the low energy electrons produced by ionisation [44]. There are very large numbers

of these; as ionisation in the atmosphere is one of the major energy loss processes for the shower, and as about 30 eV is required to produce each ion pair, about 10^{15} slow electrons will be produced by a 10^{17} eV shower.

The acceleration of this electron swarm by the earth's electric field has two aspects which make it an attractive possible mechanism for the production of low frequency radio pulses. Firstly, the low drift velocity of the electrons gives hope that the resulting radio pulse would be long enough to produce the observed spectrum (i.e. > 10 μs) and secondly the observed variability of the low frequency pulses might be explained by the variable nature of the geoelectric field or possibly by changes in the mobility or lifetime of the electrons due to changes in atmospheric conditions.

The first calculation of this effect was by Charman [45] who calculated the accelerations of the ionisation electrons in the geoelectric field, and then using the technique outlined in the previous sections, estimated that the field at 10 MHz, from an inclined shower might be as large as that produced by the charge excess or geomagnetic mechanisms.

A more complete analysis was made by Sivaprasad [46]. Three aspects of the behaviour of the electrons were considered, namely the "thermalisation" of the electrons, from their initial energy of about 30 eV to about .03 eV, in a time of about 10^{-10} secs.; the subsequent acceleration of the electrons in the geoelectric field, which occur over a time

of 10-20 ns, and results in a drift velocity of about 150 m s^{-1}; and finally the exponential depletion of the electron swarm, chiefly by attachment of O_2 molecules, which occurs with a time constant of about 10 ns. The field produced by these electron motions was calculated by integrating the contributions from each particle, with due allowance for the time of observation.

The short lifetime of the electrons means that the resulting pulse is narrow, the main contribution to its length being due to the transit time of the radiation across the disk of the shower, i.e. about 250 ns. The mechanism is thus unable to explain the shape of the low frequency spectrum, and in addition a detailed calculation shows that the magnitude of the signal will be only about 10% of that produced by the geomagnetic mechanism; far less than the observed fields.

A further effect which might produce a signal in a radio receiver, is the discharge of a static charge, induced on the antenna by the atmospheric field, by the ionisation of the shower. When an antenna is well insulated from the ground, it will take up the potential of the surrounding air - that is, approximately 100 V for an antenna 1m from the ground. If the field is discharged by the ionisation of the shower, the antenna potential will drop. This effect has been observed by Curry et al. [47], using a large, flat plate as antenna. However, the typical input impedance of a radio receiver is so low (about 50Ω), compared with the equivalent source impedance of the electric field-antenna combination (about $10^{14}\Omega$ [48])

that the antenna would be effectively grounded, and no changes would be seen. In any case, the expected time constant of any change in the field is of the order of 10s [47]; far too long to be detectable at radio frequencies.

In summary, then, under normal conditions the geoelectric field is not expected to produce pulses as large as those from the geomagnetic mechanism. However there is some experimental evidence for geoelectric charge separation under disturbed conditions. Anomalously large pulses have been recorded in several experiments, during nearby thunderstorm activity, and have been attributed to a geoelectric mechanism [23, 49, 50, 51].

2.2.3.4 Other Radiation Mechanisms

Many other mechanisms for the production of radio signals from showers have been considered, and a list of them has been compiled by Jelly [52]. Some of these are included naturally in the treatment of Allan (e.g. bremsstrahlung can be considered as resulting from the concatenation of two slightly inclined particle tracks (Section 2.2.1), synchrotron radiation is a special case of magnetic deflection); none of them will produce fields nearly as large as those resulting from the geomagnetic mechanism. However, as the fraction of shower energy converted into a radio pulse is very low (about 10^{-12} for the geomagnetic mechanism), there would appear to be ample opportunity for some other mechanism to be over-looked, because of its apparent inefficiency, although it could still be capable of producing large pulses. In the following chapters, evidence that this is indeed the case will be presented.

2.3 Determination of Primary Mass by Radio Methods

We now return to a more detailed consideration of the results of the underlying quest - the determination of the nature of the primary particles.

As has been noted, the radio technique approaches this problem through the measurement of variations in the height of shower maximum. The variations in the height of maximum are reflected in variations in lateral distribution, for the lateral distribution is the diffraction pattern produced by the source distribution, the most important feature of which is the height of maximum [50]. As the maximum moves deeper in the atmosphere, the diffraction pattern on the ground will contract, thus later development of a shower will result in a steeper radio lateral distribution.

This connection has been investigated quantitatively by Allan and his colleagues [30, 34, 35]. Their results differ somewhat over some details of the lateral distribution, but are in agreement over the important features. They find that, while the field strength in the region 50 to 100 m from the core is relatively insensitive to fluctuations, an increase of 100 gr cm^{-2} in depth of shower maximum results in a decrease in the field strength at 200 m by a factor of about 1.5, and by a factor of 2 at 300 m. The experimental task is to detect these fluctuations in the presence of background noise, uncertainties of shower analysis,drifts in receiver gain, and possibly other, unidentified, radiation mechanisms.

The experimental requirements are thus an array which can detect and analyse showers large enough to produce radio signals well above

background noise, and an array of radio receivers which can measure the radio pulse lateral distribution of single showers out to distances beyond 200 m. Only two groups, Moscow State University [23] and an Imperial College - University of Leeds collaboration (working at Haverah Park) [50] have had these resources. Both have abandoned the quest, but for different reasons.

The Moscow group has made extensive use of its detecting array to confirm the dominance of the geomagnetic mechanism, and to demonstrate the dependence of radio lateral distribution on such indicators of shower development as the muon-electron ratio. They claim to observe fluctuations in lateral distribution, and thus infer the presence of protons in the primary flux, but conclude that the theoretical basis is not sound enough to enable further deductions to be made [23].

On the other hand, the Haverah Park group appear confident of their theoretical foundations, but find that, in the important region beyond 200 m from the core, the fields are too low, in relation to the background noise, to allow the lateral distribution to be measured reliably [50].

It is difficult to understand this difference of opinion, as it would appear that the Haverah Park experiment is more sensitive; the showers detected at Haverah Park are of higher energy, and it would be unlikely that the background noise at Moscow State University, in a semi-industrial suburb of Moscow, would be significantly lower than that at rural Haverah Park. But, for whatever reasons, these investigations have been concluded, and, apart from a suggestion that there is a proton component in the flux near 10^{17} eV, they have not added to our knowledge of the nature of the primary cosmic radiation.

2.4 Optical Cerenkov Techniques

One of the factors contributing to the abandonment of radio studies of showers was the development of promising alternative techniques of determining the primary composition. Of these the most direct competitor was the Cerenkov technique. Most of the particles in a shower have energies above the Cerenkov threshold (about 20 MeV at sea level) and the resulting light pulse from a shower is readily observable under suitable conditions (i.e. clear, moonless nights). Detailed calculations have shown that, as in the case of the radio pulse, the lateral distribution depends on the height of shower maximum, but in addition, the shape of the pulse is also dependent on the shower development [53, 54]. One particularly elegant technique uses the pulse profiles from several detectors to trace the development of the shower through the atmosphere, without the need to observe the shower particles [55]. Thus the Cerenkov technique is capable of obtaining all the information that might be available through radio methods, but allows a wider range of experimental approaches to the problem.

The main drawback to the use of the technique is the limited time available for observation. However, when conditions are suitable, the pulses are relatively free of interference, and can be observed with simple, reliable equipment. The relatively high Cerenkov threshold is an advantage in calculations, for the low energy particles, so troublesome in the radio calculations, may be safely neglected. These advantages undoubtedly contributed to the demise of the radio technique.

CHAPTER THREE

THE BUCKLAND PARK EXTENSIVE AIR SHOWER DETECTOR

3.1 Introduction

The basis of a study of EAS associated phenomena is the EAS detector. Its ability to detect suitable showers, and estimate their parameters, sets a limit to the experiments that can be performed, and the accuracy of the results obtained.

The array used for these investigations was originally installed at Penticton, British Columbia. It was transferred to Adelaide, and installed at Buckland Park, about 40 km north of the city, in 1972. Since then it has been extended and improved, and currently comprises 11 detectors, with an enclosed area of about 30000 sq.m.

Although originally modelled on the Kiel array [1] no work had been done to determine the properties of the array, or the optimum methods of using it. The author was involved in the setting up of the array at Buckland Park, and designed and built the recording system. Subsequently he was responsible for the data analysis, and designed and built an improved and more extensive recording system. Some work was also done to determine the array properties and the best way of increasing the array's collecting area.

3.2 The Original Array

3.2.1 Detectors

The original array consisted of eight detectors, arranged as shown in Figure 3-1. Each detector was a 1 metre square, 5 cm thick sheet of NE102 scintillator, housed in a light-tight box, and viewed from below by one or two photomultipliers. The detectors at sites A, B, C, D and E comprised the 'fast array' and were fitted with a Phillips XP1040 photomultiplier; the resulting fast signals (rise time $\approx$ 4 ns) were used for determining the shower arrival direction, by fast timing [2]. The detectors F, G, H, and also A and D above were fitted with RCA 8055 tubes, with charge sensitive pre-amplifiers, and used for measuring the particle densities; they comprised the 'slow array'. All power supply and signal cables were brought back (underground) to the caravan C1, where the recording apparatus was housed.

3.2.2 Recording System

The original recording system is now obsolete, having been replaced by the equipment described in Section 3.3. However, as the original system was used in the experiments described in Chapters 4 and 5, it is described briefly here.

3.2.2.1 Coincidence Registration

The arrival of a shower is recognised by the coincidental detection of particles in several detectors. The simplest coincidence used was

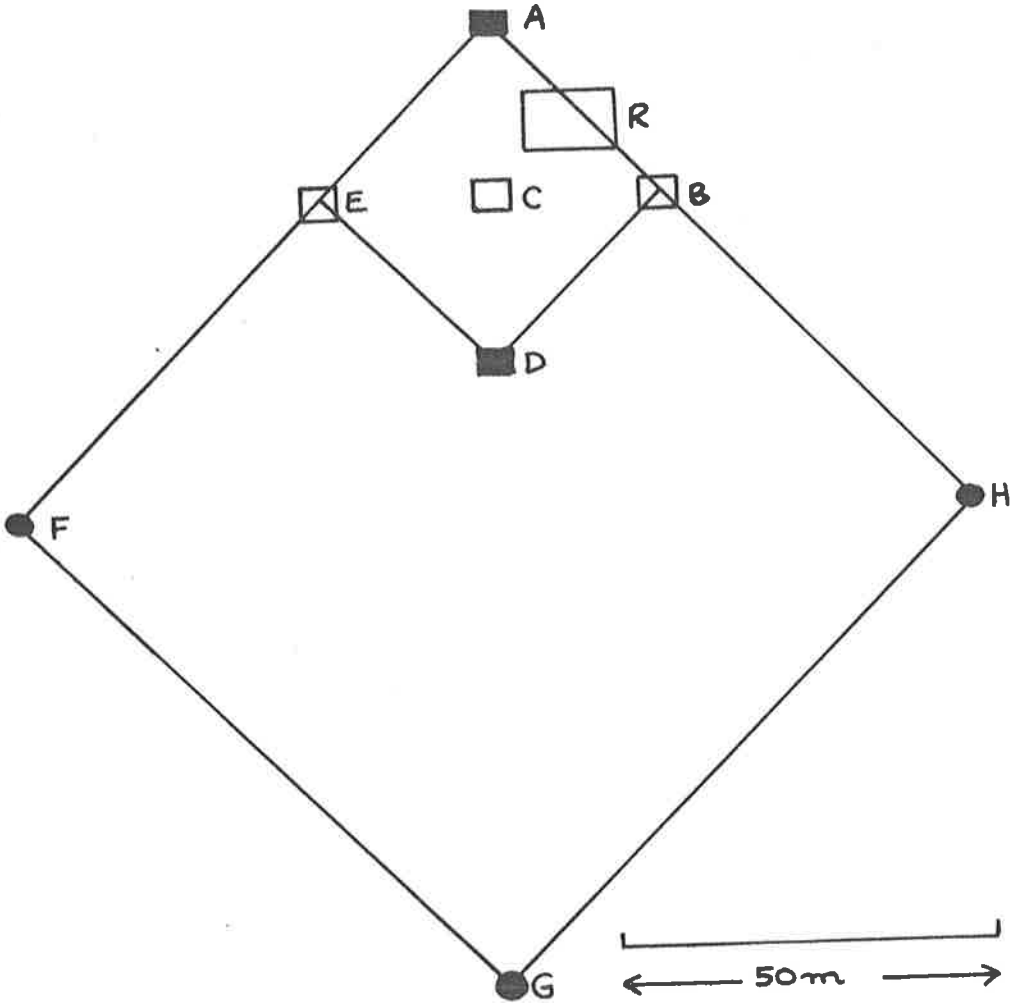

FIG 3·1 The Original Detecting Array.

□ - Fast timing detectors.

● - Particle density detectors.

■ - Fast timing and particle density detectors.

R - Recording caravan.

between C (the 'centre fast') and all four of A, B, D and E; this 'fast trigger' ensured that enough times were recorded to enable the shower direction to be over-determined. When used with thresholds of about 3 particles, this produced about 20 triggers per hour, the minimum shower size being about 8×10^4 particles. Usually a 'slow coincidence' was also required, generally any two of F, G and H at the 3 particle level, as this ensured that enough data was available to estimate the shower size and core location. The detection rate was then about 6 per hour, with a minimum size of about 1.5×10^5 particles.

3.2.2.2 Fast Timing

The relative arrival times of the shower front at the five 'fast' detectors were determined using four LRS model 108H time-to-height converters (THC). The signal from the centre fast discriminator (C) was used to supply a START to these devices, and STOP signals were obtained from the discriminators attached to the outer fast sites (i.e. A, B, D, E). (Suitable delays were inserted to ensure that a STOP could not occur before the START.) A START was obtained from every centre fast pulse; if this was not accompanied by a shower (i.e. a fast or slow coincidence) the THC's were reset. If no reset occurred, the THC's held an analogue voltage level, proportional to the time delays between START and STOP, and thus representing the difference between the shower arrival at C, and at the outer fast detectors.

3.2.2.3 Density Measurement

The amplitudes of the pulses from sites A, D, F, G and H,

representing the particle densities at these sites were recorded using EG-G AD128 A/N analogue to digital converters (ADC). Each site was connected to two ADC's, one directly, and one via a 20dB attenuator. In this way, the dynamic range of the system was extended to about 500-1.

Digitization was initiated by the fast coincidence pulse; suitable delays were inserted to ensure that the ADC's measured the peak amplitude of the density pulses.

3.2.2.4 Magnetic Tape Recording

When installed in Canada, the time and density data was punched on paper tape. However, a seven track digital tape recorder (P.I. model 1387) was to be used at Buckland Park, and so an interface unit was built to transfer the data to it.

Recording commenced with the THC's. On receipt of an OUTPUT COMMAND pulse, each THC presented its internally stored analogue data to an ADC, which digitized it to eight bit accuracy. The resulting eight bits of data were split into two four bit groups, a parity bit was calculated for each, and the resulting five bits presented to the tape recorder. Recording was accomplished by applying a STEP command to the tape recorder as each data group was presented. After completion of THC readout, the data from the 'slow' system were recorded. The output lines of these ADC's were all connected in series, so that a train of WRITE pulses caused each in turn to release its data. The resulting eight-bit groups were again split into four-bit groups and recorded. On completion of the output sequence, an end-of-record marker, and inter-record gap were written on the tape. Experimental

runs generally lasted for two or three days; at the end of this period, the tape was removed, and its data read by the University of Adelaide's CDC 6400 computer. A schematic diagram of the recording system is shown in Figure 3-2.

3.3 Improved Recording System

3.3.1 Multiplexer

As the range of experiments performed at Buckland Park was extended it became desirable to record the data from some additional experiments on magnetic tape. To enable this to be done, a multiplexer unit was built.

The most important design criterion of the multiplexer was that it should allow various experiments to be connected and disconnected at will, without affecting the recording of the basic array data, and this was achieved by writing the data from each experimental device as a separate record. Although wasteful of tape, as each record had to be terminated with an inter-record gap, this ensured flexibility of use. To change the number of experiments being recorded, it was only necessary to connect the appropriate devices to the multiplexer, and indicate, by means of a thumbwheel switch, the number of such devices.

The major components of the multiplexer are an address control section, a data control section, and one decoder-buffer for each device that is to write on the tape. The address control section, and the decoder-buffers control the output cycle, by allowing data from

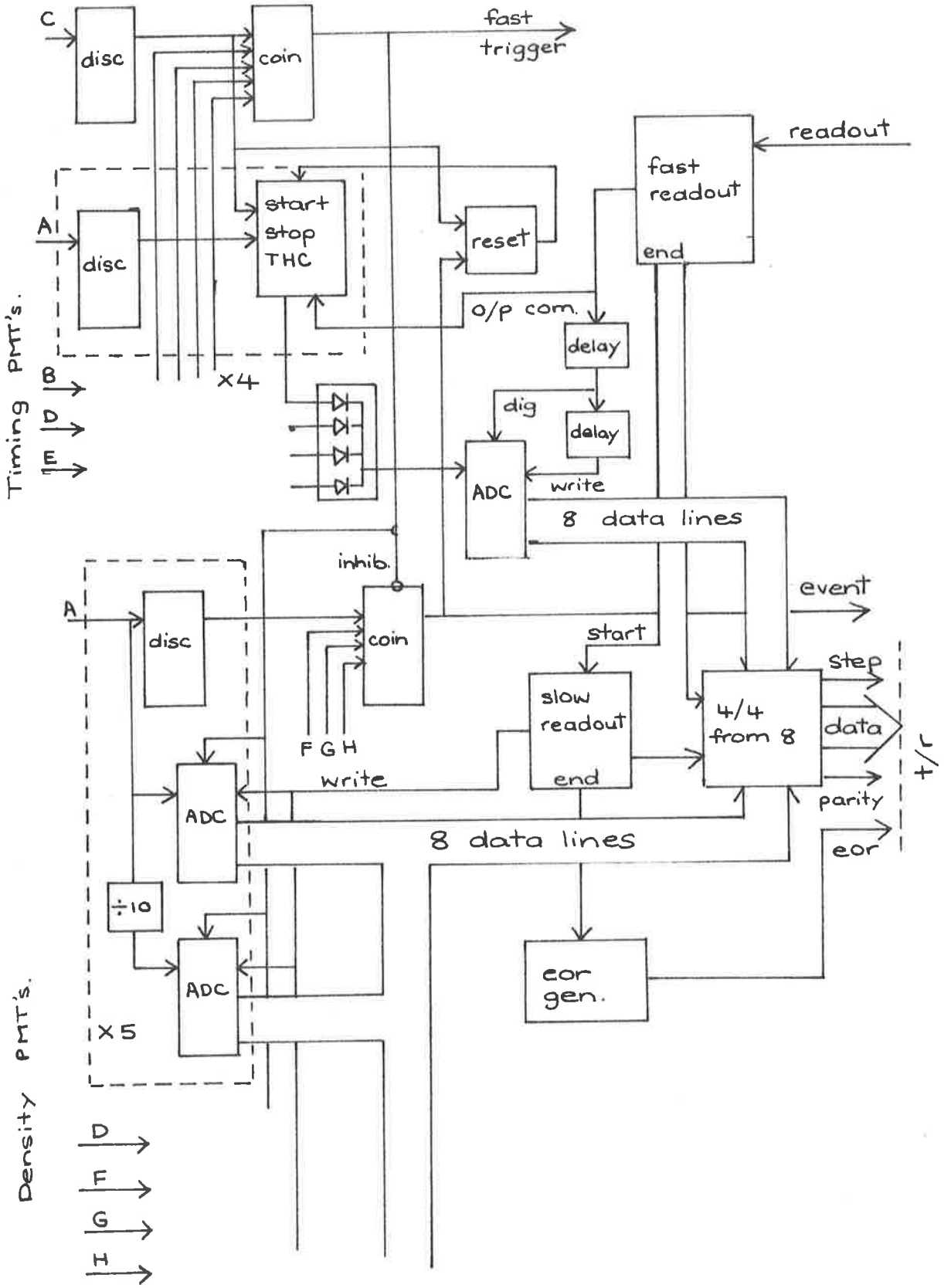

FIG 3·2

The original recording system.

each device in turn to flow through its decoder-buffer to the tape recorder. The data control section writes sequencing information at the head of each record, and writes an end of record after each device has transferred all its data.

In operation the address control section receives a trigger when a shower is detected. This readies the tape recorder, and sets the address counter to the first address, i.e. 1. Control then passes to the data control section, which writes a sequencing word, consisting of the current address and a two bit sequencing counter, onto the tape. A 'GO' signal is then sent to all decoder buffers, but only the one whose address equals the current value of the address counter can accept it. This decoder buffer then initiates the output cycle of its attached device, and allows the resuling six-bit data words, each accompanied by a STEP pulse, to pass through to the tape recorder. The external device indicates its completion of data transfer, by removing its BUSY signal, and this is used, by the data control section, to write an end-of-record on the tape, thus completing the block of data from the current device.

When the tape recorder has completed the end-of-record, the address control section checks to see if the correct number of output devices (as indicated by the thumbwheel switch) have transferred their data. If not, the address is incremented, and the next device read out, otherwise the address is reset, and the readout sequence terminates.

A schematic diagram of the multiplexer is shown in Figure 3-3.

3.3.2 Clock

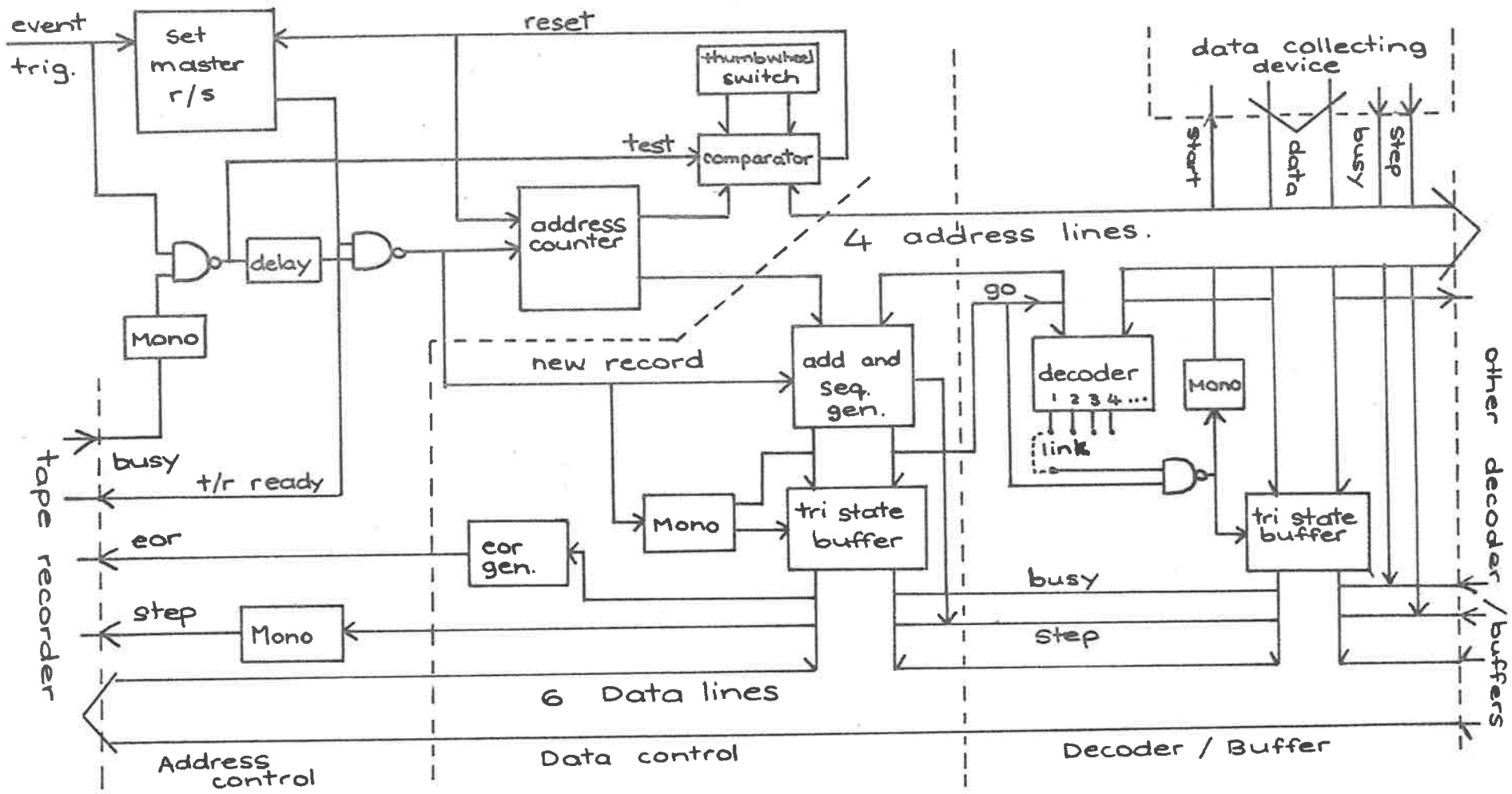

FIG 3·3
The Multiplexer.

A clock was added to the system as soon as the multiplexer was available. In addition to recording the time of the event, to the nearest second, the clock can be used as a buffer, to allow other slowly varying data, such as meteorological data, to be recorded on tape.

The major parts of the clock are a system of counters, connected in the usual way to allow time of day to be derived from the 50 Hz mains supply, and a 256 bit parallel input shift register. When a shower trigger is received, the data on the clock counters, and any other digital data supplied from other devices is read into the shift register. Then, when the multiplexer issues an output command to the clock, the shift register data is stepped along to a 4 bit serial-to-parallel converter, a parity bit is calculated, and the resulting data words are transferred to the multiplexer, and recorded on tape.

3.3.3 PAJAMAS *

* (Phil and Jim's Amazing Measurer of Air Showers)

When the decision to extend the Buckland Park array was made, it was obvious that more recording equipment would be required, and as it was also apparent that the ADC's of the recording system described earlier were becoming increasingly unreliable, it was decided to replace this old system.

The requirements of the new system were:- (1) digitize the time delays between the fast timing detectors to within about 2 ns. (2) digitize the pulse amplitudes from up to 12 density detectors, with a dynamic range of at least 500:1, and (3) be compatible with the

existing multiplexer-tape recorder combination.

3.3.3.1 Pajamas Fast Timing

The heart of the fast timing section of the new particle recorder is an LRS model 2228 time-to-digital converter (TDC). This device digitizes the time delays between a START signal, and up to eight separate STOP signals. The digitized times are stored in the TDC until readout is requested.

In use, the START pulses are supplied by the centre fast detector (C) and STOP pulses from the outer fast detectors A, B, D, E. Most centre fast pulses are, of course, not accompanied by a shower, and so the TDC is reset immediately if no slow coincidence follows the START. If a slow coincidence occurs, then, on command from the multiplexer, the readout sequence is initiated.

Readout is achieved by applying a WRITE COMMAND signal to the TDC. The eight stored times can then be read by applying the binary numbers 0-7 in turn, to its address register. The 12 bits of data produced for each time channel are then split into two six bit groups, and, together with a STEP pulse, transferred to the multiplexer, for recording.

3.3.3.2 Pajamas Pulse Amplitude Measurement

This part of pajamas was designed and built by Mr J.D. Kuhlmann, but is described briefly here for the sake of completeness.

The three main sections of the pulse amplitude measuring system are

a series of sample-and-hold amplifiers (SHA), a Datel 'DAS 16' data acquisition system, and a 192 bit shift register. The output of each density detector preamplifier is connected into a fast sample and hold amplifier (SHA) (Teledyne Philbrick 4853). These SHA's are given a HOLD command whenever a fast coincidence is detected; delays inserted to compensate for the cable transit time from distant sites and the rise time of the preamplifier pulses, ensure that the amplitude is sampled at the peak of the pulse. The SHA's hold the amplitude for about 400 us, to allow the DAS time to digitize all channels.

The DAS has two main components, a 16 channel analogue multiplexer, and a 12 bit analogue-to-digital converter. On receipt of a fast trigger, the DAS begins its digitizing sequence. The analogue multiplexer presents the output of each SHA in turn, to the ADC, which then digitizes the amplitude. The DAS itself contains sufficient circuitry to control these operations. The output from the DAS is taken into the shift register via a 12 bit parallel to serial converter. The shift register is clocked along as each channel is digitized, so that after all 16 channels are digitized, the shift register is full. This data is then held until the data from the fast timing section has been transferred to the multiplexer. The shift register data is then repeatedly clocked into a 4 bit serial to parallel converter, a parity bit is produced, and the resulting 5 bit data words are transferred to the multiplexer for recording on tape.

A schematic diagram of Pajamas is shown in Figure 3-4.

3.4 Array Improvements

The design of an array presents a conflict between the close

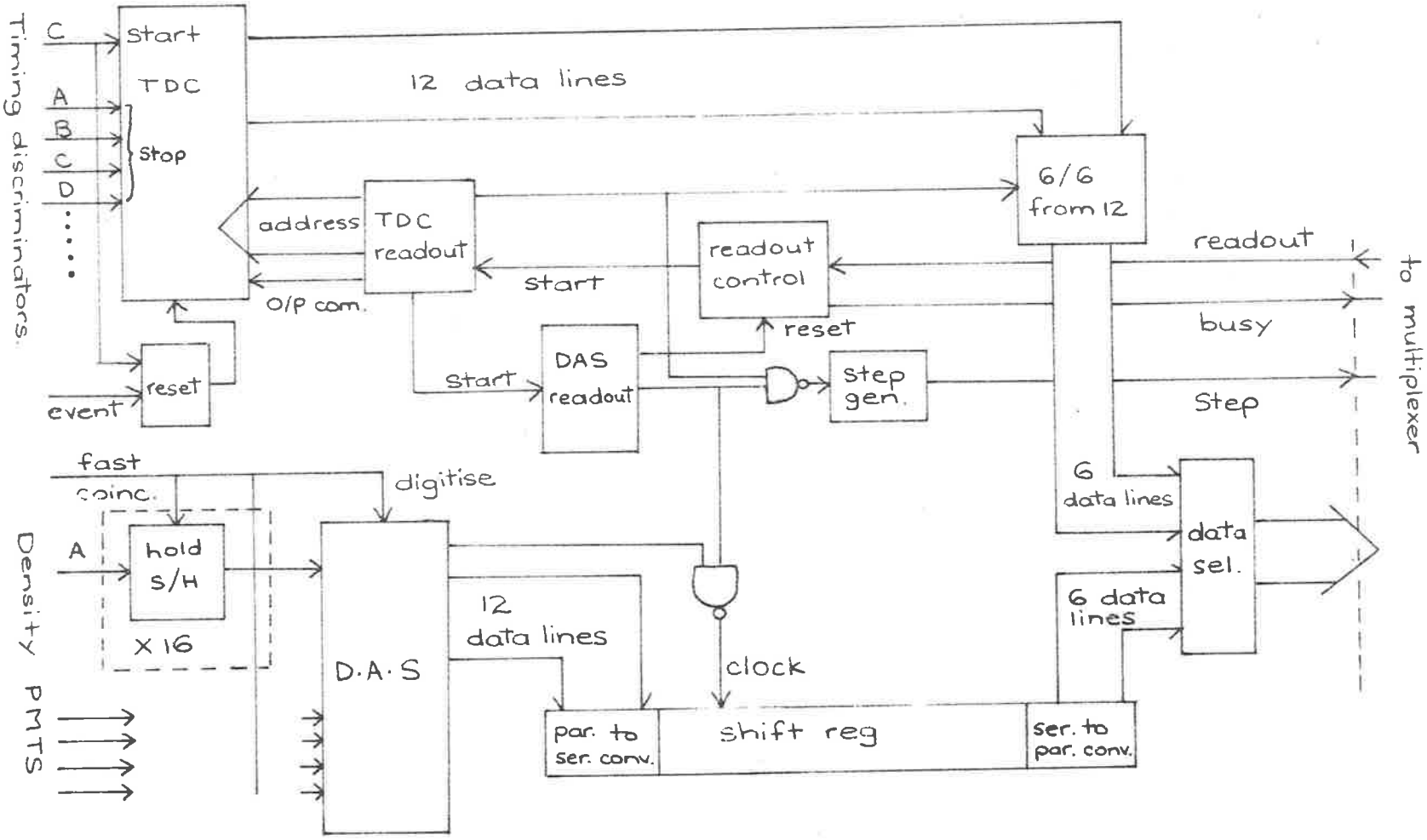

FIG 3·4 PAJAMAS ®

detector spacing required to accurately determine the shower parameters, and a wider spacing, allowing showers to be detected over a larger area. The nature of the experiments currently being performed at Buckland Park emphasises this conflict; one group is concerned with fluctuations in the Cerenkov light emission from showers, and requires as many large showers as possible, while another group, interested in the spectrum and anisotropies near the shower spectrum 'break' (about 7×10^5 particles) requires accurate analysis of these smaller showers.

Ideally perhaps, one would design an array by determining the set of showers of interest to the experiments contemplated, determine triggering requirements that would select this set, and then determine the detector arrangement required to measure these showers to the required accuracy. However, in designing extensions to the Buckland Park array, the presence of the existing sites, and the conflict outlined above limited this approach. Initial investigations showed that suitable detection and analysis of small showers presented greater problems than the large showers, and so it was decided that the approach adopted would be to choose a triggering scheme that selects showers which could be well analysed by the existing array, and then determine where the new detectors should be placed to give the best analysis of larger showers falling outside the present array.

3.4.1 Triggering Conditions

3.4.1.1 Method

The effects of various triggering criteria were estimated using a

computer program. The triggering probability at a point on the array, for a shower of given size, was found by the following method. First, the density at each detector was calculated using the lateral distribution given by Greisen [3]. A random Poisson fluctuation was then introduced, to estimate the number of particles that would be observed by the scintillator, and this number was compared with the threshold set for that detector. If the required number of detectors exceeded the threshold, then a shower was recorded. This process was repeated ten times at each point on a 5m x 5m grid covering an area 200m square, centred on the array. By repeating this process for different shower sizes, the triggering probability $P(N,x,y)$ was calculated as a function of shower size, and core location, for each triggering scheme. The effective triggering area $\iint P(N,x,y)dxdy$ was also calculated, and by multiplying this by the flux of showers in each size range (derived from the shower size spectrum, given by Hillas [4]), the expected rate of observed showers was obtained.

Two approximations were made to facilitate the calculations. Firstly, only vertical showers were considered. As the apparent detector spacing, in the plane of the shower-front, is less for inclined showers than vertical ones, this approximation underestimates the triggering area. However, this was found not to be important when making comparisons between different triggering schemes, as they were all affected similarly. The second approximation was the use of the Normal approximation to the Poisson fluctuations in the number of particles observed by each detector. This gives quite accurate results for particle densities above about 6 particles, but below this leads to a slight underestimation of the triggering area. The Landau distribution of pulse heights produced by a single particle passing through a scintillator is much narrower than the Poisson, and was

ignored.

A common feature of all schemes investigated was the requirement of a 'fast coincidence' (Section 3.2.2). Not only does this ensure that the shower direction can be determined, but it has also been found to give a suitable rate of prompt triggers for certain experiments. Thus only 'slow coincidence' requirements were investigated.

3.4.1.2 Results

The result of several representative triggering schemes, expressed as an expected differential size spectrum, is shown in Figure 3-5. The scheme requiring 3 of A, F, G and H, at the 3 particle level appears to be superior to the others, as it gives a sharp cut-off to small showers, a broad maximum near the size spectrum break (about 7×10^5 particles) and good sensitivity to larger showers outside the array. However, further work showed that such a triggering system, i.e. coincidence between a number of widely spaced detectors with low thresholds, was not very satisfactory, particularly when this involved using many of the density measuring scintillators in the triggering scheme. Under these conditions, showers are preferentially selected if the densities measured are upward fluctuations of the mean particle densities at the detectors, resulting in systematic overestimation of the shower size. This is illustrated in Figure 3-6, which shows the result of different coincidence levels on the calculated size of simulated showers, analyzed using the technique described in the next section. It is apparent that as the triggering probability falls below 50% the shower size is increasingly overestimated, and as is shown in Figure 3-7a the requirement of 3 out of A, F, G and H results in many showers being detected in these 'low probability' regions. A

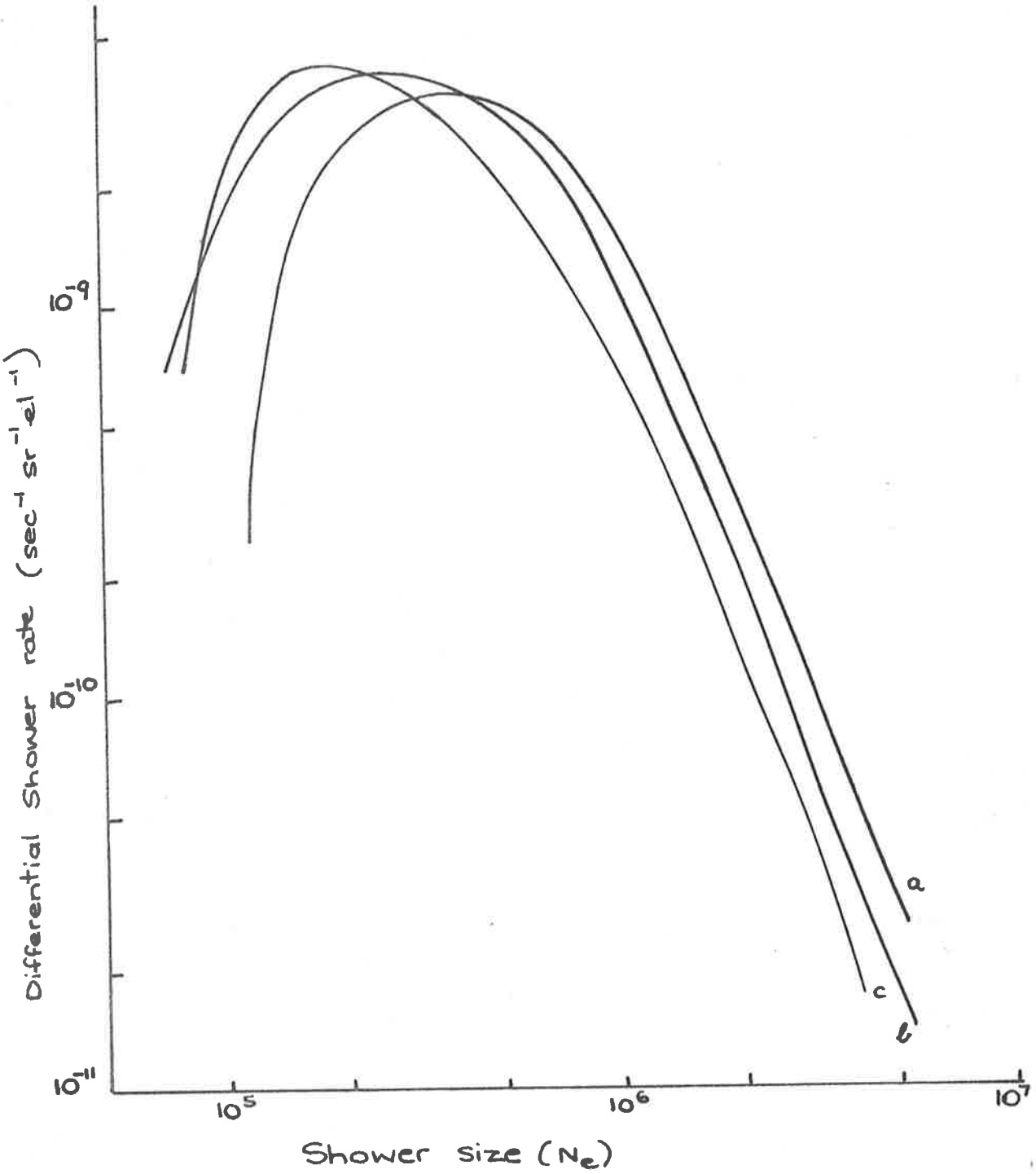

FIG 3·5

Comparison of shower rates expected from different triggering criteria.

(a) Fast coincidence + 3 of A F G H ⩾ 3 parts.
(b) Fast coincidence + A ⩾ G and D ⩾ 8
(c) Fast coincidence + D ⩾ 18.

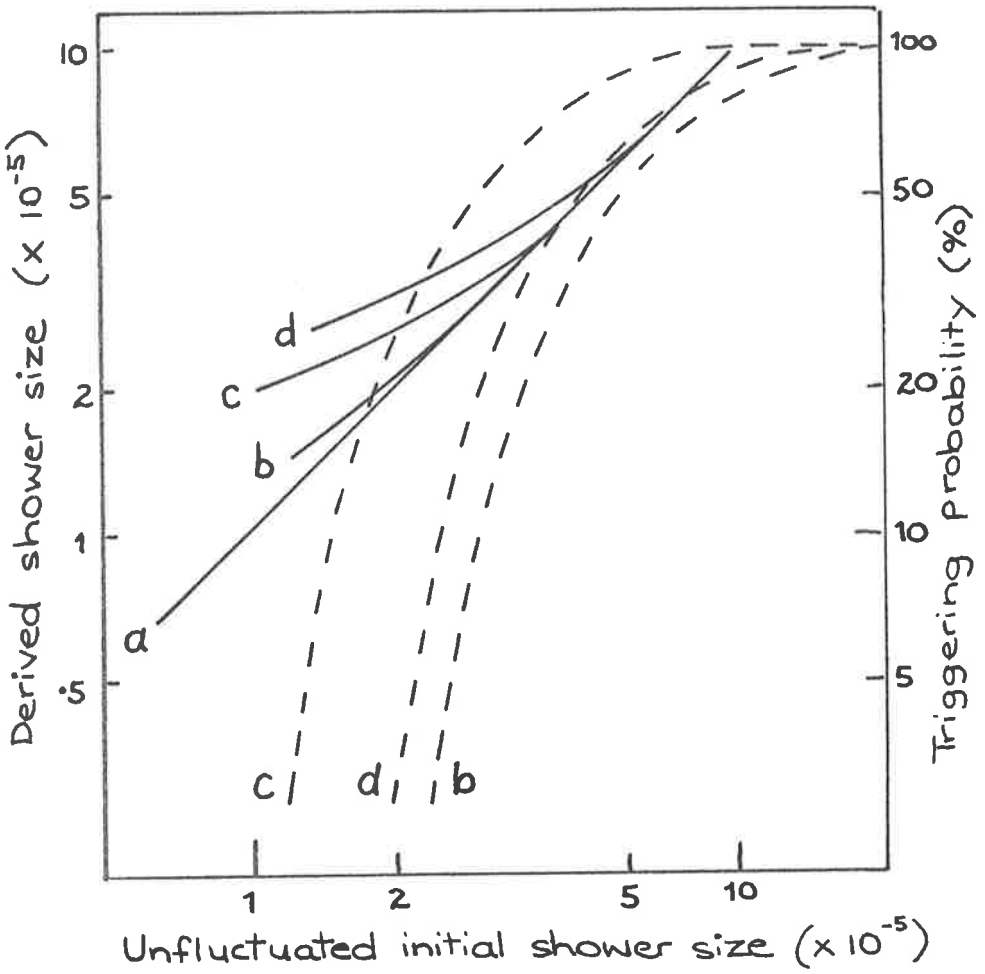

FIG 3·6

Effect of triggering conditions on calculated shower size.

—— Shower size

--- Triggering Probability

a - no triggering conditions.

b - coincidence between A (6 parts) and D (8 parts.)

c - coincidence between any 3 of AFGH (3 parts.)

d - coincidence between all 4 of AFGH (3 parts.)

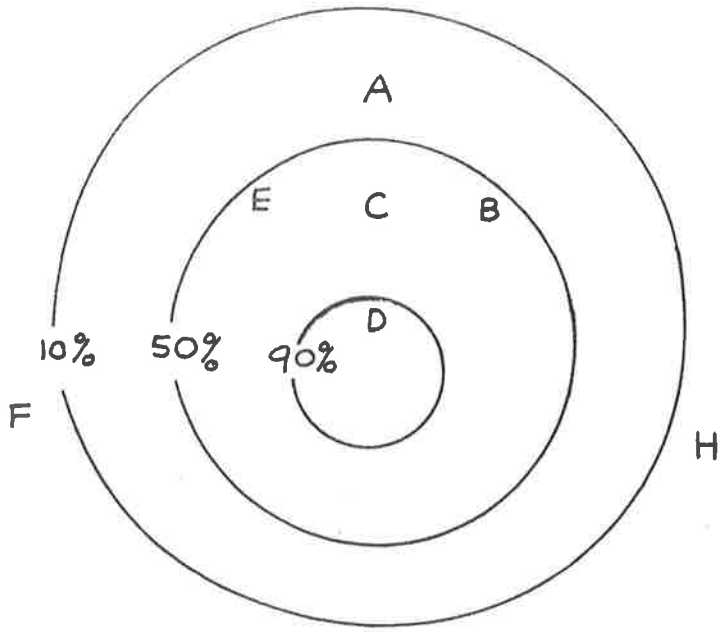

(a) Fast coincidence
+3 of A,F,G and H ⩾ 3 parts.

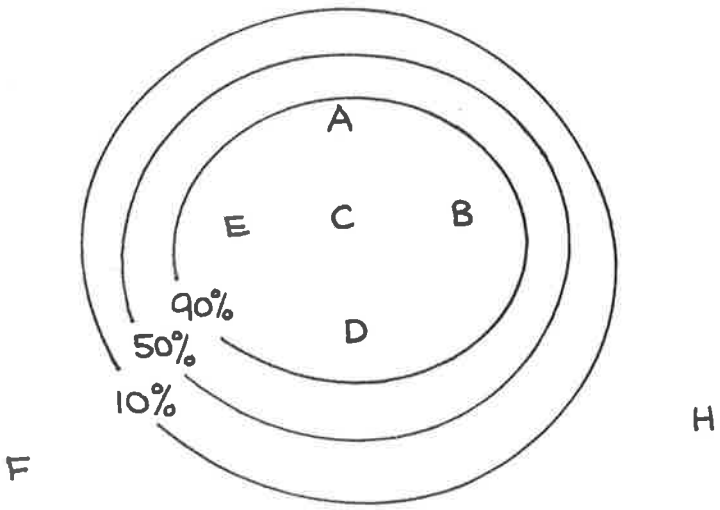

(b) Fast coincidence
+ A ⩾ 6 parts. and
D ⩾ 8 parts.

FIG 3·7

Comparison of triggering probabilities for two triggering schemes.
The effective collecting areas are approximately equal.
(Shower size 4×10^5 particles.)

system requiring a coincidence between fewer detectors, at higher thresholds was thus required, and the most suitable was found to be a two-fold coincidence between A (6 particles) and D (8 particles). As can be seen in Figure 3-7b, this also results in most of the small showers being detected inside the fast timing array, where the close detector spacing allows better shower analysis.

Having chosen the triggering conditions to be used, inclined showers were included in the calculation of collecting area, and the result, the spectrum of showers expected to be observed, together with the spectrum actually recorded under these conditions, is shown in Figure 3-8. The agreement is considered very good, the discrepancy being consistent with a systematic error of shower size estimation of less than 10%.

3.4.2 Array Extensions

Having now determined the selection of showers that would trigger the array, a program was written to determine how additional density detectors could best be used to improve the analysis of showers falling outside the array, and also how the installation of density recording equipment at the 'fast' sites B, C and E would improve analysis.

3.4.2.1 Method

The program first set up the coordinates of the array to be used, and the sizes and core locations of the showers to be tested were determined. Then the particle densities at each site were calculated, and random fluctuations introduced, as previously described. The

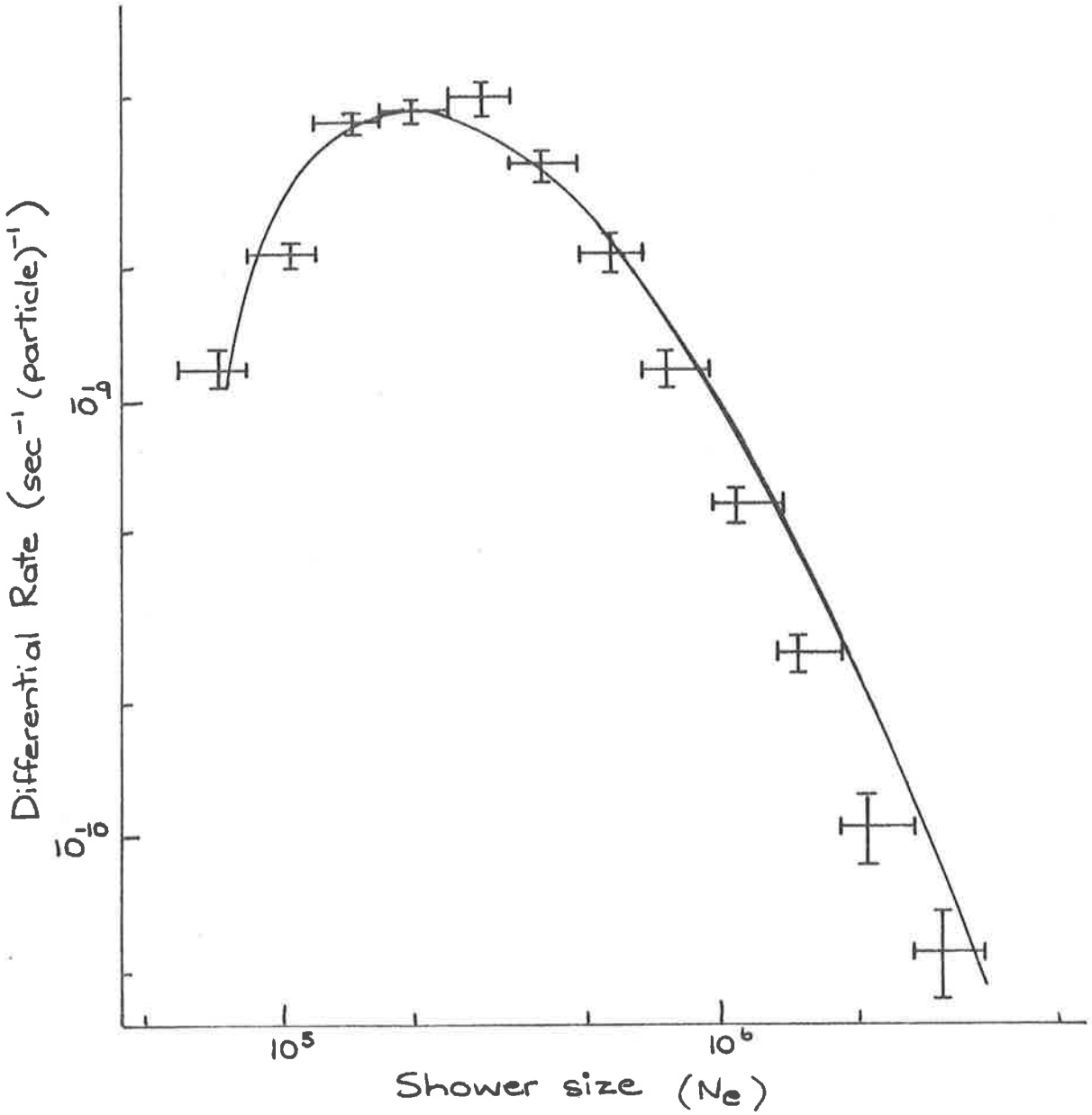

FIG 3·8

Size spectrum of showers triggering the Buckland Park Array.

____ - Predicted

Data Points - Observed.

resulting 'observed' densities were then checked to see if the triggering criterion had been satisfied. If so, an attempt was made to reconstruct the shower from these observed densities, using the analysing techniques outlined in Section 3.5. The shower parameters derived from this analysis were then compared with those of the original shower, to determine the accuracy of the analysis. For each combination of detecting array, core location and shower size, this procedure was repeated ten times, enabling the mean core location, mean size and rms core error to be estimated. All showers were again assumed to be vertical. The core errors found for inclined showers were not significantly different, for, although in the plane of the shower the projected areas of the detectors were smaller, they are closer to the axis, and so the number of particles observed, and thus the relative statistical errors are not greatly changed. No allowance was made for instrumental errors in recording the densities; these are expected to be less than 5% [5] and so are less than statistical fluctuations at all but the highest densities.

In optimising the array, most attention was paid to the rms core error, as at an early stage of the investigation it was found that, although core and size errors are related, greater inaccuracies would be introduced by typical core errors than size errors, particularly in experiments which determine a lateral distribution.

It should be noted that as no instrumental errors are included, and as some analysis problems were circumvented by using the original core as the starting point for locating the 'fluctuated core' (see sect. 3.5), the errors obtained are those applicable to an ideal array, and would not be approached in practice.

3.4.2.2 Results

The results of including density measurements at the 3 'fast only' sites, B, C and E are illustrated in Figure 3-9; the reduction in core error was typically greater than 50% for the test showers used. As a result it was decided to include density recording equipment at these sites, and all eight existing detectors were included in evaluations of array extensions.

The only extensions considered in detail were to the north of the present array, for extensions in other directions did not improve the analysis of the large number of showers detected just outside the fast array. The first configuration considered was with the 3 new detectors at the corners of a square of side 180m (i.e. twice the present array) with the fourth corner the existing site G (Figure 3-10).

The accuracy of the array was assessed in 13 circular areas of radius 25 m, covering the eastern side of the array (no analysis was made of the western side, because of the symmetry of the array).

The core errors obtained were generally less than 12m, with a typical size error of 10% (for a shower of 2×10^6 particles) except in the area approximately halfway between A and J, where the poor east-west location, due to the low densities recorded at I and K, increased the core errors to more than 15 m. This could be improved, at the expense of collecting area, by moving huts I and K inwards. The most suitable compromise obtained is shown (by the sites marked (b)) in Figure 3-10. This arrangement reduced the core errors in the centre of the extensions to about 10m, the collecting area being

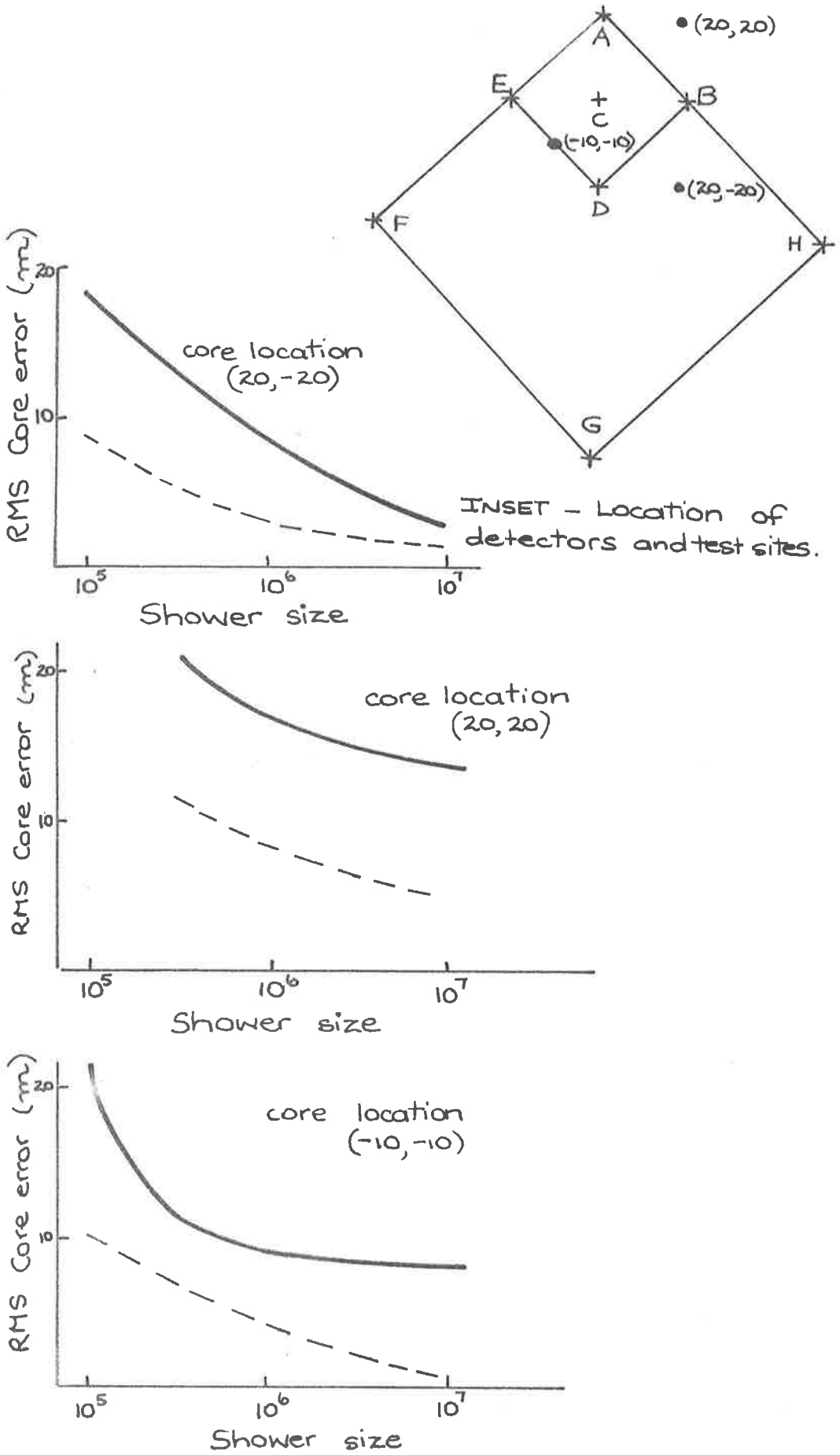

FIG 3·9 Improvement in core location by using density recording at sites B, C, E.
—— 5 sites, ---- 8 sites.

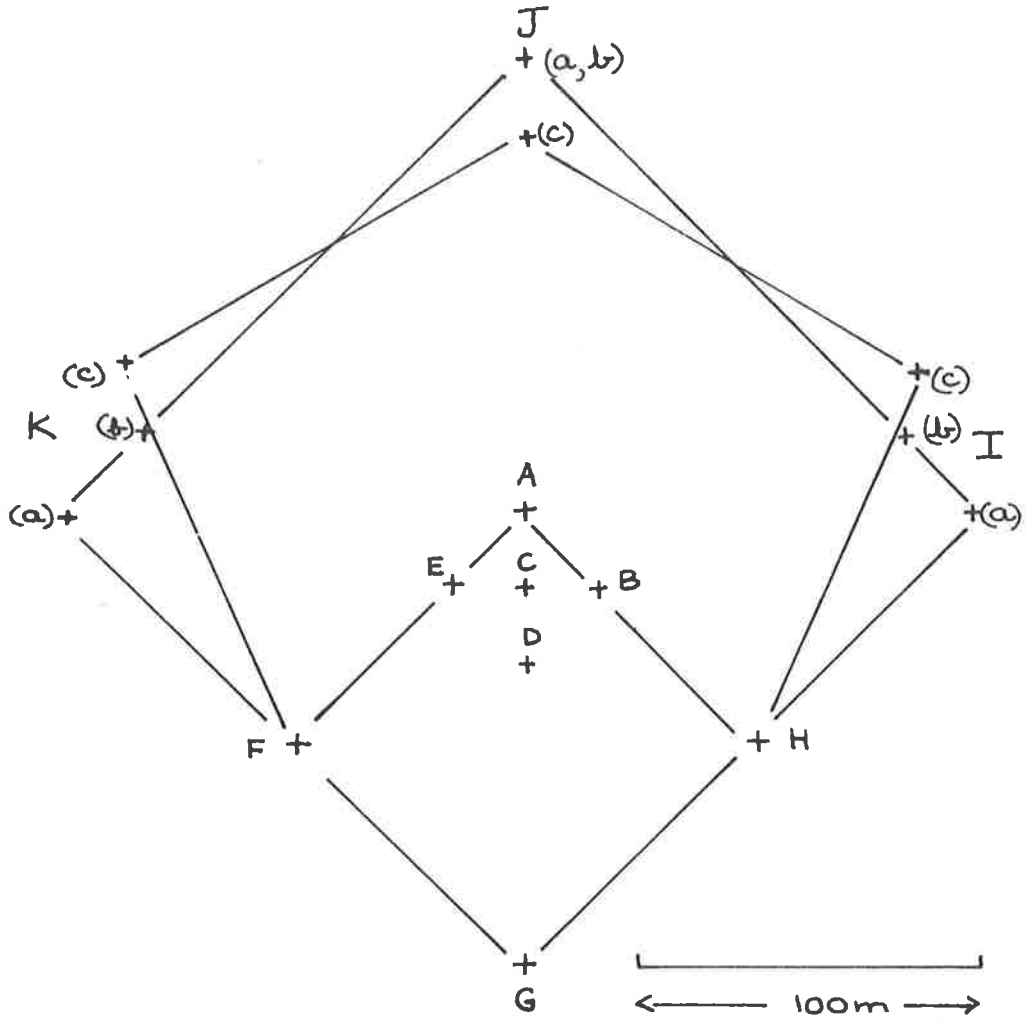

FIG 3·10

Extensions to the Air Shower Detecting Array.
A–H - existing sites.
I–K - extensions.
I (a) – K (a) - initial choice of sites.
I (b) – K (b) - improved locations.
I (c) – K (c) - final locations.

reduced by about 10%.

Further consideration showed that the area near J was so far from the fast array that it was insensitive to all but the largest showers. It was found that moving J towards A, and I and K northwards (sites '(c)' of Figure 3-10) increased the useful collecting area, and also further improved core location.

Several other schemes were tried, but none which gave better results, for a similar collecting area, was found. Accordingly, this array (Figure 3-10c) was adopted. (Site K was found to be located at the deepest part of a small swamp, convincingly demonstrating the correctness of this decision.)

A comparison of the three arrays referred to above is given in Table 3-1, while Figure 3-11 shows the core errors expected in the final array.

3.5 Analysis of Air Shower Data

3.5.1 Shower Direction Determination

The arrival direction of the shower is determined from the time delays between the arrival of the shower front at the five 'fast' detectors [2].

If we have detectors at $\underset{\sim}{r}_i = (x_i, y_i, z_i)$

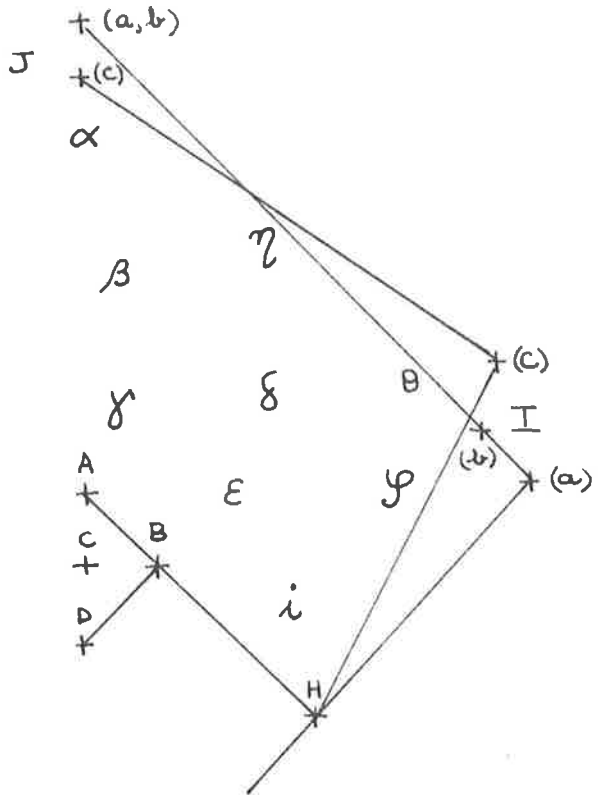

	Array	α	β	γ	δ	ε	φ	η	θ	i
size = 2×10^6	a	8·7	15·2	4·9	11·3	3·0	5·5	15·3	6·8	2·9
	b	9·9	9·1	5·5	6·4	3·1	4·8	9·5	5·7	3·1
	c	5·5	7·9	3·0	6·9	3·1	5·8	7·3	5·3	4·0
size = 5×10^5	a			7·3		7·6				9·2
	b	*	*	7·5	*	7·6	*	*	*	9·2
	c			6·8		6·8				10·7

Table 3·1

A comparison of RMS core errors for three array configurations. The locations of the test areas are shown in the figure.

[* - triggering probabilities too low for analysis.]

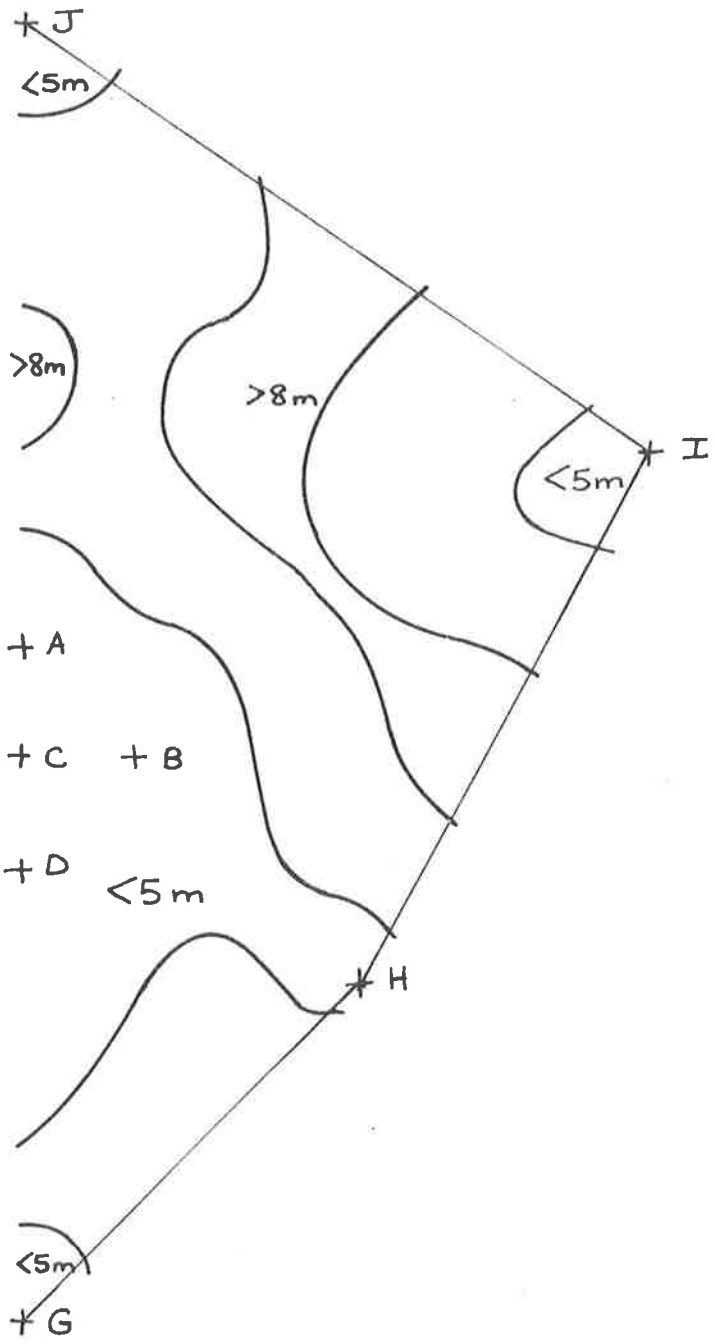

FIG 3·11

Estimated RMS core errors for extended array.

Shower size 2×10^6 parts.

and the shower front (assumed plane) moves in the direction $\underset{\sim}{u}$ = (l,m,n) with velocity c, then the shower front will pass through the detectors at times

$$t_i = t_0 - \frac{1}{c}\,\underset{\sim}{r}\cdot\underset{\sim}{u}$$

where t_o is the time that the shower passes through the origin. If we measure the arrival time at detector i to be T_i, then we can obtain the 'best fit' arrival direction by a 'least squares minimisation' [6], i.e. by minimising

$$\chi^2_T = \frac{1}{m-3}\,C \sum_{i=1}^{m} (T_i - t_i)^2$$

For our array, where hut C is the centre of the coordinate system, and all times are measured relative to the arrival at C, this reduces to

$$\chi^2_T = \frac{1}{m-3} \sum_{i=1}^{m-1} (cT_i - \underset{\sim}{r}\cdot\underset{\sim}{u})^2$$

This is readily solved to give the shower direction [7].

The timing errors (about 4ns) are too large to enable departures from a plane wavefront to be measured by the fast array [8]. An analysis of the minimum values of χ^2_T obtained in this way has shown that the typical error in shower direction determination is about 2.5 sec (θ) degrees, where θ is the zenith angle of the shower [5].

3.5.2 Size Determination and Core Location

The size and core location of the shower are determined from the recorded particle densities. Again, a least squares method is used,

but as the equations contain non-linear elements, the problem is somewhat more difficult. If d_i is the density expected at hut i when a shower of size N falls at (x,y), and D_i is the density actually recorded, then the most probable shower will be found by minimising

$$\chi^2_D = \frac{1}{m-3} \sum_{i=1}^{m} w_i (D_i - d_i)^2$$

The weighting functions w_i used are those applicable to Poisson statistics, i.e.

$$w_i = \frac{1}{d_i}$$

The determination of the location of the minimum of χ^2_D must be done by numerical means, i.e. by evaluating χ^2_D at a series of trial core locations, chosen so that the value of χ^2_D decreases at each trial [7]. The original analysis program, which was brought from Canada with the array, used a 'grid search' technique, where the new trial locations were found by alternately moving the trial core parallel to the x and y axes. However, for the array evaluation program, a 'gradient search' technique was used, where the trial core was moved in the direction of maximum decrease of χ^2_D. As this proved to be much more efficient, this was adopted for analysis of the array data.

This technique proved quite satisfactory for the data from the original array, but some problems were encountered with the analysis of data from the extended array. These are due to the existence of 'local minima' in the χ^2_D surface, separated by 'ridges' of high χ^2_D, which generally join adjacent detectors. If the initial choice of core is on the wrong side of one of these ridges the searching routine will not, in general, cross it to find the 'true' minimum, and hence the most probable shower parameters.

Some preliminary attempts to solve this problem were made, and some success was achieved by performing a preliminary analysis using the data from the outer sites only, and then refining this result by repeating the analysis, including the less distant huts in turn. However, these attempts were superseded by the purchase of the powerful function minimisation routine MINUIT [9], which can use a variety of techniques to ensure that the 'best' minimum is found. This program has been used successfully in similar applications [10], and is being incorporated into the Buckland Park analysis routines.

CHAPTER FOUR

EXTENSIVE AIR SHOWER ASSOCIATED RADIO PULSES AT FREQUENCIES BETWEEN 2 AND 22 MHZ

4.1 The Problem of Low Frequency Pulses

Although anomalous radio pulses have been observed in many experiments [1, 2, 3, 4], the results obtained in the frequency region from 20-120 MHz have generally been well explained by the geomagnetic and charge excess theories [1, 4, 5, 6]. However, in the frequency range below 22 MHz, there is a great deal of confusion. Hough et al. [7], working at a frequency of 3.6 MHz, detected pulses with field strengths an order of magnitude greater than those observed in the 'geomagnetic' region (i.e. 20-120 MHz), and this result was confirmed by measurements at 2 MHz [8, 9] and 6 MHz [10]. This rise in field strength at low frequencies is in disagreement with the theory discussed in the previous chapter, while Allan [11] has shown that even the most extreme theoretical estimate of the field strength from the geomagnetic or charge excess mechanism will fall far short of the fields observed. This complete disagreement between theory and experiment will be discussed in the following sections.

4.1.1 Previous Results at Low Frequencies

Felgate and Stubbs [10] have presented a frequency spectrum of the

low frequency results mentioned above [7, 8, 9], which shows that these results, together with the 22 MHz measurements of Hough et al. [12] are all consistent with a power law spectrum, with exponent of about -1.5. The underlying unity suggested gives added weight to the individual results, and so it will be used as a basis for an appraisal of these experiments.

4.1.1.1 22 MHz Experiments

The 22 MHz result is not only the most firmly established result, but is unique in being consistent with both conventional geomagnetic theory, and the Felgate-Stubbs spectrum. In a series of experiments [12-15] not only was the field strength measured, but its dependence on shower size, core distance, and shower direction was determined. The most important of these was the last, which indicated clearly the dominance of the geomagnetic mechanism at this frequency. In two virtually independent experiments [13,14], using two different antennae, a linear relationship between pulse amplitude and 'geomagnetic factor' $\underset{\sim}{X}.\underset{\sim}{V} \times \underset{\sim}{B}$ (where $\underset{\sim}{X}$, $\underset{\sim}{V}$ and $\underset{\sim}{B}$ are unit vectors in the direction of the antenna axis, the shower axis and the geomagnetic field respectively) was demonstrated. By extrapolation a non geomagnetic component (i.e. independent of $\underset{\sim}{X}.\underset{\sim}{V} \times \underset{\sim}{B}$) approximately 15% of the maximum geomagnetic signal, was also inferred.

Apart from the obvious and elegant confirmation of theoretical predictions, this experiment has other features which make it most unlikely that the result is seriously contaminated by spurious effects. Firstly, the signal-to-noise ratio (S/N) was such that at times clear pulses could be observed above the background noise, and this, together with the availability of the air shower parameters,

enabled possible errors, which could be concealed by the averaging techniques necessary with low S/N ratios, to be found by checks on individual showers. Secondly, the antennae used were of a conventional design (arrays of folded dipoles used above an earth screen) and so their properties could be accurately estimated. In particular, although the individual elements were identical, they were connected and used in quite different arrays. One (the 'cross polarised' array) had a wide angular response and thus showers from a large region of the sky were available for analysis. The 'main array', however, was connected to give four narrow, high gain beams, and only showers with arrival directions in these beams were used. As the same result was obtained in each experiment, it would appear unlikely that the pulses observed are anything other than the conventional radiated fields assumed in the antenna calculations.

While the dependence of the radio pulse amplitude on shower arrival direction thus gives strong support for the geomagnetic theory, the lateral distribution does not. The field strength measurements 50m from the core [12] are in reasonable agreement with theoretical predictions [4, 16, 17] but the field strength is found to increase rapidly closer to the core [12], in contrast to the decrease predicted theoretically [16, 18]. This would appear to imply the existence of an additional, non geomagnetic component, which dominates near the core. However, this is in disagreement with the result quoted above, where the non geomagnetic component, near the cores of a similar set of showers, was only 15% of the geomagnetic [13, 14]. This confusing result may be related to some early Russian results, where, at a frequency of 30 MHz, large fluctuations in the field strength were observed near the core [19]. This was interpreted in terms of fluctuations in the height of shower maximum, but this explanation is

not supported by the detailed calculations referred to above [16, 18]. No further studies of this effect have been reported.

4.1.1.2 3.6 MHz

None of the experiments at lower frequencies have all of the advantages of the 22 MHz experiments, viz. individual shower analysis, good S/N ratio, and well understood antenna. The Calgary 3.6 MHz experiment [7], which first showed the presence of high field strengths at low frequencies had only the last of these. The antenna used was a single folded dipole, and although complicated by the presence of the steel framed building below it, its properties could be readily estimated. A simple geiger counter coincidence system was used to detect showers, so no data on individual shower parameters was available, and the background radio noise was too high to enable individual pulses to be observed.

A good deal of care was taken to avoid biasses in the analysis of the data, and in extracting the signal from the background noise, and checks were made to exclude the possibility that the pulses observed were due to spurious electronic 'pick up'.

4.1.1.3 2 MHz - Haverah Park

At Haverah Park [8], the experiments did have the advantage of an established shower detecting array, but again no pulses could be seen above the background noise, despite the fact that the mean shower size was about a hundred times greater than that used by Hough et al. Even on selected traces (large showers during quiet periods) no pulses were observed [20]. This is rather surprising for it implies that the

noise background must have been very high. The antenna used was a top loaded Hertzian dipole. Although its properties are amenable to calculations, they are fairly sensitive to the small capacitance between the antenna and ground. It would also appear that this type of antenna would be more sensitive to some types of non-radiated signal (e.g. discharge of the geo-electric field) than a balanced dipole. However, care was taken to check the antenna gain, and to check that interference was not present.

4.1.1.4 2 MHz and 6MHz - Adelaide

Perhaps the most interesting experiments in this frequency range were those of Stubbs and Felgate [9, 10]. They used a large antenna array, connected to give a high gain beam directed at the zenith, and a highly directional optical Cerenkov coincidence system was used to detect showers directed along the axis of the beam. This, of course, necessitates working only at night, when the background noise is high, but the extra sensitivity of the antenna was sufficient to compensate for this.

High field strengths, consistent with the previous 2 MHz and 3.6 MHz results were measured at 2 MHz, and 6 MHz, and in addition, the 6 MHz pulses were found to be somewhat polarised in the E-W direction, as predicted by the geomagnetic mechanism.

As single radio pulses could not be observed above the background, an averaging technique had to be employed. This was done by means of a high speed multi channel counter, which was used to record, digitally, the output of the receiver in the time interval following the arrival of the shower. Although eliminating observer bias, this

device did not allow the exclusion of excessively noisy events, and also did not allow the signal to be extracted from the noise by means of quadratic subtraction, although the error introduced is small [10].

In order to test for the presence of spurious signals, the apparatus was operated with radio and Cerenkov beams out of alignment. No signal was observed. This would appear to confirm not only that the apparatus was free from interference, but also that the assumption of a radiated field, originating high above the array, implicit in the calculation of the antenna response, was correct.

However, the field strengths quoted, particularly at 6 MHz would appear to be underestimated, for no allowance has been made for the lateral distribution of the radiation. The calcultion of the antenna gain, and hence the field strength was made under the assumption that the antenna was illuminated uniformly over its aperture. Thus the field strength estimate is based on the average power absorbed over the whole array, not the larger intensity which could be expected in the region near the core. It is difficult to estimate a correction, as there is no information on the lateral distribution at these frequencies. If the lateral distribution is the same as that at 22 MHz [12] the field will be underestimated by a factor of about 10, but it is probably more reasonable to assume that the width of the distribution is proportional to wavelength [21], in which case the field is underestimated by factors of about 3 at 6 MHz, and about 2 at 2 MHz. This 2 MHz result is still compatible with the Haverah Park measurement, particularly as this would also be increased by a correction for lateral distribution, but the 6 MHz field is now greater than the 3.6 MHz result; the correction to the latter would be small as the antenna was close to the cores of the showers detected.

4.1.2 Summary of Previous Results

The correction to the 6 MHz field strength destroys the smooth spectrum of Felgate and Stubbs [10], for the 6 MHz measurement is now greater than that at 3.6 MHz. Nevertheless, the fact remains that three independent groups, two of them with a good deal of experience in the field, observed field strengths very much greater than those expected and observed in the 20-120 MHz band, and, as Allan has shown, completely inexplicable in terms of conventional theories [11]. The range of techniques used to detect showers, whose size ranged over 3 orders of magnitude, and the variety of radio systems used would appear to exclude the contention that they are all subject to some common spurious effect.

4.2 Present Experimental Work at 2 MHz

4.2.1 Particle Trigger Experiments

The 2 MHz field strengths quoted above suggest that showers of primary energy above 10^{15} eV should produce pulses which are clearly observable above the daytime noise at a quiet site, and so an experiment was set up to observe these pulses.

The Buckland Park antenna array consists of 89 pairs of crossed half-wave dipoles arranged on a square lattice with 95 m spacing, and covering an area approximately 1 km in diameter [22]. The dipoles are matched into the connecting cables by 'baluns', tuned to enable operation at both 1.98 MHz, and its third harmonic 5.96 MHz. The

cables connecting the antennae to the central hut are all cut to electrical lengths which are multiples of a half wavelength (at 1.98 MHz) ensuring that signals from the zenith all arrive at the central site in phase.

The receiver used had a 3dB passband from 1.7 to 2.4 MHz, with a maximum gain of 85dB at the centre frequency. No detector stage was used. Recording of the r.f. signal was by means of a Biomation Transient Recorder (Model 610). This device consists of a high speed 6 bit analogue to digital converter (ADC), a 256 word shift register memory, and a digital to analogue (DAC) output stage, with associated control circuitry. In operation, the ADC can be made to continually sample and digitize the input signal, at a preset sample rate, and store its output in successive words of the shift register, earlier data being discarded at the end of the register as current data are added at the beginning. Thus, at any time, the shift register contains a record of the input signal for the preceding 256 sample intervals. On command, storage of data may be effected by continually circulating the data in the shift register, returning the data discarded at the end to the beginning of the register. By delaying the beginning of storage for a suitable time after receipt of a trigger, data preceding or following the trigger can be stored. Output can be effected either digitally, or, using the DAC, as analogue signal, in which case only 224 data words are available. For this experiment, the sample interval was 0.1 usec, the storage delay was adjusted so that the shower arrival was near the centre of the output record, and output was to a chart recorder. Thus for each event a 22 usec sample of receiver output, including the shower arrival was available for analysis.

Showers were detected by means of a coincidence between any 3 of the 1 m sq scintillator counters A F G H (Figure 4-1) of the Buckland Park air shower array. The minimum shower size was about 10^5 particles.

As a preliminary experiment, only one dipole ((1) of Figure 4-1) was used as antenna, and it was connected directly to the 50 Ω input impedance receiver. About 500 events were recorded, and of these 157 quiet traces were examined for the presence of bandwidth limited pulses immediately following the shower arrival. No clear unambiguous pulses, standing well above the noise were observed. A more careful check was made by examining 3 separate regions, each 2.2 us wide (i.e. approximately one reciprocal bandwidth), one before the shower arrival, one immediately after the trigger, and one approximately 5 usec later. For each event, these three regions were compared to see which contained the largest pulse; traces in which two were equal being disregarded. No excess of pulses in the expectation region was observed under this criterion.

This result was a surprise, as showers of this size were expected to produce field strengths above 5 uV m^{-1} MHz^{-1}, which should have been readily observable during quiet periods. A more sensitive experiment was therefore undertaken to check this contradiction.

For this experiment, four E-W polarised dipoles ((1), (2), (3) and (4) of Figure 4-1) were connected as a broadside array, to give greater gain at the zenith, and some reduction of noise from the horizon. A good deal of attention was paid to matching the antenna to the receiver, however as the dipoles became highly reactive away from resonance, the usable bandwidth was restricted to about 400 kHz. Some

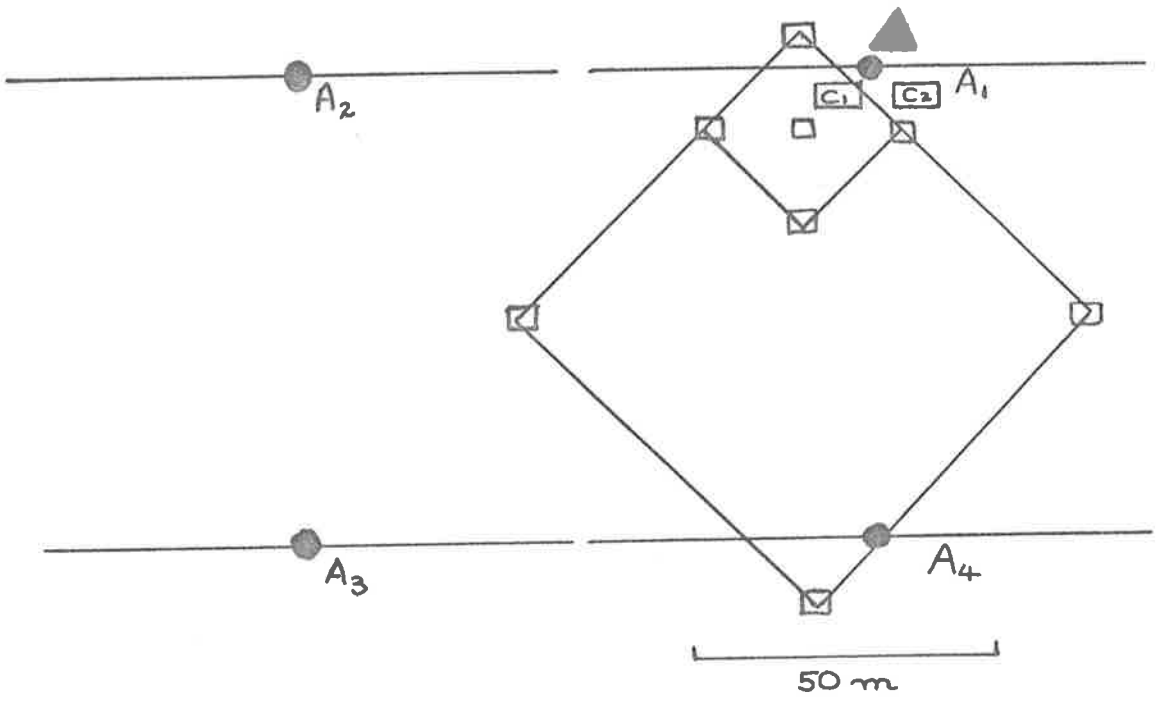

FIG 4·1

The Buckland Park Array, showing location of 2 MH_2 Antennae.

□ - Particle detectors.
$A_1 - A_4$ - 2 MH_2 Antennae
C_1, C_2 - Recording Caravans.
▲ - Čerenkov light detector.

(Antenno A_1 is the centre of the full 89 dipole E-W polarised array.)

adjustments were made to the receiver passband, in order to give a steeper cut-off at lower frequencies, so as to reduce the interference from radio transmissions at a frequency of 1.6 MHz. The shower detection criterion was changed to a coincidence between 3 of ABDE, and 2 of FGH, but the threshold shower size was still about 10^5 particles. The recording system was unchanged.

As it now appeared that the S/N ratio would be low, it was necessary to allow for the background noise. This was done using the technique described by Allan [8] and used generally in this work [7, 12, 15]. As the impulse from the EAS signal will occur at a random time relative to the background noise, the output of the receiver will, on the average, contain the signal and noise added in quadrature. Thus to extract the signal from the noise, the amplitude at the time the EAS associated pulse is expected, and thus representing the signal plus noise, is squared, and the mean squared noise, determined from measurements at other times on the trace, subtracted. The result, when averaged over a number of events is the mean squared signal for those events. The only significant variation in the technique is the number of samples of noise taken on each trace; generally more samples give a better estimate of noise, and thus signal, especially when the S/N ratio is low.

After rejecting traces in which the noise level exceeded a pre-determined level, 396 events were available for analysis. For each trace the amplitude was measured in seven 2 us wide regions - the expectation region immediately following the shower arrival, and six others, two preceding the shower, and four following. The mean square amplitude for each time region was calculated and the results are shown in Figure 4-2; there is no evidence for any pulse associated

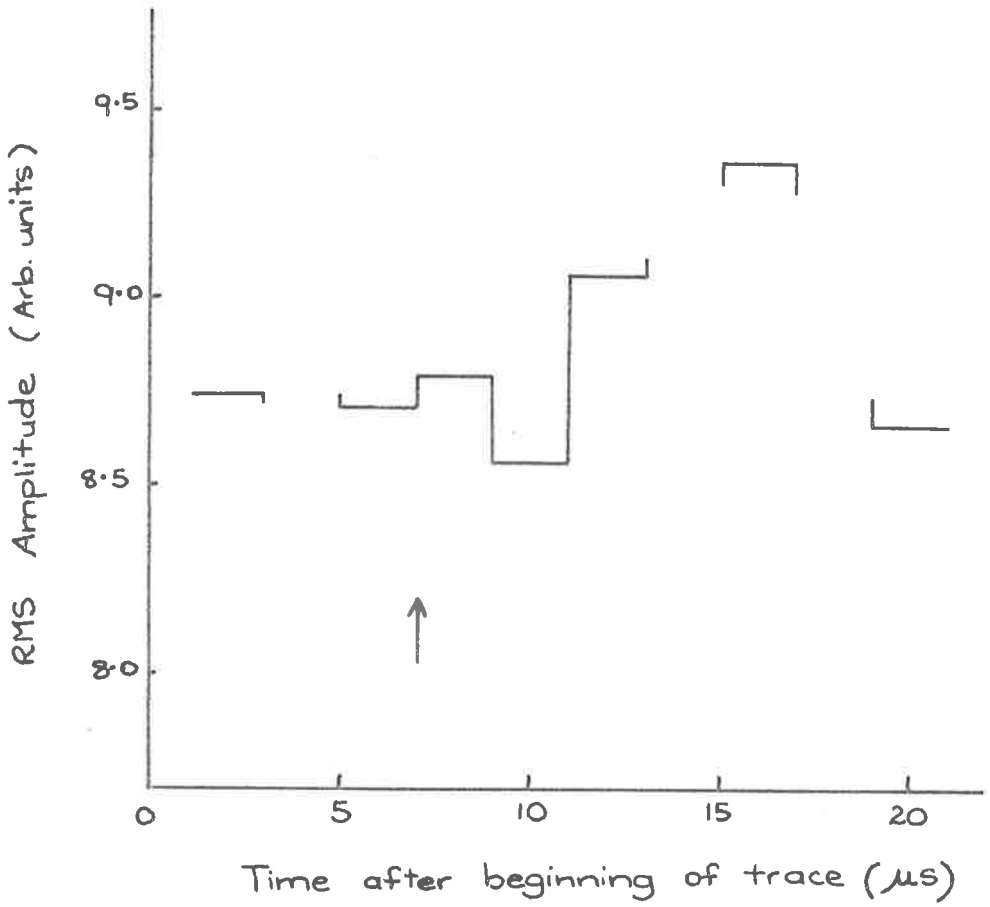

FIG 4·2 RMS signal amplitudes ($2\,MH_2$) in time intervals near the arrival of a shower. The time of shower arrival is indicated by an arrow.

with the showers. The gain of the antenna was estimated to be 12, and from this a 95% confidence level upper limit for any signal associated with the shower was estimated at 0.3 uV m^{-1} MHz^{-1}. This is to be compared with Stubbs' figure of 1 uV m^{-1} MHz^{-1} for showers at least 3 times smaller [9].

4.2.2 Cerenkov Trigger Experiments

After this failure to detect 2 MHz pulses, it was decided to repeat the original experiment of Stubbs.

Showers were detected by means of their Cerenkov light, using two 112 cm diameter searchlight mirrors, each with an RCA 6199 photomultiplier at its focus, as detectors. The mirrors were carefully aligned, so that the axis of each detector was vertical, and were swept with warm air to prevent misting. Each photomultiplier output was fed to a discriminator and a shower arrival was indicated by a coincidence between them. The mean rate of detection was about five showers per hour, corresponding to a minimum primary energy of about 3×10^{14} eV [23].

All 89 E-W polarised dipoles of the antenna array were connected together, to form a broadside antenna giving a pencil beam of half-width 4^{o}, directed at the zenith. The signal from the antenna was matched, by means of a length of 70Ω cable, into the 50Ω input of a solid state receiver. The bandwidth was 30 kHz, centred on 1.98 MHz. The undetected receiver output was recorded with a transient recorder and chart recorder, as previously described. The sample interval was 0.1 usec, thus 22 usec of receiver output were recorded for each event. The only changes made to Stubbs' apparatus were (1)

replacing the discriminator and coincidence unit with commercial NIM units, (2) replacing the receiver with a new solid state unit, with improved skirt selectivity, and (3) using the transient recorder - chart recorder combination rather than the multi-channel counter. This last change was responsible for a considerable improvement in the sensitivity of the experiment, as excessively noisy events could be rejected. It was found that a large contribution to the mean background noise was made by bursts of high intensity noise, lasting for from 0.1 to 2 seconds, and rejecting events during these periods resulted in a marked reduction in the apparent background. This change also allowed correct quadratic extraction of the signal, but as will be seen, this was unimportant.

The apparatus was run on clear moonless nights in February and March 1975, and 214 events were recorded. After rejection of noisy events, 139 were available for analysis. The maximum peak to peak excursion was measured in five 42 usec wide regions, including the expected pulse location immediately following the shower arrival. The amplitudes for all traces were squared and added and the r.m.s. signal for each region calculated. The result is shown in Figure 4-3. It is apparent that there is no signal associated with the arrival of the shower. The upper limit for any such signal was estimated at about 0.1 uV m^{-1} MHz^{-1} (95% confidence level) again to be compared with Stubbs' 1 uV m^{-1} MHz^{-1}.

A number of checks were made to determine whether this discrepancy was due to some artefact of the experiment. The reading of the charts was repeated by an independent reader. No significant systematic errors were revealed, and the same result was obtained. A linear addition of traces, simulating the operation of Stubbs' counter, also

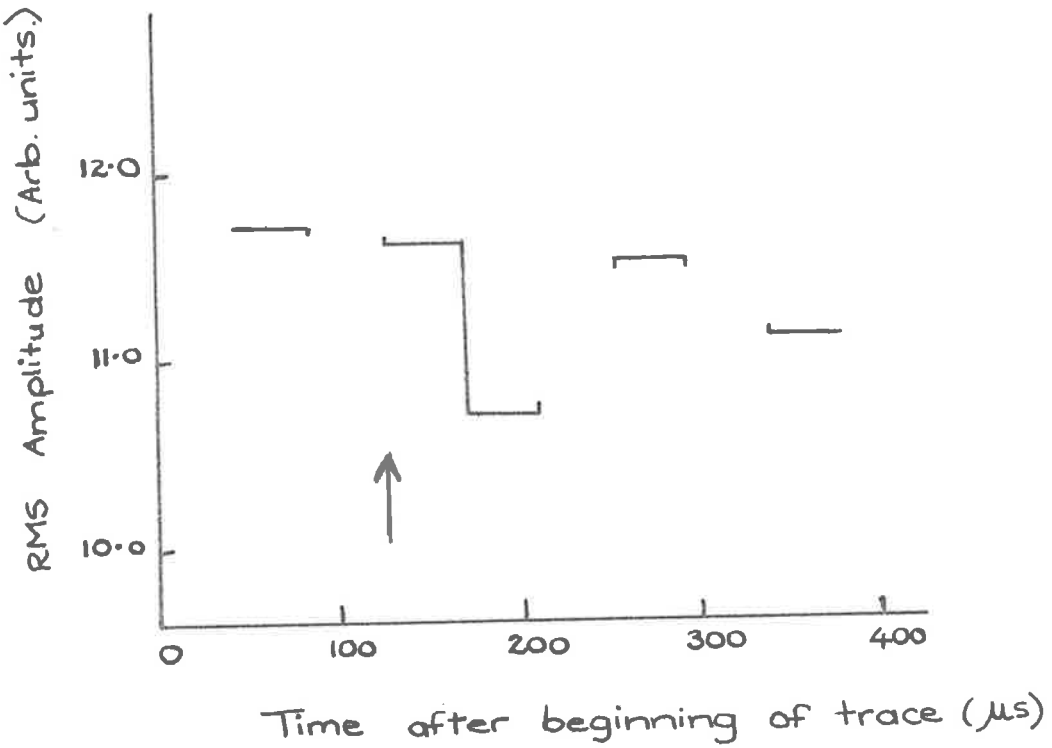

FIG 4·3

RMS signal amplitudes ($2MH_2$) in time intervals near the arrival of a shower (Cerenkov detected.) The time of shower arrival is indicated by an arrow.

failed to reveal any signal.

It has been observed that a too rigorous rejection of noisy events can lead to a reduction in signal, as genuine signals can be rejected as noise [7]. This was considered an unlikely source of error, as most of the rejected events were well above the noise threshold, few being borderline cases. However, the analysis was repeated using relaxed noise rejection criteria; no signal was seen.

The most likely source of error considered was incorrect alignment of the Cerenkov beam with the antenna beam. Following Stubbs, the latter was assumed to be vertical, as during construction a good deal of effort was made to ensure that all antennae fed in phase [24]. The mirrors were adjusted by allowing a 1 cm steel ball to roll to the lowest point of the mirror, which was then adjusted so that the lowest point coincided with the optical centre marked by the manufacturer. A plumb bob was then used to ensure that the photomultiplier was positioned vertically above this point. The technique was easy and gave consistent results, an error of 1^{o} being readily detected. The alignment was checked by focussing the images of stars onto the faces of the photomultipliers. Further evidence that the optical axes were parallel was obtained by monitoring the single photomultiplier count rates as well as the coincidences. At discrimination levels well above background noise, more than 60% of pulses in one tube were accompanied by a pulse in the other. The output of a 1 m^{2} scintillator (B of Figure 4-1) approximately 20 m from the Cerenkov detector showed that particles were arriving in coincidence with the Cerenkov trigger, and was consistent with the estimate of the shower energy. Careful checks of the receiver used revealed no abnormality.

It was thus considered unlikely that the null result of the experiment was due to an experimental defect.

4.2.3 Analysis of an Experiment at 3.6 MHz

These failures to detect 2 MHz pulses raised doubts on the reported observations at other frequencies, and Dr J.H. Hough was approached for further information on the 3.6 MHz experiment. He very generously allowed the author to examine the records from a previously unanalysed 3.6 MHz experiment.

The experiment had been conducted at Penticton, B.C., using the University of Calgary scintillator array [15]. The antenna was a 3.6 MHz folded dipole, polarised E-W and suspended 10 m above the ground. The undetected output from the receiver was displayed on an oscilliscope screen, and photographed whenever a trigger was received from the scintillator array. The system bandwidth was 0.4 MHz. Thus, for each event a film record of 20 usec of receiver output, and full shower analysis (i.e. size, core location and axis direction) was available. The mean shower size was about 2.10^6 particles.

After excluding all events where the noise exceeded a pre-determined level, and those where the film image was too faint for accurate reading, 568 events remained. The peak to peak amplitude of the trace was measured at fourteen points, seven in a 3.6 usec interval containing the air shower arrival and seven in a similar interval 4.5 usec later. The amplitudes were squared and added, and the resulting rms amplitude for each sample point is shown in Figure 4-4. There is no evidence for any signal associated with the shower.

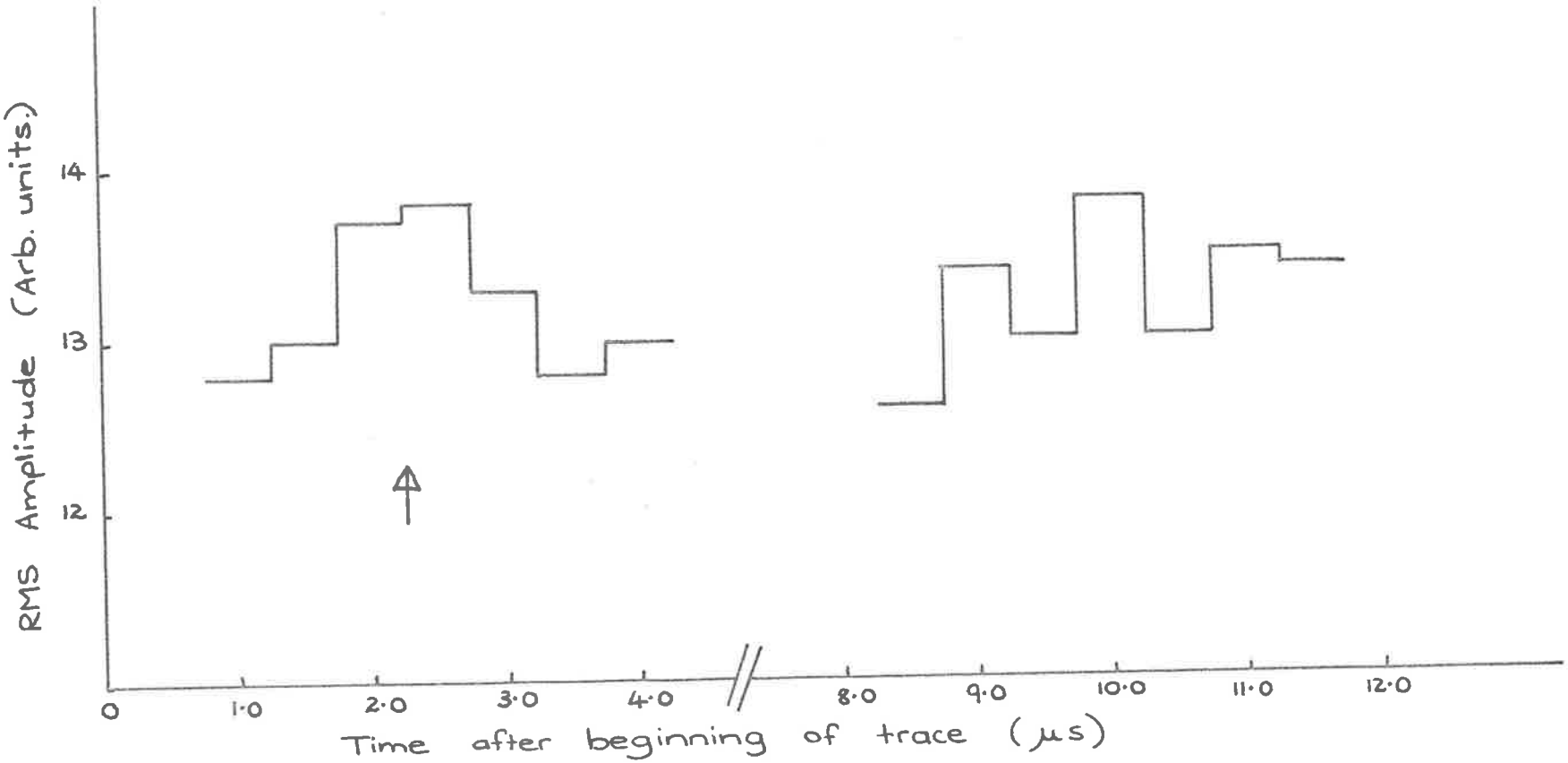

FIG 4·4

RMS signal amplitudes (3·6 MH_2) in time intervals near the arrival of a shower. The time of shower arrival is indicated by an arrow.

Various subsets of the showers were examined to see if any signal could be observed. In particular the 44 largest showers, the 30 showers with largest (size x geomagnetic factor) and 68 particularly quiet events were examined, but no signal was observed in any case.

The upper limit, at the 95% level, for any excess signal at the receiver input was 1.2 uV. From this, the maximum field strength produced by a shower of size 2×10^6 particles, was estimated to be about 0.5 uV m^{-1} MHz^{-1}. This should be compared with Hough et al's figure of 2.5 uV m^{-1} MHz^{-1} for showers of mean size 5×10^5 particles.

4.2.4 Association Between Pulses at 2MHz and 100 kHz

As will be described in the following chapter, several short experiments were conducted during the setting up of the 100 kHz recording system. In one of these, both 100 kHz and 2 MHz signals were recorded simultaneously, the 2 MHz using the four antenna system previously described, and the 100 kHz using antenna A1 and the recording system described in Chapter 5. During this run large pulses were detected by the 100 kHz system.

After rejecting noisy events, 94 2 MHz traces remained, and they were analysed in the manner previously described. Figure 4-5a shows the result. The 100 kHz records were now examined for the presence of large signals, and 30 events were selected. The rms amplitudes for the corresponding 2 MHz traces were calculated, and are shown in Figure 4-5b.

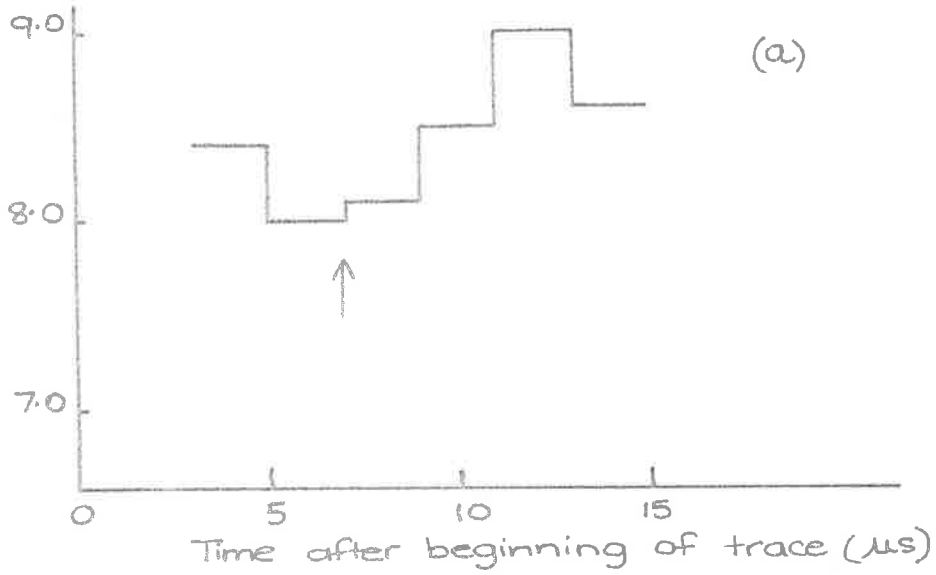

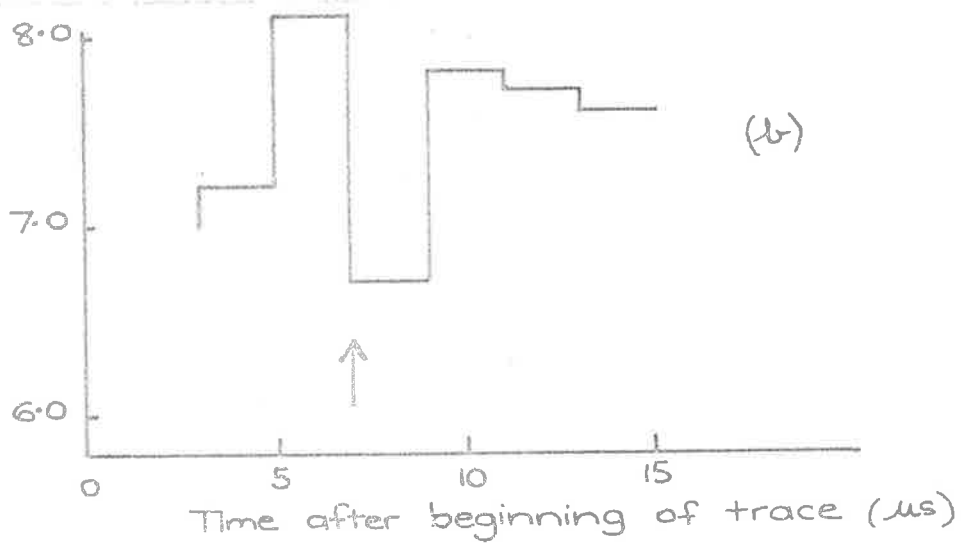

FIG 4·5

2 MH_2 Amplitudes in time intervals near the arrival of an air shower, measured during a period in which 100 KH_2 pulses were observable.

(a) all events
(b) events with large 100 KH_2 signals.

The time of shower arrival is indicated by arrows.

There is no indication in either case of any 2 MHz signal produced by the showers. The upper limits for any such signal were estimated at 0.4 uV m^{-1} MHz^{-1} and 0.5 uV m^{-1} MHz^{-1} respectively.

These results should be treated with some caution. As will be described in Chapter 5, this run was a pilot run, intended to test the recording system, and ensure that no interference was present in or generated by the apparatus. Consequently calibrations and other tests were not carried out as thoroughly as in the regular runs described earlier. However, when after the disappearance of the 100 kHz signals, it became apparent that the experiment might not be able to be repeated, the system was rechecked carefully. No sources of error were found, and the calibrations were found to be correct.

Thus, although no source of error is known, these problems, and the relatively small number of events available, reduce the weight which should be accorded to the result.

Although the obvious implication of this result is that the 2 MHz and 100 kHz signals are not due to a common mechanism, this conclusion cannot be reached without knowing the 100 kHz field strength during periods in which 2 MHz pulses were observed. It may be that the 100 kHz signals at such times are much larger than those so far observed.

4.3 Further Reported Work at 2 MHz

While these 2 MHz experiments were in progress two other experiments at this frequency were reported. One was performed at Yakutsk [4], where, although some signals were observed, no signal as large as one-tenth of the previously reported field [8, 9] was observed, even

with showers as large as 10^8 particles. The other experiment was at Haverah Park, where Allan et al. [1] were also unable to detect any signal. They estimated an upper limit of 0.6 uV for 10^{17} eV showers - this value is comparable with the signal expected from the geomagnetic mechanism.

Both these results are in sharp disagreement with the early, high field strengths reported, and are consistent with the lack of signal reported here.

CHAPTER FIVE

EAS ASSOCIATED RADIO PULSES AT A FREQUENCY OF 100 KHz

5.1 Discovery of 100 KHz Pulses

As has been noted, the conventional theories of radio emission (geomagnetic and charge excess) predict a monotonic fall in signal strength at low frequencies. The reported rise in signal between 22 MHz and 2MHz thus aroused interest in the behaviour at still lower frequencies.

Immediately below 2MHz, the presence of medium wave broadcasting makes detection of small signals difficult, but in Australia, the frequency region below this band (i.e. < 500 KHz) is relatively unused. Taking advantage of this, Clay and Gregory [1,2] performed a search for radio pulses at 100 KHz. The results were spectacular. Large pulses, standing well above the noise were observed on a large number of events; the mean signal to noise ratio was about 2, far greater than that observed at any other frequency. The field strength measured was hundreds of times greater than that observed at 2 MHz [3,4] and indeed was consistent with an extrapolation of Felgate and Stubbs' spectrum [5]. A second unexpected result was that the observed pulse amplitudes were variable, both diurnal variations, and irregular fluctuations on a timescale of a few days being observed.

These results were even more wildly at variance with theory than

those at 2 MHz [6]. In particular, calculations showed that if the spectrum continued rising for an octave or so below 100 KHz, the total energy in the radio pulse would approach the total shower energy. It was obvious, if the result was not spurious, that this was some new phenomenon.

A great deal of effort was applied to ensuring that no spurious effects were present. Random pulses were fed, in various ways, into the shower detecting system, in order to trigger the recording system. No signal was observed in coincidence with these 'artificial showers'. In order to check the possibility of pulses being picked up from the scintillation detector cables or photomultipliers, runs were made with the EHT supply disconnected from each detector in turn. Only slight changes in signal strength, which could be explained by the different shower triggering conditions, were observed.

Although no shower analysis was available, a positive correlation between signal strength and shower size was observed. In one experiment, the shower triggering thresholds were increased; the mean pulse amplitude was found to increase also. In a second experiment, the outputs of discriminators connected to the scintillation detectors F, G and H (Figure 5.1) (which were not used to obtain an EAS trigger) were recorded. A positive correlation between 100 KHz signal and the number of sites recording particle densities above the discriminator thresholds, was obtained. Both of these experiments indicated that larger showers produced larger 100 KHz signals, a result unlikely to be obtained from spurious signals originating in the recording electronics, although it does not exclude the possibility of pick-up from apparatus carrying particle density signals [7].

These tests appeared to confirm that the radiation detected was not of spurious origin. An attempt was made to measure the lateral distribution, using an antenna approximately 400 m from the array, but this attempt failed, as the fluctuations in pulse amplitude became so large that it was impossible to obtain valid estimates of the mean signal. Signals were, however, observed at the 400 m site [7].

Shortly after this, the signals disappeared completely. Apart from intermittent monitoring, which showed that the signals returned in the following summer [7], no further experiments were performed by Clay and Gregory.

5.2 Experimental Work at 100 KHz

Following the completion of the 2 MHz experiments, work was commenced at 100 KHz. The first aim was to check the validity of the Clay-Gregory results, chiefly by an exhaustive check of possible sources of interference. If the effect was found to be genuine, then further experiments to determine the relationships between pulse size and shower parameters would be performed.

A modified recording system (described in the following section) began operating in December 1974, and immediately 100 KHz pulses, for which no spurious cause could be found, were observed. A series of short pilot experiments were then undertaken, in order to test various aspects of the system, while the EAS particle recording system was completed. These experiments were abruptly terminated when the local rabbits developed a taste for cables, making it necessary for all unburied cables to be raised above their reach. All apparatus was completed in March 1975, and recording of two 100 KHz channels, and

shower parameters commenced. Recording continued for 10 days, and strong 100 KHz pulses were observed. However, a fault developed in the shower recording system, and during repairs, it was found that a change in a colleague's experiment had contaminated some of the previous events by adding a spurious signal to the observed pulse. (This contamination, and its treatment, is discussed in Section 5.2.2.) Eight days later, when recording recommenced after completion of repairs, no signal could be observed. Recording continued for several months, but without success.

This behaviour seemed to confirm the seasonal effects observed by Clay and Gregory [1,2], although the observable period seemed rather shorter, and the pulses were expected to return in the following summer. Further extension of the recording system, with additional antennae, and a device for recording the earth's electric field were prepared in anticipation, however no signal was observed during the summer 1975-76. Monitoring continued to the summer 1976-77. Again no clear signal was observed, although there was some indication of weak pulses during one week in early 1977.

The available data thus consist mainly of a 10-day run in March 1975, with full shower analysis, the radio pulses being recorded with antennae A_1 and A_2 of Figure 5.1. Data from the short test runs between December 1974 and February 1975 were generally without shower analysis, however some of these events could be used, particularly to compare various antennae systems. This is obviously not enough data to enable the parameters of 100 KHz radiation to be fully investigated, particularly as the mean pulse amplitude appeared to fluctuate a good deal in the first period. However, the data was sufficient to show some relationships between parameters, and these

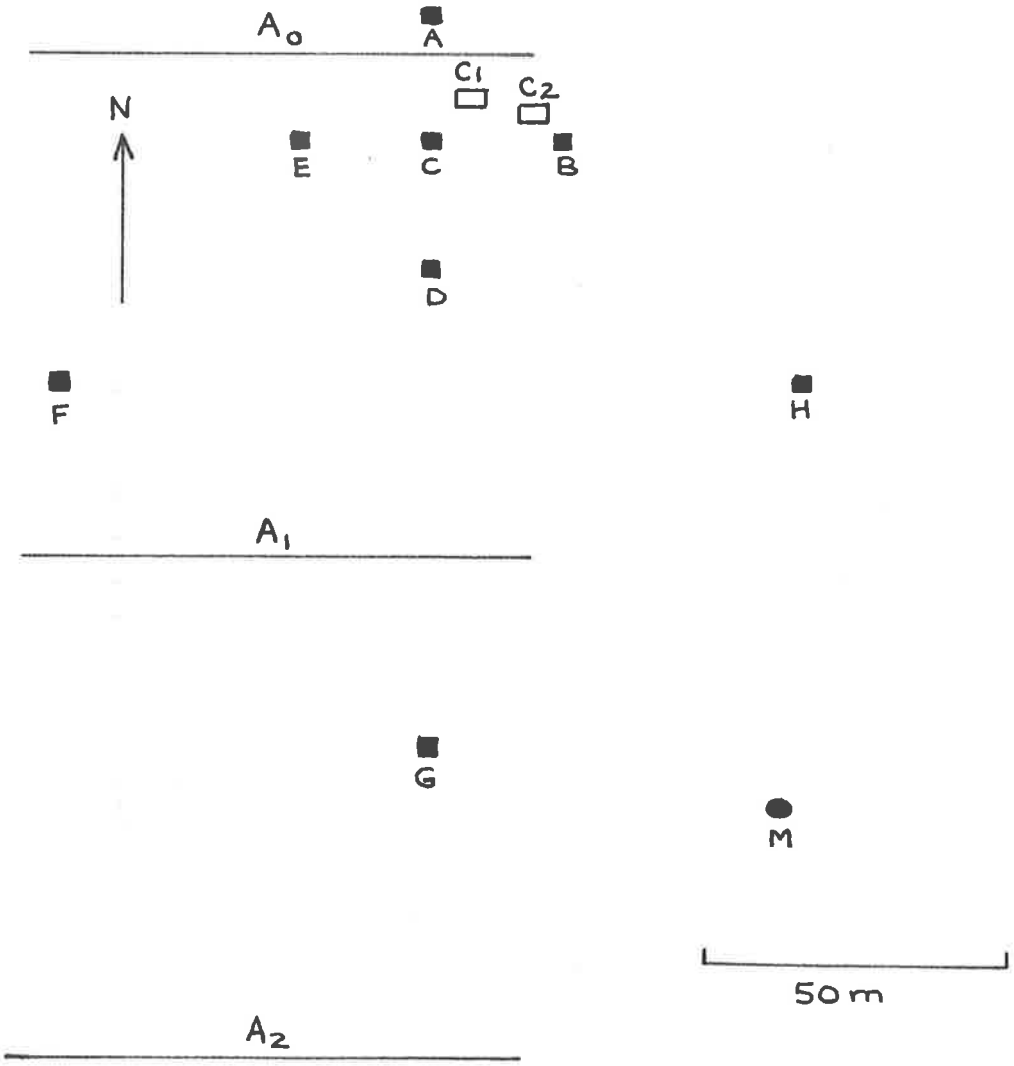

FIG 5-1

Plan of the Buckland Park Array, showing 100 kHz antennae.
■ Particle detectors.
A_0, A_1, A_2 - horizontal antennae.
M - monopole antenna.
C_1, C_2 - recording caravans.

are discussed in the following sections.

5.2.1 Apparatus

Although Clay and Gregory were unable to find any spurious source for the 100 KHz pulses they observed, it was decided, in view of the unusual nature of the effect, to use a new system for these further experiments. The three most important changes were the mounting of the (battery powered) receivers directly below the antennae, rather than in the recording caravan; the resiting of the radio recording equipment in a second caravan, separate from the EAS recording equipment; and the use of antennae at some distance from the EAS recording caravan. The main aim of these changes was to remove the radio system from the vicinity of possible sources of interference in the particle system, however, the first change had the desirable effect of minimising the capacitive loading of the antennae.

The location of the radio equipment is shown in Figure 5.1. A_0 is Clay and Gregory's original antenna, A_1 and A_2 are similar, that is, approximately 95 m long, and suspended about 3 m above ground. Each receiver is fed from the eastern end of the antenna, through about 2 m of bare wire, and 1 m of coaxial cable. M is the 'monopole' antenna, a 10 m length of wire, supported vertically by a wooden pole and feeding a receiver at its foot, through 1 m of coaxial cable.

The radio recording equipment was housed in caravan C_2. Each receiver was fed through a high pass filter, designed particularly to reduce interference picked up at a frequency of about 30 KHz, to a Biomation 610 Transient Recorder - Chart recorder combination, as

described in the previous chapter. The sampling rate used on the transient recorder was 1 usec, thus about 220 usec of receiver output was recorded for each event. Approximate timing information was obtained by producing a blank event every 2 hours.

The receivers used, with bandwidth of 80 KHz, centred on 100 KHz, were identical with the one used by Clay and Gregory.

The air shower recording equipment was in caravan C_1. The air shower triggering criterion was again 3 of A, B, D or E, and 2 of F, G or H, as in the 2 MHz experiment; the minimum shower size was about 10^5 particles.

5.2.1.1 Tests for Spurious Responses

Two general approaches available to show that signals are not spurious are firstly, to anticipate possible interference sources, and show that they are not responsible for the observed signals, and secondly to show that the signals have properties (e.g. correlation with EAS parameters) which would not be expected with spurious mechanisms. Neither technique is foolproof, as they are both based on preconceived notions of the properties of signal or interference; both were used in this case.

In the first approach, EAS derived signals were systematically replaced with 'random' signals, and the receiver output was checked for the presence of (spurious) signals. This was a fairly simple matter for signals inside the recording caravan; the whole recording system could be triggered by replacing the pulses from the particle detectors with pulse generator signals, or by changing the coincidence

arrangements so that the array triggered off the (unaccompanied) signal from each detector in turn. The latter also tested for pick-up produced by the scintillation detectors, and their associated cables; a further test of this section of the apparatus was made by introducing large pulses into the detector preamplifiers, and triggering off these. No signal was observed associated with any of these non-EAS triggers. In addition, a large amplitude 100 KHz sine-wave signal was injected into all signal-carrying cables in the EAS array. Again no signal was observed on the receiver output.

The original experiments of Clay and Gregory used only the fast timing section of the EAS array to detect showers, the remaining sites were not operating. A test was therefore made by detecting showers with the 'slow' array only; the slight change of signal observed was consistent with the change in shower size resulting from the changed coincidence requirement.

The second approach to the identification of spurious signals was based on the assumption that EAS associated signals would be correlated with the shower size. As will be shown in Section 5.2.3.3 this was found to be the case. This does not eliminate the contention that a spurious signal was produced by the output of a particle density detector, for this would also be expected to be correlated with shower size. However, as can be seen in Figure 5.2, the dependence of 100 KHz signal on density at the detector D is very weak, and is even weaker for the other detectors.

Further evidence for the dependence of 100 KHz signal on EAS size, but independence from the pulses representing particle densities, was obtained in a run in which the EHT supply to the particle detector

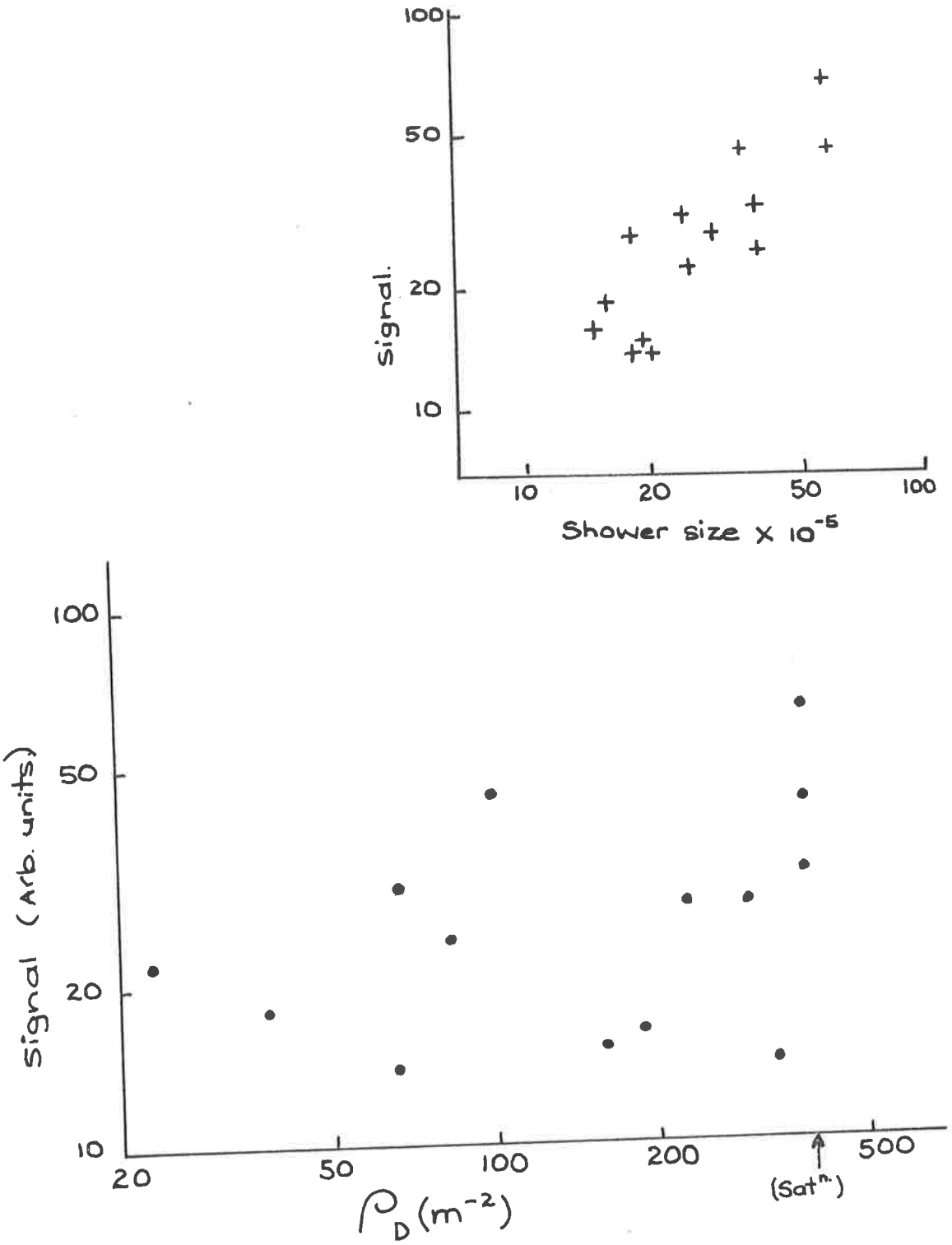

FIG 5.2

Relationship between signal amplitude and particle density at detector 'D'
The 14 largest showers recorded are plotted.
The relationship between signal amplitude and shower size is shown for comparison.
(see fig 5.7.)

photomultipliers was reduced by 100 V. This resulted in the detector gains being reduced by a factor of about 2, thus the minimum size of showers triggering the array was doubled, while the detector signals were unchanged. The ratio of the mean 100 KHz signal during this run to that obtained before and after was 2.7 ± 0.6.

Thus, two independent experiments show a relationship between shower size and signal, and in addition, a smaller but significant dependence of signal on the shower core location will be demonstrated (Section 5.2.3.4). Both of these properties are reasonable a priori assumptions about the behaviour of EAS generated signals, and appear unlikely to be satisfied by a spurious mechanism. It is concluded that the 100 KHz signals observed are not a spurious artifact of the experiment.

5.2.2 Analysis

The technique used to extract the signal from the background noise was similar to that used in the 2 MHz experiments. As the signal to noise ratio was generally high, the noise was estimated by measuring the maximum p-p amplitude in only three 30 usec wide intervals, two immediately preceding the air shower arrival, and one some 70 usec later. The signal plus noise was measured as the maximum amplitude in a similar interval commencing at the time of shower arrival (the expectation region). Events with the background noise above a predetermined criterion were rejected, and in order to be more certain that noise pulses were not included as signal, isolated quiet events in otherwise noisy conditions were also rejected.

As has been noted, much of the data was contaminated with pulses produced by a colleague's apparatus. The pulses were found to be entering the 100 KHz system via the antennae, and occurred approximately 750 ns after the air shower arrival. As this time is much less than one period at 100 KHz, this pulse would be expected to add linearly to any EAS generated signal.

Some evidence for this assumption is presented in Figure 5.3, where, using the methods outlined in Section 5.3.3 following, the pulse amplitude from antenna A_1 has been plotted against shower size. Figure 5.3(a) was taken from data recorded before the advent of the interference, while Figure 5.3(b) represents the bulk of the data, including interference. Both sets of data are consistent with a straight line, the difference in slopes being due to the different mean signal. The amplitude of the interference was measured to be 9.5 units, in excellent agreement with the intercept in Figure 5.3(b). Interpreting Figure 5.3(b) as a linear size dependence with the addition of a constant interference signal, leads to the conclusion that the true signal can be obtained by linear subtraction of the 9.5 unit interference. This correction has been made wherever necessary.

It should perhaps be noted that the interference could be recalled at will: the true signal could not.

5.2.3 Results

5.2.3.1 Field strength measurement

The field strength estimates made by Clay and Gregory suffered from

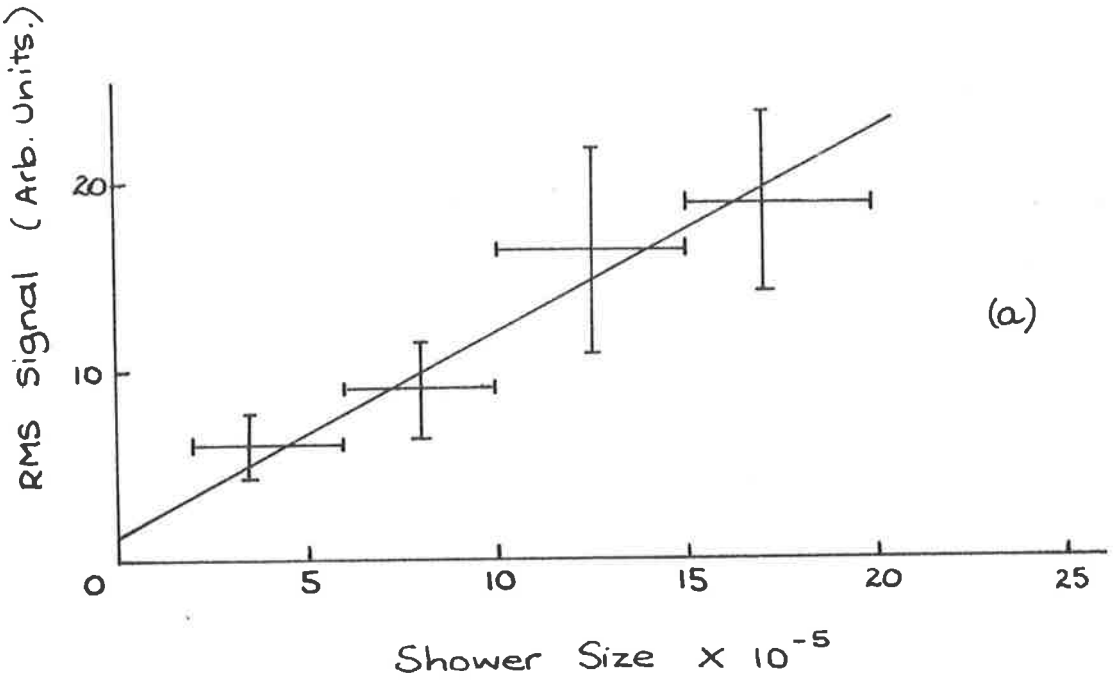

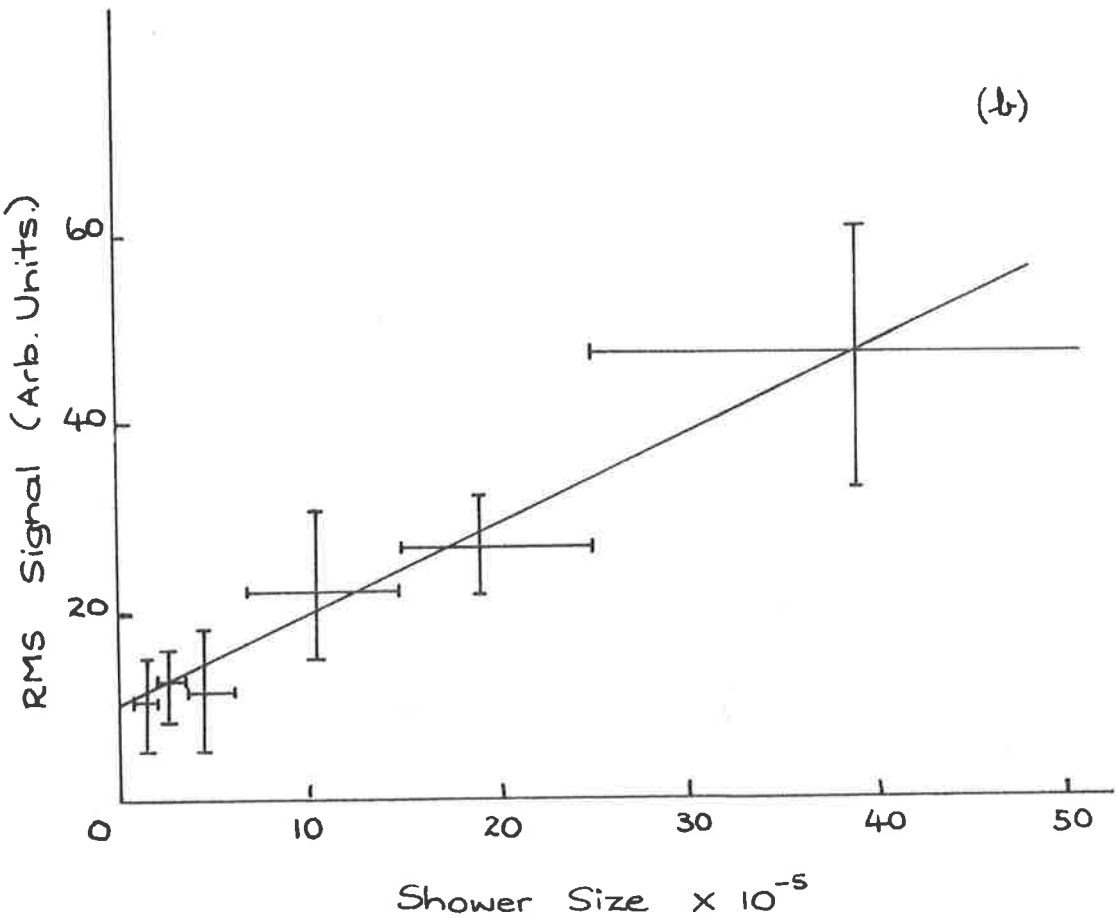

FIG 5·3

The relation between "apparent signal" and shower size, showing the effect of interference.

(a) without interference.
(b) interference present.

the disadvantage that the antenna used was attached to one of the poles of the 2 MHz antenna array, and thus was in close proximity to the 2 MHz feeder cables. To overcome this problem a new antenna was built, consisting of a 10 m vertical wire, supported on a wooden pole located equidistant between 4 of the 2 MHz antenna poles (point M of figure 5.1). The receiver, mounted at its base was fed through about 1 m of coaxial cable. Six 20 m long copper wires were buried, radiating from the antenna to form a ground plane. This antenna was used to measure the background noise level, using the method described by Watt [8], and the result is shown in Figure 5.4, together with the predicted noise level [8]. The observed noise level was typically 4 to 6 db below the predictions. Some of this discrepancy was due to the receiver saturating during excessively noisy periods, while it would also be expected that the surrounding 2 MHz array might modify the observed field.

Only a few events (63) were recorded on this antenna and available for calculation of the mean signal field strength. However, examination of the pulses recorded simultaneously on the horizontal antenna A_1 showed that their amplitudes were typical of the whole period, although only about 70% of the overall mean. The vertical component of the mean pulse field strength, as recorded on the monopole antenna was calculated, again using the method of Watt [8], and was found to be 150 uV m^{-1} MHz^{-1}. Allowing for the lower mean field strength for this period, the overall mean field strength from showers of about 3×10^5 particles was 200 uV m^{-1} MHz^{-1}. Although this measurement is only half of the mean signal reported by Clay and Gregory, it is well within the observed range of variation.

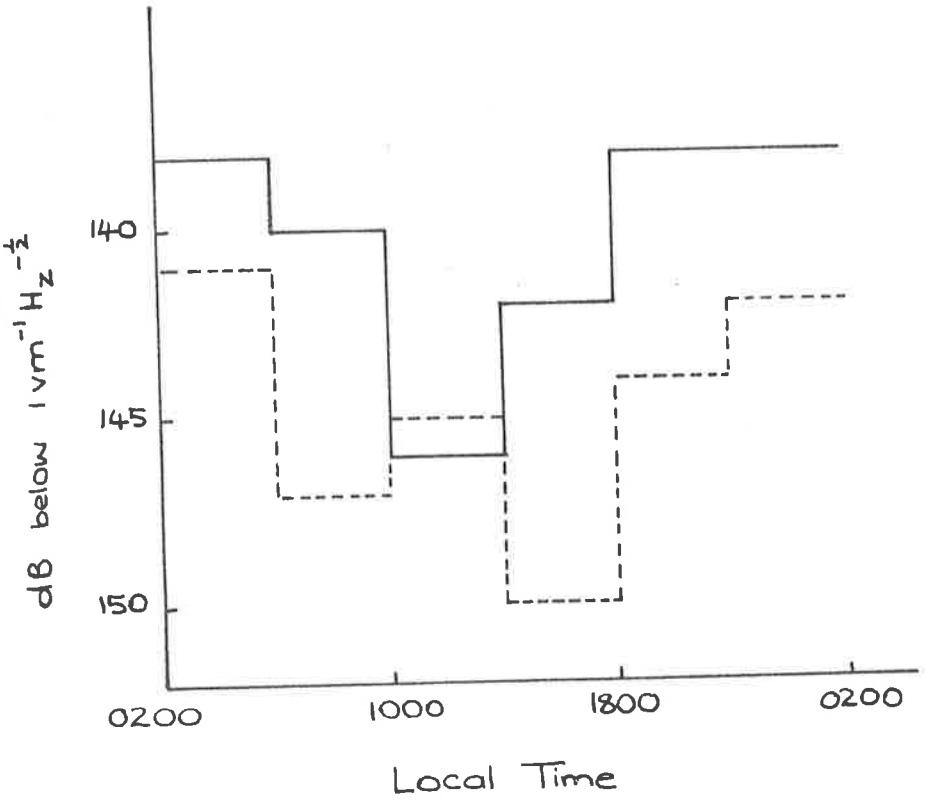

FIG 5·4 100 kH_z Radio Noise

——— From Watt [8]

- - - - - Measured at Buckland Park.

5.2.3.2 Signal Strength Variations

Clay and Gregory observed that the mean 100 KHz signal varied, both diurnally, and also on a time scale of several days. This effect was investigated by measuring the mean signal, from antenna A_1, in four-hour intervals over the 10-day period of the experiment. The result is shown in Figure 5.5 ; an overall decline in amplitude over the period is apparent. Eight days later, as already noted, the signal could not be observed at all; it had declined to less than 10% of its previous value. Changes of this scale are comparable with those observed by Clay and Gregory.

It has been suggested by many colleagues that atmospheric conditions may be responsible for the signal variations, either directly, by affecting the emission mechanism, or by an indirect effect, for example on the antenna characteristics. An indication of the weather, including the maximum temperature and humidity, is included in Figure 5.5 : no effect is evident. The weather remained warm and fine for the week following this period, during which the signals disappeared.

The mean diurnal variation obtained is shown in Figure 5.6, with Clay and Gregory's data for comparison. The magnitude of the variation is similar, but the phase is different, and thus this data does not support the suggested geoelectric mechanism [1].

5.2.3.3 Shower Size Dependence

A more rigorous noise selection criterion was now applied to the data used in the previous section, and the resulting events were sorted into six shower size groups. The noise threshold was then

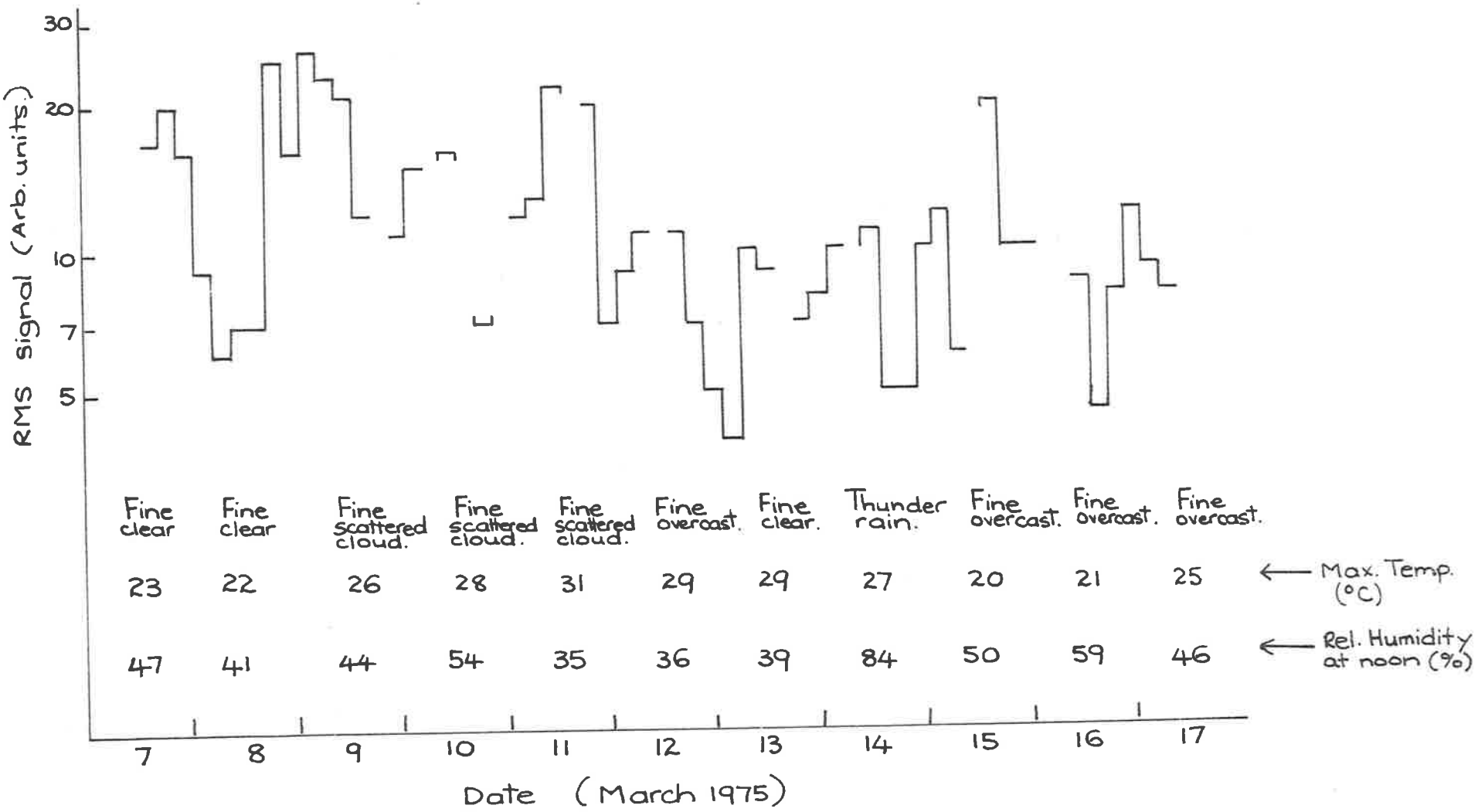

FIG 5·5

Variations in 100 KHz signal strength.

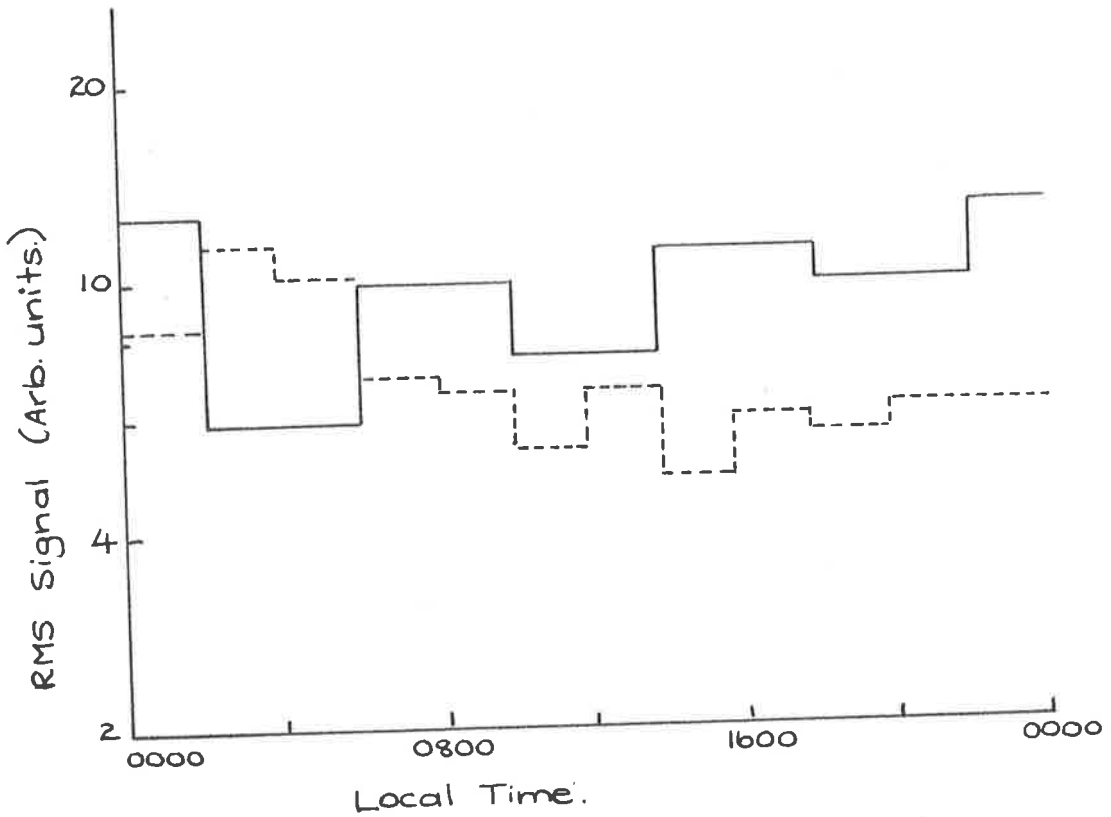

FIG 5·6 Diurnal variations of 100 KHz Signal.

—— Present work.

----- Clay et al [1]

relaxed somewhat for the two largest shower size groups, resulting in a total of 143 showers being selected. The mean signal in each shower size group was then calculated, and the result is shown in Figure 5.7. The fourteen largest showers are also plotted individually on this figure, the mean S/N ratio for these showers being greater than 3. It is evident that there is a strong linear dependence of signal amplitude on shower size (correlation coefficient $r^2 = 0.95$).

It may be argued that the 100 KHz pulses are a purely local effect, for example, caused by the discharge of the atmospheric electric field in the immediate vicinity of the antenna. This would be expected to produce a strong correlation between pulse amplitude and local particle density. In Figure 5.8 the pulse amplitude of the 14 largest showers is plotted against the number of electrons falling within 1 m of the antenna. The relationship is obviously very much weaker than that with shower size and can be explained by the correlation between the particle density at the antenna and shower size. (Only the largest showers were investigated in this way; small showers showed a stronger relationship. This is because, as the small showers were detected only if their cores fell in a fairly small region (near detector C), changes in antenna density were strongly dependent on shower size.)

5.2.3.4 Lateral Distribution

As the 100 KHz pulses from the showers used in the previous section were measured on two antennae (A_1 and A_2 of Figure 5.1) spaced 95 m apart, it was possible to measure the lateral distribution of the pulses out to core distances of about 200 m.

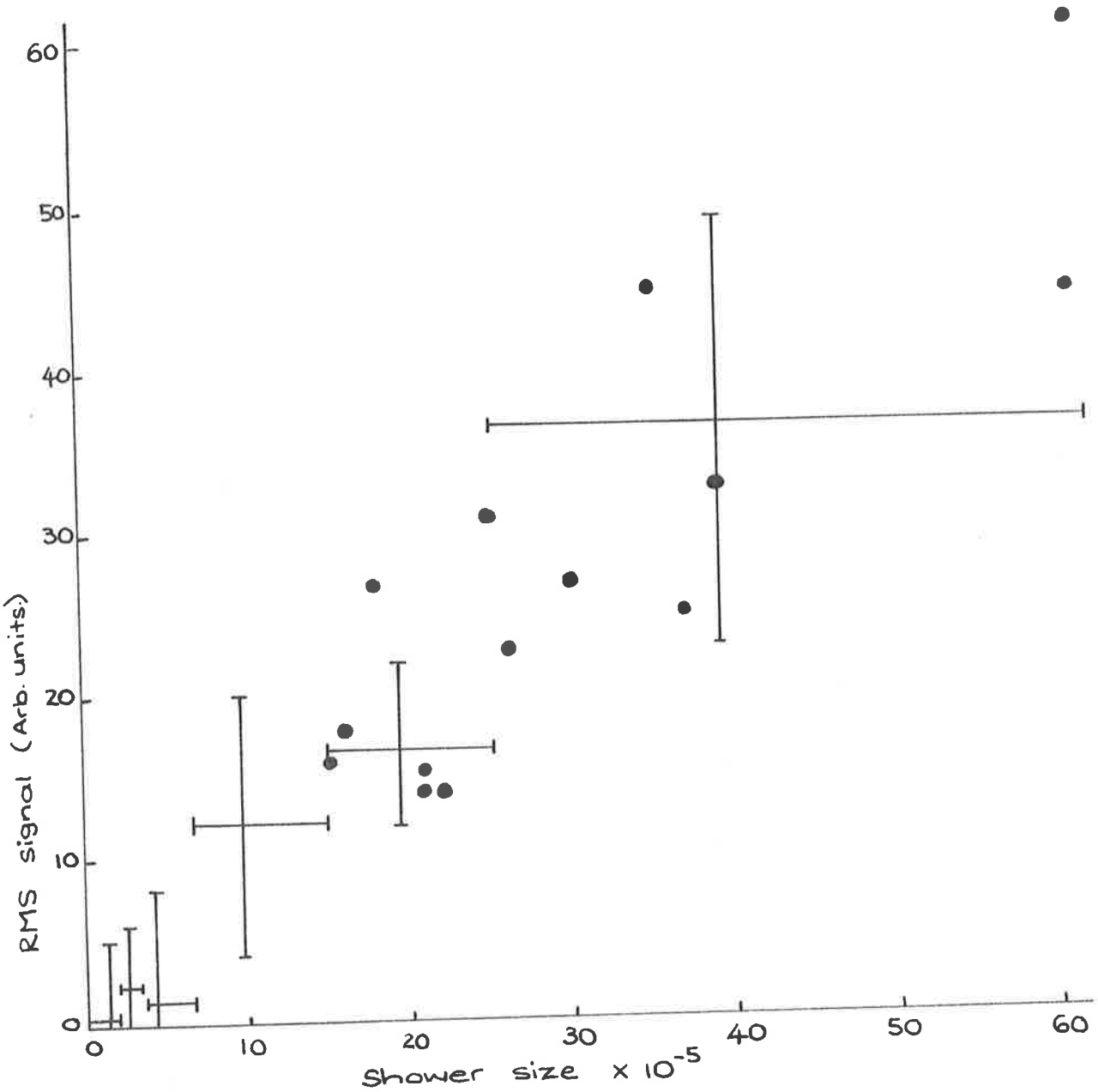

FIG 5·7

Relationship between 100 kHz signal and shower size. The 14 largest showers are plotted individually.

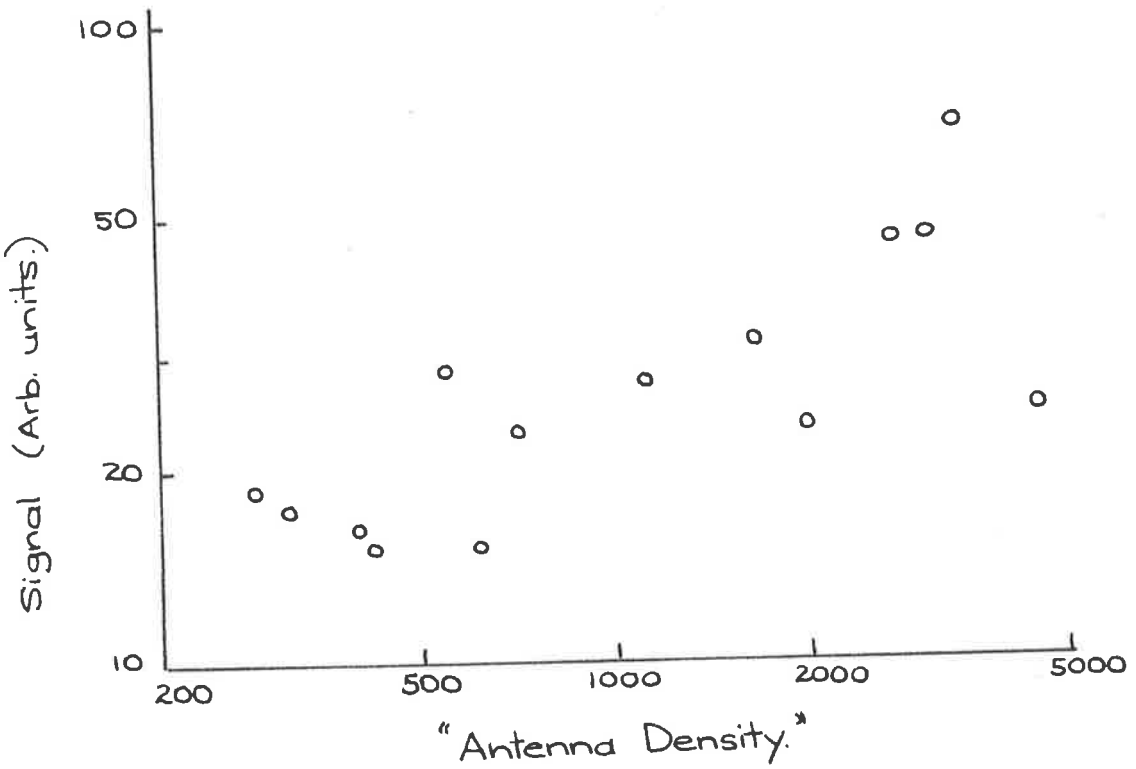

FIG 5·8
Relationship between 100KHz signal and number of particles falling near the antenna.

By measuring the background noise observed by both antenna-receiver combinations, the relative system gain was calculated; both for average background levels, and for impulsive noise. The ratios were the same, and equal to the ratio of receiver gains measured in the laboratory, indicating that the antenna characteristics were similar.

The analysis of the relationship between shower size and pulse amplitude was now repeated, using antenna A_2. A similar straight line plot was obtained, but the slope, after allowing for the receiver gain difference was 0.67 ± 0.13 of that obtained with antenna A_1, indicating that the field was reduced by this amount.

The showers were now sub-divided into three groups, according to the distance of their cores from antenna A_1. (Again only larger showers ($Ne > 6.5\ 10^5$) were used, to avoid biases due to the irregular distribution of small showers.) The mean pulse amplitude at each antenna was calculated, and these data, corrected linearly for the small size differences between shower groups, are shown in Figure 5.9. These results are consistent with an exponential distribution, of the form $s = \exp(a/r)$, where a is approximately 200m. Note that two substantially independent experiments are represented in Figure 5.9, viz. the measurement of single groups of showers on different antennae, and the measurement of different groups on a single antenna. The consistency of the results gives further weight to the validity of the data and analysis procedure.

5.2.3.5 Angular Dependence of Signals

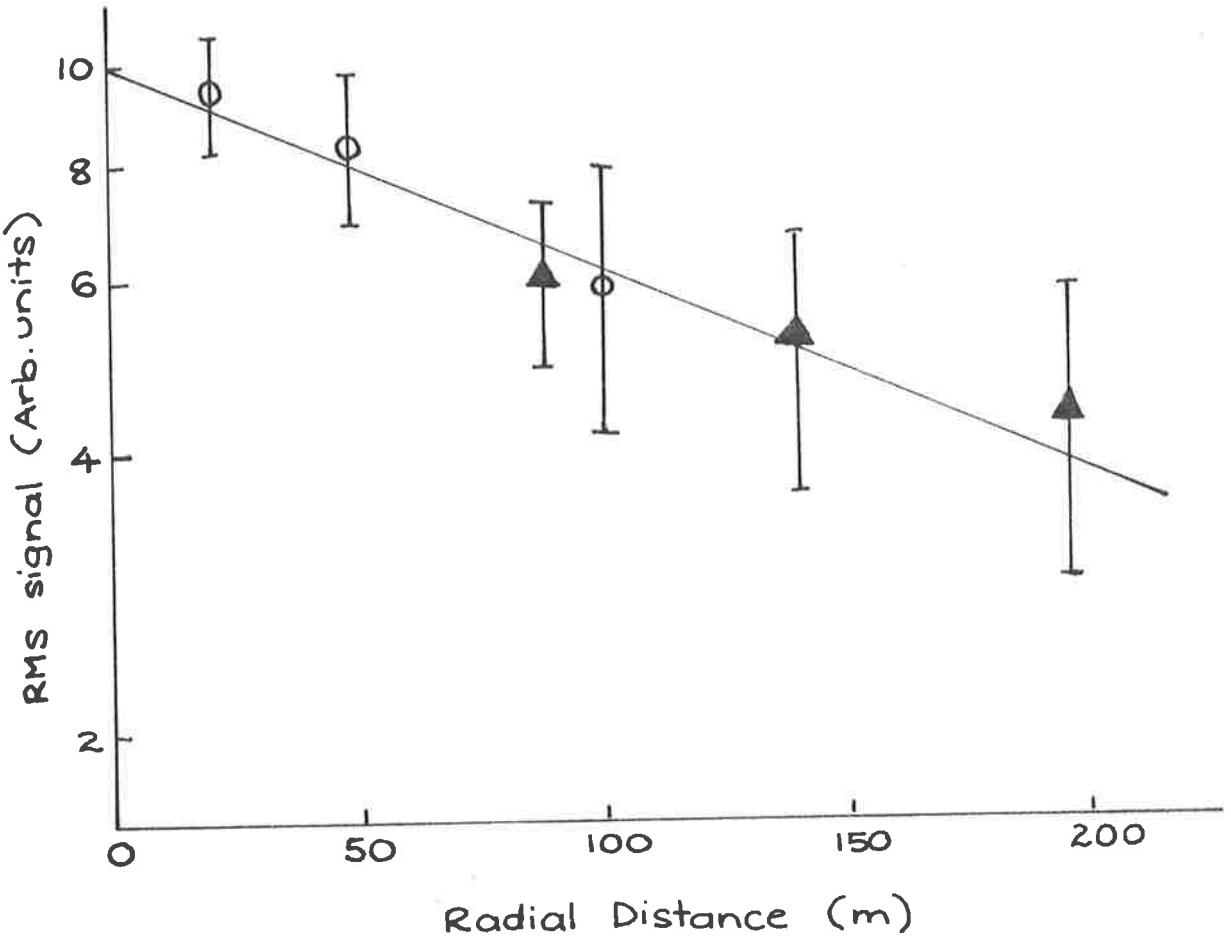

FIG 5·9

Lateral distribution of 100 KHz signals.

○ Measurement with antenna A1.

▲ Measurement with antenna A2.

Straight line $S = e^{-\frac{R}{200}}$

(1) Zenith Angle

The 143 quiet showers were divided into 3 groups, with zenith angles less than 15^{o}, 15^{o} to 35^{o}, and greater than 35^{o}, and the mean signal for each group calculated. No significant variation was observed.

(2) Azimuth Angle

The showers were divided into 4 groups with azimuth angles 45^{o} to 135^{o}, 135^{o} to 225^{o}, 225^{o} to 315^{o} and 315^{o} to 45^{o}, and the mean signal for each group calculated. No significant variation was observed.

(3) Geomagnetic Angle

The showers were divided into 3 groups, with angles between the shower axis and the geomagnetic field, less than 15^{o}, between 15^{o} and 35^{o}, and greater than 35^{o}. again, no significant effect was seen.

5.2.3.6 Pulse Frequency Spectrum

As can be seen from Figure 5.10, the shape of the EAS associated pulse differs from the impulse response of the receiver, implying that the spectrum is not flat across the receiver pass-band. To investigate this, several pulses with high signal to noise ratio were digitized by measuring the amplitude at 2 usec intervals, and, using a

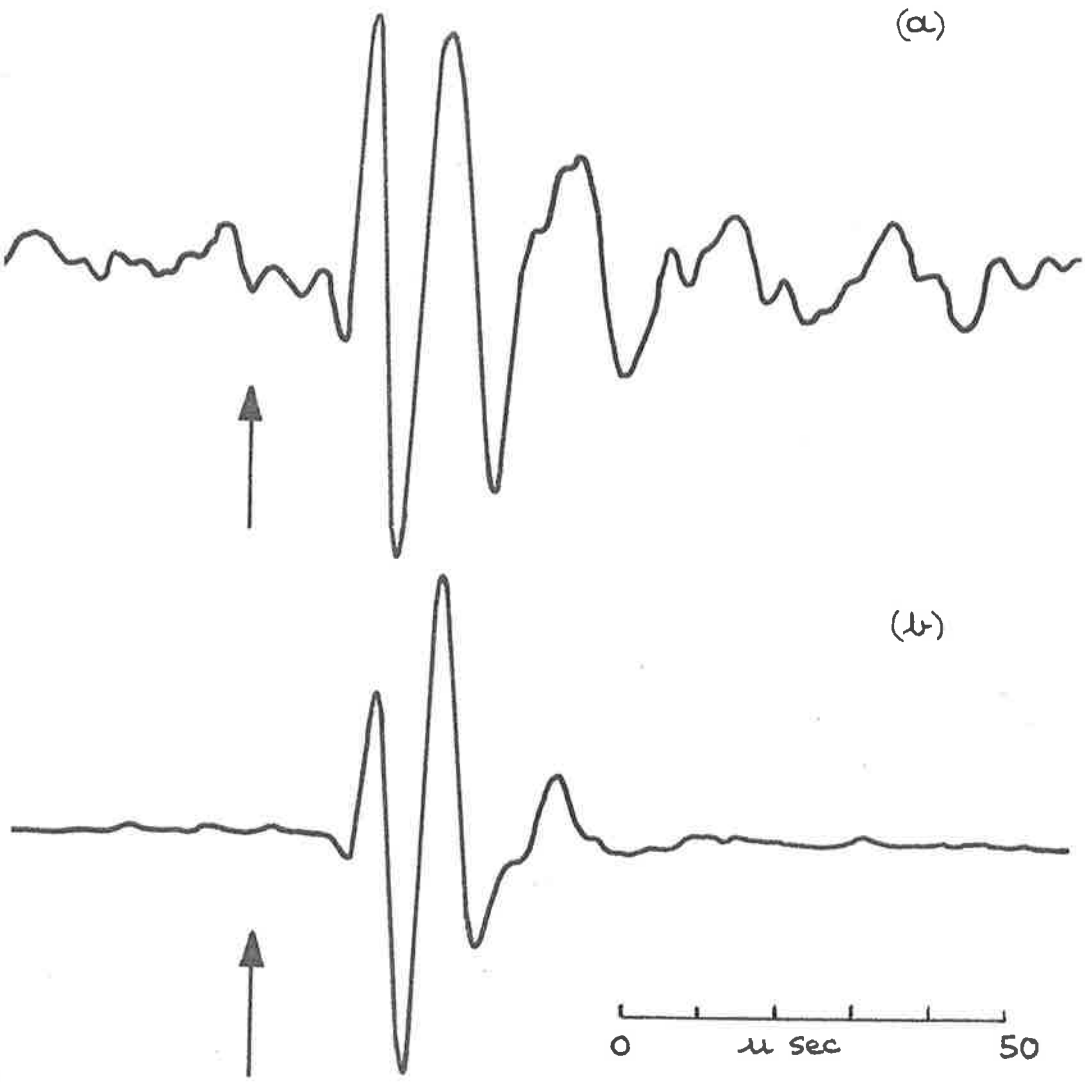

FIG 5·10

Pulses from a 100 KH_2 Receiver.

(a) typical large shower associated signal.

(b) response of receiver to a narrow impulse.

The time of shower arrival or input impulse is indicated.

The delay between input and response is due to the limited receiver bandwidth.

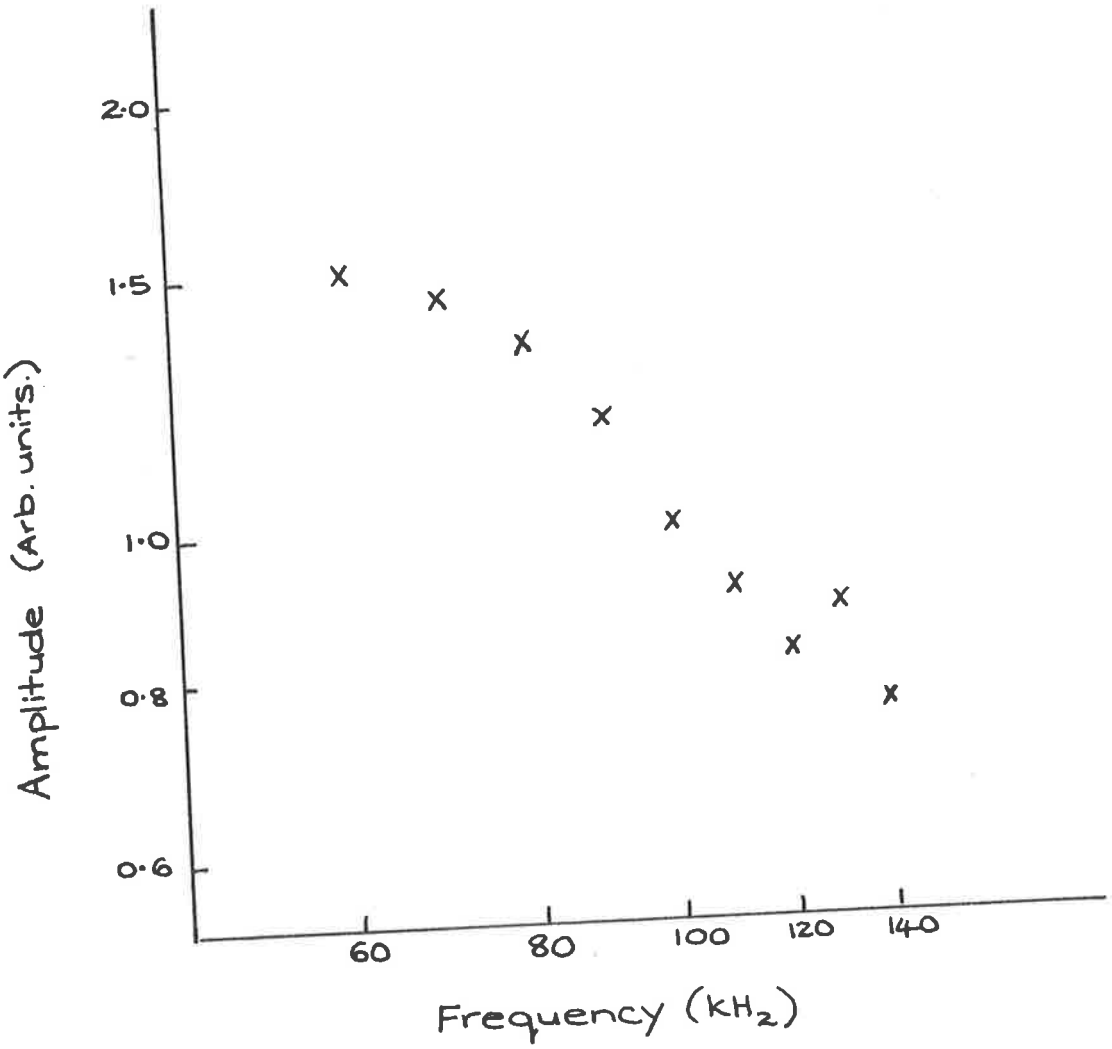

FIG 5·11 Frequency spectrum of a typical, large, shower associated pulse.

fast Fourier transform computer program, the Fourier components of the waveform were calculated. In addition, the Fourier components of the impulse response (obtained by applying a 100ns wide pulse to the receiver input) and several examples of impulsive noise on otherwise quiet traces, were obtained in the same way; both of these spectra agreed well with the receiver frequency response curve. The EAS associated signal, however, was found to be strongly peaked towards the low frequency end of the spectrum. Figure 5.11 shows the ratio of EAS associated signal to impulse response across the receiver pass-band. This rise towards low frequencies is in qualitative agreement with the spectrum presented by Felgate and Stubbs [5].

CHAPTER SIX

CONCLUDING REMARKS

> Of making many books there is no end; and much study is a weariness of the flesh.
>
> Let us hear the conclusions of the whole matter.
>
> Ecclesiastes

6.1 The Observations

In a series of observations, conducted at a frequency of 2 MHz, no radio signal which could be associated with air showers was observed. This result has been supported by more recent reports, but is in direct contradiction with a number of previously published results.

However, at 100 kHz, the existence of strong signals was confirmed. The mean signal was found to be proportional to shower size, and decreased exponentially with distance from the shower core. No dependence on the shower direction was observed. The signal strength was subject to wide variations, and remained below a detectable level for many months.

6.2 The Mechanism

At a frequency of 100 kHz, extreme fluctuations in the mean radio emission from air showers have been observed directly. If the mechanism responsible for the 100 kHz pulses can also produce pulses at higher frequencies, it is reasonable to assume that these signals will also be variable. This assumption can explain the contradictory results obtained between 2 and 6 MHz, the confusion over the high field strength observed near the core at a frequency of 22 MHz, and the variations in lateral distribution near the core, at a frequency of 30 MHz, observed by the Moscow group. In addition, the apparent polarization at 6 MHz would be more plausibly explained by a change in the field strength during the experiment, than as the result of a geomagnetic origin of the pulses. Such a postulate is weak, for apparent variations due to poor experimental technique can be concealed within it; however, the alternative appears to be that, for the reasons discussed in Chapter 4, incompetence is a common feature of experimental investigations of radio emissions from EAS (including the present work).

High, variable field strengths have also been observed in the 30 to 60 MHz frequency region, and their association with thunderstorm activity has been interpreted as evidence of a geoelectric mechanism. At 100 kHz some very indirect evidence for a geoelectric mechanism has been reported, but is not supported by this work, and theoretical considerations make it unlikely that it can produce the observed low frequency field strengths.

There is no direct evidence to support any production mechanism, and the author is quite unable to suggest a plausible explanation for these observations.

6.3 The Future

The discontinuance of attempts to use radio techniques for the study of cosmic ray primaries has effectively made this work irrelevant to the mainstreams of cosmic ray physics.

If radio techniques had been continued as a serious tool in cosmic ray research, this work would certainly need further close examination, for serious doubts would be cast on any interpretation of radio pulse fluctuations in terms of fluctuations in shower development, when an erratic, unexplained mechanism was possibly active at frequencies only an octave below those used in the fluctuation studies.

However, if there is now little in this subject to excite the interest of cosmic ray physics, the puzzle still remains. Perhaps it may find a home in the field of atmospheric physics.

> 'And what do you believe about them now?' asked Cebes.
>
> 'Why upon my word, that I am very far from supposing that I know the explanation of any of these things'
>
> Socrates

REFERENCES

Note the abbreviation P.nth ICCR stands for Proceedings of the nth International Conference on Cosmic Rays.

CHAPTER ONE

1 JELLEY J.V. et al Nature 205 p327 (1965)

2 ASKARYAN G.A. Sov. Phys. JETP 14 p441 (1962)

3 JELLEY J.V. et al Nuovo Cim X46 p649 (1966)

4 GREISEN K. Phys. Rev. Letts 16 p748 (1966)

5 LINSLEY J. Phys. Rev. Letts 10 p146 (1963)

6 FEGAN D.J. et al Can. J. Phys. 46 pS250 (1968)

7 CHARMAN W.N. et al Can. J. Phys. 46 pS220 (1968)

8 VERNOV S.N. et al Can. J. Phys. 46 pS241 (1968)

9 HILLAS A.M. Physics Reports 20 p59 (1975)

10 ATRASHKEVICH V.B. et al P 13th ICCR 4 p2399 (1973)

11 ALLAN H.R. et al P 13th ICCR 4 p2407 (1973)

12 ALLAN H.R. Rapporteur Paper 15th ICCR (to be published)

13 ALLAN H.R. Prog. Elementary Particle and Cosmic Ray Physics 10 p170 (1971)

14 ALLAN H.R. Nature 237 p384 (1972)

15 GINZBURG V.L. and SYROVATSKII S.I. The Origin of Cosmic Rays (Pergammon, 1964)

16 EDGE D.M. et al J. Phys. A 6 p1612 (1973)

17 LINSLEY J. and WATSON A.A. Nature 249 p816 (1974)

18 BRECHER, K. and BURBIDGE G.R. Ap. J. 174 p253 (1972)

19 STECKER F.W. Phys. Rev. Letts. 21 p1016 (1968)

20 HILLAS, A.M. and OULDRIDGE M. Nature 253 p609 (1975)

21 EDGE D.M. et al J. Phys. G 4 p133 (1978)

22 SYROVATSKII S.I. Com Astrophys. and Space Phys. 3 p155 (1971)

23 CUNNINGHAM G. et al P 15th ICCR 2 p303 (1977)

REFERENCES CONTINUED

CHAPTER TWO

1 HAYAKAWA S. Cosmic Ray Physics (Wiley 1969)

2 DIXON H.E. et al Proc. Roy. Soc. A339 p133 (1974)

3 BARRET M.L. et al P 15th ICCR 8 p172 (1977)

4 TOMASZEWSKI A and WDOWCZYK J. P 14th ICCR 8 p2899 (1975)

5 DIXON H.E. et al Proc. Roy. Soc. A339 p157 (1974)

6 DIXON H.E. and TURVER K.E. Proc. Roy. Soc. A339 p174 (1974)

7 FEYNMAN R.P. Phys. Rev. Letts. 23 p1415 (1969)

8 PROTHEROE R.J. and TURVER K.E. P 14th ICCR 8 p2847 (1975)

9 GAISSER T.K. et al P 15th ICCR 8 p314 (1977)

10 KALMYKOV N.N. and KHRISTIANSEN G.B. P 14th ICCR 8 p2861 (1975)

11 GRIEDER P.K.F. Rev. Nuovo. Cim. 7 p1 (1977)

12 GAISSER T.K. Rapporteur Paper 15th ICCR (to be published)

13 McCUSKER C.B.A. Phys. Reports 20 p229 (1975)

14 BOHM E. et al Can. J. Phys. 46 pS41 (1968)

15 DAKE S. et al P 12th ICCR 3 p948 (1971)

16 GRIEDER P.K.F. P 15th ICCR 8 p370 (1977)

17 GREISEN K. Ann. Rev. Nucl. Sci. 10 p80 (1960)

18 NISHIMURA J. Handbuch Der Physik 46,2 p1 (1967)

19 BUTCHER J.C. and MESSEL H. Nucl. Phys. 20 p15 (1960)

20 ALLAN H.R. et al P 14th ICCR 8 p3071 (1975)

21 BRADT H.V. and RAPPAPORT S.A. Phys. Rev. 164 p1567 (1967)

22 HILLAS A.M. et al P 12th ICCR 3 p1001 (1971)

23 ATRASHKEVICH V.B. et al P 14th ICCR 8 p3086 (1975)

24 ORFORD K.J. and TURVER K.E. Nature 219 p706 (1968)

25 EARNSHAW J.C. et al J. Phys. A 6 p1244 (1973)

26 JELLEY J.V. Nuovo Cim. S8 p578 (1958)

27 KAHN F.D. and LERCH I. Proc. Roy. Soc. A 289 p206 (1966)

28 ALLAN H.R. Prog. Elementary Part. and Cosmic Ray Physics 10 p170 (1971)

29 HOUGH J.H. J. Phys. A 6 p892 (1973)

30 SHUTIE P.F. Thesis, University of London (1973)

31 FEYNMAN R.P. et al The Feynman Lectures in Physics Vol 1 (Addison - Wesley)

32 JACKSON J.D. Classical Electrodynamics (Wiley)

33 BRACEWELL R. The Fourier Transform and its Application (McGraw - Hill 1965)

34 HOUGH J.H. J. Phys. A 6 p892 (1973)

35 ALLAN H.R. et al P 14th ICCR 8 p3077 (1975)

36 ASKARYAN G.A. Sov. Phys. JETP 14 p441

37 FUJII M. and NISHIMURA J. Acta Physica Hung. 29 S3, p709 (1970)

38 CASTAGNOLI C. et al Nuovo. Cim. 63B p373 (1969)

39 FUJII M. and NISHIMURA J. P 12th ICCR 3 p1131 (1971)

40 ALLAN H.R. et al P 14th ICCR 8 p3077 (1975)

41 PRESCOTT J.R. et al Nature P.S. 233 p109 (1971)

42 VERNOV S.N. et al Sov. Phys. JETP Letters 5 p157 (1967)

43 CHALMERS J.A. Atmospheric Electricity (Pergammon)

44 WILSON R.R. Phys. Rev. 108 p155 (1957)

45 CHARMAN W.N. J. Atm. Terr. Phys. 30 p195 (1968)

46 SIVAPRASED K. P 15th ICCR 8 p484 (1977)

47 CURRY A. ET AL J. Atm. Terr. Phys. 36 p215 (1974)

48 CROZIER W.D. J. Geophys. Res. 68 p5173 (1963)

49 HAZEN W.E. and HENDEL A.Z. P 12th ICCR 3 p1137 (1971)

50 ALLAN H.R. et al P 14th ICCR 8 p3082 (1975)

51 MANDOLESI G. et al J. Atmos. Terr. Phys. 36 p1431 (1974)

52 JELLEY J.V. P 9th ICCR 2 p698 (1965)

53 SMITH G.J. and TURVER K.E. P 13th ICCR 4 p2369 (1973)

54 FOMIN Y.A. and KHRISTIANSEN G.B. S.J.N.P. 14 p360 (1972)

55 ORFORD K.J. and TURVER K.E. Nature 264 p727 (1976)

CHAPTER THREE

1 BAGGE E. et al P 9th ICCR 2 p738

2 BASSI P. et al Phys. Rev. 122 p637 (1961)

3 GREISEN K. Ann. Rev. Nuc. Sci. 10 p80 (1960)

4 HILLAS A.M. Phys. Reports 20 p59 (1975)

5 PATTERSON J.R. Pers comm.

6 CLARK G. et al Nuovo Cim. Supp. 8 ser 10 p623 (1958)

7 BEVINGTON P.R. Data Reduction and Error Analysis (McGraw Hill 1969)

8 SMITH A.C. Nuc. Inst. and Meth. 154 p573 (1978)

9 JAMES F. and ROOS M. Comp. Phys. Comm. 10 p343 (1975)

10 SMITH A.C. and THOMPSON M.G. Nuc. Inst. and Meth. 145 p289 (1977)

CHAPTER FOUR

1 ALLAN H.R. et al P 14th ICCR 8 p3082 (1975)

2 HAZEN W.E. and HENDEL A.Z. P 12th ICCR 3 p1127 (1971)

3 MANDOLESI N. et al J. Atmos. Terr. Phys. 36 p1431 (1974)

4 ATRASHKEVICH V.B. et al P 14th ICCR 8 p3086 (1975)

5 MANDOLESI N. et al P 13th ICCR 4 p2414 (1973)

6 HAZEN W.E. et al Phys. Rev. Letts 24 p476 (1970)

7 HOUGH J.H. et al Nature P.S. 232 p14 (1971)

8 ALLAN H.R. et al Nature 225 p253 (1970)

9 STUBBS T.J. Nature P.S. 230 p172 (1971)

10 FELGATE D.G. and STUBBS T.J. Nature 239 p151 (1972)

11 ALLAN H.R. Nature 237 p384 (1972)

12 HOUGH J.H. and PRESCOTT J.R. Nature 227 p590 (1970)

13 HOUGH J.H. et al Proc 6th Inter-American Seminar on Cosmic Rays (La Paz) 2 p527 (1970)

14 PRESCOTT J.R. et al Nature P.S. 233 p109 (1971)

15 CLAY R.W. et al P 12th ICCR 3 p1132 (1971)

16 HOUGH J.H. J. Phys. A 6 p892 (1973)

17 ALLAN H.R. et al P 14th ICCR 8 p3077 (1973)

18 SHUTIE P.F. Ph D Thesis, University of London (1973)

19 ATRASHKEVICH V.B. JETP Letters 13 p51 (1971)

20 CLAY R.W. Pers. Com.

21 CLAY R.W. Ph D Thesis, University of London (1970)

22 BRIGGS B.H. et al Nature 223 p1321 (1969)

23 JELLEY J.V. Cerenkov Light and its Applications (Pergammon) p228

24 SMITH J.W. Pers. Com.

CHAPTER FIVE

1 CLAY R.W. et al P 13th ICCR 4 p2420 (1973)

2 GREGORY A.G. et al Nature 235 p86 (1973)

3 ALLAN H.R. et al Nature 225 p253 (1970)

4 STUBBS T.J. Nature P.S. 230 p172 (1971)

5 FELGATE D.G. and STUBBS T.J. Nature 239 p151 (1972)

6 ALLAN H.R. Nature 237 p384 (1972)

7 CLAY R.W. Pers. Com.

8 WATT A.D. VLF Radio Engineering (Pergammon 1967)

Better is the end of a thing
than the beginning thereof.

Ecclesiastes